

THERMAL REARRANGEMENT OF *O*-VINYL-PHENYLISOCYANATES.  
EXPERIMENTAL AND COMPUTATIONAL PROBES OF SUBSTITUENT EFFECTS  
ON PERICYCLIC REACTIONS

By

LIAN LUO

A DISSERTATION PRESENTED TO THE GRADUATE SCHOOL  
OF THE UNIVERSITY OF FLORIDA IN PARTIAL FULFILLMENT  
OF THE REQUIREMENTS FOR THE DEGREE OF  
DOCTOR OF PHILOSOPHY

UNIVERSITY OF FLORIDA

1998

To the Lord my God

for giving me the freedom of choice  
to believe in science

## ACKNOWLEDGMENTS

There are a great number of people I would like to thank for assisting me in the completion of this dissertation, however, I might leave some of them out inadvertently.

I am certainly indebted to the supervision from my advisor, Professor William R. Dolbier, Jr. As a scientist, Professor Dolbier furnishes us with not only his vast knowledge of chemistry, but his methods of motivating and inspiring students as well. Chemistry is joyful and all the problems are solvable with Professor Dolbier. As an ordinary person, Professor Dolbier provides us with friendship, which is precious especially for us who are far away from home. Professor Dolbier was my boss once at the University of Florida, he will be my supervisor for life.

Greatly appreciated are the professors in my committee and the professors whose courses I have taken. Their inspiration and their knowledge benefited me to in building my chemistry intuition. Through my stay in the Dolbier Research Group, I received countless hours of help. Thanks are due to all my colleagues: Michael Bartberger, the computer wizard in our group, for his help and time in the computational studies, which gave me the confidence that my experimental were on the right track; Conrad Burkholder for numerous discussions and the tricks in organic laboratory; Michelle Fletcher and Alex Roche for their patience to correct the grammatical errors in the thesis; Bruno Delest, Henu Koroniak, Rogelio Ocampo, Luz Amalia Rios, and recently, John Baker, Sasha Shtarev, Virginie Kruger, all for providing valuable friendships. Thanks also go to the

three senior undergraduate students, Tinh Tam, Alex Papangelou and Mike Henderson, for making some of the starting materials and for helping me understand life in America (especially for life of people in generation X). Also, thanks go to my friends from mainland China: Duan Jianxin, Li Anrong, Huang Bingnan, Rong Xiaoxin, Tian Feng, Xu Yuelian, Zhang Li and Zhang Lianhao for making me “at home” in the lab.

I thank Dr. Ion Ghiriviga and Dr. Roy King for teaching me how to run all the NMR machines, and Dr. Mike Peterson for help in retrieving the “old” spectra.

Outside the research group, thanks are required to a number of friends: Hu Jian, Kang Fan, Lang Lisa, Liu Fang, Shi Jia, Tang F. Xing, Tao Li, Tian Fang, Wang Jianmao, Wu Yee and Z. Dawn Power, for not only providing the friendships, but also showing me the truth that friendship is the most beautiful and valuable thing in the world.

I thank my Mom, my sisters and brothers for their love and for letting me go abroad. No matter how far away from them, I always feel their love, support and encouragement. Last, but certainly not the least, what will always be remembered was the influence from my Dad. After years, I still can see the never-satisfied look in his face and it is still leading me to a higher level.

## TABLE OF CONTENTS

ACKNOWLEDGMENTS .....	iii
ABSTRACT .....	vii
CHAPTER	
I AN OVERVIEW OF SUBSTITUENT EFFECTS ON PERICYCLIC REACTIONS.....	1
1.1 Introducing Torquoelectronic Selectivity .....	1
1.1.1 Stereochemistry of thermal cyclobutene/1,3-diene inter-conversion .....	1
1.1.2 Theoretical rationales of the thermal cyclobutene/1,3-diene interconversion.....	8
1.2 Introducing Pseudo-Pericyclic Reactions .....	15
1.3 A View on Rotational Kinetic Isotope Effects .....	20
II THERMAL REARRANGEMENT OF <i>O</i> -VINYL-PHENYLISOCYANATES .....	25
2.1 Introduction.....	25
2.1.1 Development of a suitable 6- $\pi$ electrocyclic system .....	29
2.1.2 Thermal rearrangement of the parent system. A mechanistic approach.....	32
2.1.3 Conclusions.....	46
2.2 Investigating the Isotope Effects at the $\beta$ -Position .....	47
2.3 Polar Effects of the $\alpha$ -Substitutions.....	56
2.3.1 Thermal rearrangement of iso-propenyl phenylisocyanate .....	56
2.3.2 Thermal rearrangement of $\alpha$ -trifluoromethyl system.....	59
2.4. Investigation of Torquoelectronic Selectivity on 6 $\pi$ System.....	65

2.4.1 Thermal rearrangement of <i>o</i> -( <i>E/Z</i> ) propenyl phenylisocyanate.....	66
2.4.2 Thermal rearrangement of <i>o</i> -( <i>E/Z</i> )-3,3,3-trifluoropropenyl phenylisocyanate.....	71
2.4.3 Thermal rearrangement of <i>o</i> -iso-(1-fluoro)-propenyl phenylisocyanate.....	76
2.4.4 Thermal rearrangement of <i>o</i> -( <i>E/Z</i> ) $\beta$ - fluorovinyl phenylisocyanate.....	82
2.4.5 Conclusions.....	86
III SUMMARY .....	91
IV EXPERIMENTAL.....	97
General Methods.....	97
Experimental Procedures.....	98
APPENDIX.....	122
REFERENCES .....	141
BIOGRAPHICAL SKETCH .....	150

Abstract of Dissertation Presented to the Graduate School  
of the University of Florida in Partial Fulfillment of the  
Requirements for the Degree of Doctor Of Philosophy

THERMAL REARRANGEMENT OF *O*-VINYL-PHENYLISOCYANATES.  
EXPERIMENTAL AND COMPUTATIONAL PROBES OF THE SUBSTITUENT  
EFFECTS ON PERICYCLIC REACTIONS

By

Lian Luo

May, 1998

Chairman: William R. Dolbier, Jr.  
Major Department: Chemistry

Thermal rearrangement of *o*-vinyl phenylisocyanate(**52**) to quinol-2-one (**56**) was examined in C<sub>6</sub>D<sub>6</sub> around 110°C. The rearrangement was proven to be a smooth and well behaved first-order reaction, via a 6- $\pi$  electrocyclic process. Analysis of the transition structure from theoretical calculations revealed that the electrocyclization of such a compound proceeds via a novel pseudopericyclic process, *i.e.*, a process that the overlapping orbitals are mutually orthogonal.

This newly developed system led to the evaluation of torquoelectronic selectivity in a 6- $\pi$  electron system disrotatory process, which was experimentally unprecedented, with only one case from computational studies in the literature. The novelty of the system was the absence of a substituent at the isocyanate terminus of its 6- $\pi$  system. This eliminated the steric effects which had hampered the earlier investigations on

torquoelectronic selectivity on disrotatory process. The successful syntheses of various isomeric  $\beta$ -substituted vinyl phenyl isocyanates and the kinetic experiments on them made it possible to evaluate the substituent effects on the electrocyclization. The experimental results, corroborated by the computational investigations, made it patently clear that the major contributing factor on the electrocyclization was the electronic property of the substitutions, instead of the sterics. This was based on the facts that the smallest substituent (F, **105**) gave rise to the largest observed kinetic effects ( $k_Z/k_E=82.1$  at  $101.6^\circ\text{C}$ ), whereas the largest ( $\text{CF}_3$ , **96**) gave rise to the smallest ( $k_Z/k_E=3.2$  at  $182.3^\circ\text{C}$ ).

Substantial polar effects were found at the  $\alpha$ -position. With respect to the parent system, putting a electron donor ( $\text{CH}_3$ , **72**) at the  $\alpha$ -position lowered the temperature for the rearrangement by *ca.*  $80^\circ\text{C}$ , whereas an electron acceptor ( $\text{CF}_3$ , **79**) raised the temperature by *ca.*  $40^\circ\text{C}$ . This polar effect was understood in terms of donor/acceptor type interactions. An electron donating group at the  $\alpha$ -position can induce polarization of the transition state and results in a lowering of the barrier to bond formation.

Normal kinetic isotope effects were observed by putting deuterium at the  $\beta$ -position(**63**). It was explained by the rotational isotope effect. That is, when a hydrogen attached to a carbon is substituted with a deuterium, the carbon's ability to rotate is subsequently retarded. The weak normal isotope effects for the overall reactions ( $(k_H/k_D)_{\text{cis}}=1.11$ ;  $(k_H/k_D)_{\text{trans}}=1.07$ ) and the relatively larger isotope effect for the product formation step ( $k_H/k_D=2.5$ ) combined with the lack of equilibrium between the isomers asserted the electrocyclization was rate determining.

## CHAPTER I

### AN OVERVIEW OF SUBSTITUENT EFFECTS ON PERICYCLIC REACTIONS

In the last few decades, a great deal of efforts have been directed at understanding the nature of pericyclic reactions, which indeed have been widely applied in organic syntheses and mechanisms. Fundamental principles of orbital theory have provided guidelines for chemists to predict stereochemistries and mechanisms of pericyclic reactions. However, pericyclic reactions, as one of the most important chemical reactions, are still “pregnant” with intriguing mysteries, stimulating controversies and inspiring ambiguities.

#### **1.1 Introducing Torquoelectronic Selectivity**

##### **1.1.1 Stereochemistry of thermal cyclobutene/1,3-diene inter-conversion**

In 1965, in a series of communications<sup>1</sup> which shocked the chemistry world, R. B. Woodward and R. Hoffmann laid down some fundamental bases for the theoretical understanding of all concerted reactions. According to their theory, “the basic principle enunciated was that reactions occur readily when there is congruence between orbital symmetry characteristics of reactants and products, and only with difficulty when that congruence does not obtain-or to put it more succinctly, orbital symmetry is conserved in concerted reactions.”<sup>2</sup> Since then the properties of molecular orbitals and their

interactions have been widely used to predict the stereochemistry and mechanisms of organic reactions. Woodward and Hoffmann identified electrocyclic rearrangements, such as a  $4\text{-}\pi$  electron conrotatory interconversion of cyclobutene to butadiene, and a  $6\text{-}\pi$  electron disrotatory 1,3,5-hexatriene conversion to 1,3-cyclohexadiene as occurring through thermally allowed concerted pathways.<sup>2</sup> They proposed that a path which conserves the orbital symmetry from reactants to products is the lowest energy pathway by which the process may occur. To maintain the symmetry for the thermal  $4\text{-}\pi$  process, C3 and C4 of cyclobutene must rotate in the same direction upon breaking the  $\sigma$  bond, thereby defining a conrotatory process. As shown in Figure 1-1, two equivalent stereodistinct, conrotatory processes are allowed by orbital symmetry for  $4\text{-}\pi$  thermal reactions, each leading to a different conjugated diene. Theoretical studies show that a concerted transition structure does not exist for the thermally forbidden disrotatory process, and Breulet and Schaefer estimated that the non-concerted path involving the allylmethylene diradical is 9-11 kcal/mol above the concerted conrotatory transition state.<sup>3</sup>

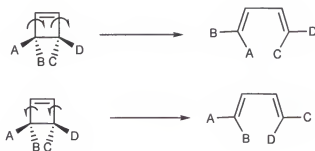


Figure 1-1 Thermal Conrotatory  $4\text{-}\pi$  Electrocyclic Process

In a somewhat “taking it for granted” manner, the stereochemistry of butadiene products from early studies of C3 and C4 alkylated cyclobutenes were rationalized using a strictly *steric* argument. Such C3 and C4 methylated cyclobutenes yielded butadienes in which the bulkier substituents had stereospecifically rotated outward to form the *E*-alkenes (Figure 1-2)<sup>4,5,6,7</sup>

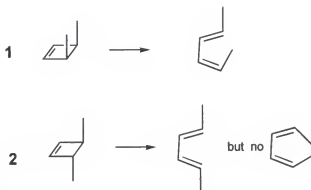
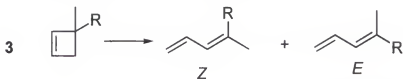


Figure 1-2 Thermal ring opening of methyl substituted cyclobutenes

In 1980, Curry and Stevens reported a series of 3,3-disubstituted cyclobutenes which yielded products contrary to those which would have been predicted on steric grounds.<sup>8</sup> Figure 1-3 illustrates their results in which ethyl, *n*-propyl and *i*-propyl favor



Ratio of Products

R	Z	E
ethyl	2.1	1
<i>n</i> -propyl	1.6	1
<i>iso</i> -propyl	1.9	1
<i>t</i> -butyl	1	2.1

Figure 1-3 Thermal ring opening of 3,3-dialkylcyclobutenes

inward rotation over methyl, the less bulky group, to predominately form *Z*-butadienes. Surprisingly, *t*-butyl yields 32% of the product where this very bulky group has rotated inward! More intriguing examples have followed as illustrated in Figure 1-4.<sup>9,10,11</sup> In each of these cases, the reaction is 100% stereoselective and occurs contrary to expectations based on steric interactions.

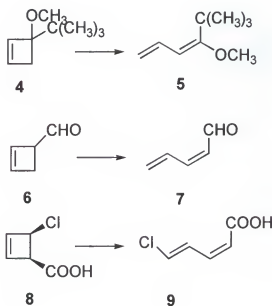


Figure 1-4 Examples of un-intuitive thermal ring openings in substituted cyclobutenes.

More convincing and inspiring examples were provided by Dolbier's group when they were investigating the ring openings of the fluorinated cyclobutenes. An understanding of the unique properties of fluorine is imperative since it is utilized as a mechanistic probe for some of the systems for the author's project. The effects exhibited by fluorine as a substituent are due to three intrinsic characteristics of the fluorine atom: its extreme electronegativity, non-bonded electron pairs and small relative size. Fluorine

is the most electronegative of all elements 4.10 on the Pauling scale as compared with oxygen (3.50), chlorine (2.83), bromine (2.74) carbon (2.50) and hydrogen (2.20).<sup>12</sup> Strong polarization of fluorinated molecules through the  $\sigma$  bonding framework and through space (field effects) are results of fluorine's large electronegativity. The atom is mono-valent and accommodates three non-bonded electron pairs in orbitals of similar dimension to hybridized orbitals on carbon.<sup>13</sup> Because of these two preceding factors, fluorine exhibits an interesting donor/acceptor contradiction under certain circumstances in that the strong removal of electron density from a bound atom can be offset by back donation of density from the non-bonded electrons.<sup>14,15</sup> The van der Waals radius of fluorine is 1.47 Å as compared with chlorine (1.73 Å), bromine (1.84 Å), iodine (2.01 Å) and hydrogen (1.20 Å).<sup>16</sup> In fact, a fluorine substituent is the smallest of all non-hydrogen substituents. Thus, it should exhibit minimal spatial requirement as a substituent. Examples of single fluorine substituents exerting a steric influence on the outcome of a reaction are rare.<sup>17</sup> Therefore, it makes the substitution of hydrogen by fluorine in many hydrocarbon system a promising mechanistic tool. Returning from the digression, Dolbier et al. investigated a series of fluorocyclobutene/fluoro-1,3-diene inter-conversions in the 1980s.<sup>18,19</sup> In all the cases studied in the Dolbier's group, fluorine, a  $\pi$  electron-donor substituent, kinetically preferred outward rotation and in some cases, outward rotation of fluorine was favored even at the expense of rotating a much bulkier -CF<sub>3</sub> group, which is attached at the same carbon as the fluorine, *inward*! (Figure 1-5)

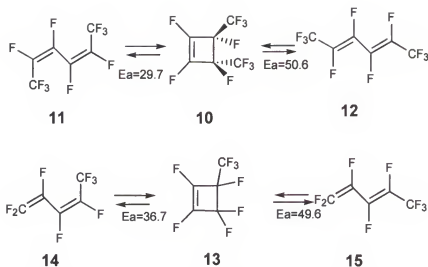


Figure 1-5. Thermal polyfluorinated cyclobutene/1,3-diene interconversions

In the investigations of the thermal opening of perfluorinated cyclobutenes it was demonstrated that the formation of product via outward rotation of a fluorine atom and inward rotation of the  $\text{CF}_3$  group was preferable kinetically by 21.5 kcal/mol and 12.9 kcal/mol, respectively. In another study, the effect of a lone fluoro or trifluoromethyl substituent was determined unambiguously, Figure 1-6.<sup>20</sup> A thorough investigation of the opening of the rings of 3-fluoro, 3-trifluoromethyl and 3,3-difluorocyclobutene showed the individual dienes are formed, while the opening of trifluoromethylcyclobutene leads to a mixture of *E* and *Z* isomers. The rotation of the fluorine atom inward proceeds with an energy of activation that is 10.2 kcal/mol greater, while rotation outward proceeds with an energy of activation that is 3.6 kcal/mol lower, than for unsubstituted cyclobutene. Also note that the activation energy for ring-opening of 3,3-difluorocyclobutene is 16.9 kcal/mol greater than the monofluoro analogue. It is clear that when a fluorine substituent must rotate inward, this rotation significantly increases activation energy.

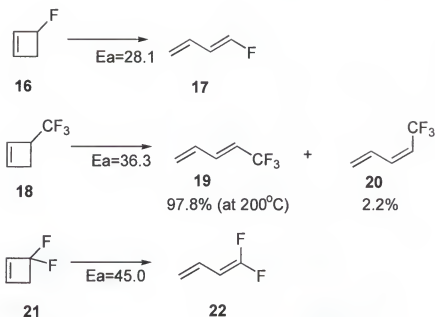


Figure 1-6 Thermal ring opening of partially fluorinated cyclobutenes. Activation energies are in kcal/mol

It is interesting to compare the data on the openings of 3-fluorocyclobutene and 3-trifluoromethylcyclobutene. In the former case only *E*-diene is formed. While, in the latter case, 2.2% *Z*-isomer is formed. Since a trifluoromethyl group is much bulkier than a methyl group, the simple fact of formation of *Z*-diene, although in small amount, constitutes evidence that the electronic properties rather than the steric properties of the substituents are the major factors involved in determining the stereoselectivity of ring openings of cyclobutenes.

Related results are also found in other  $4n \pi$  electron electrocyclic processes, such as in the cyclizations of pentadienyl cations (Nazarov cyclization)<sup>21</sup> and the cycloaddition reactions of ketene-imine (Staudinger reaction).<sup>22</sup>

### 1.1.2 Theoretical rationales of the thermal cyclobutene/1,3-diene interconversion

When this unintuitive result could not be understood by a simple steric rationale, there arose a need for an alternative approach. Besides the size of the substituent, another factor which plays an important role in chemical reactions is its electronic properties. From the variety of examples and the nature of substituents examined for all these 4- $\pi$  electron thermal processes, it has become obvious that the observed stereoselectivity originated from a strong electronic effect involving interaction of cyclobutene C3 and C4 position substituents with the molecular orbitals of the 4- $\pi$  transition state. Electron donors and mild electron acceptors at C3 and C4 positions kinetically favor outward rotation to form an *E*-diene, whereas powerful  $\pi$ -electron acceptors favor inward rotation to form a *Z*-diene.<sup>23,24</sup>

The initial theoretical studies were carried out in Houk's group<sup>23</sup>. They developed a hypothesis based on results obtained by theoretical *ab initio* level calculations on the cyclobutene/1,3-diene thermal conrotatory process. Figure 1-7 is a representation of their proposed interactions between the breaking  $\sigma$  bond orbital and the substituent p orbital upon the inward and outward rotations. The dashed line represents bonds to carbons 1 and 2 of 3-substituted cyclobutene. The drawing shows the  $\sigma^*$  and  $\sigma$  orbitals of the breaking  $\sigma$  bond and a p orbital on a substituent at C-3.

Electron-donor substituents at a saturated carbon of cyclobutene have very little effect on the stability of the reactant but stabilize the transition state to a large extent due to overlap and mixing with the  $\sigma^*$  orbital.<sup>25</sup> Electron-withdrawing groups also influence the transition state, but not the reactant energies. The electron-donor groups attached to

the breaking bond will either maximize (in the process) the stabilizing two-electron interaction of the substituent with the C3-C4  $\sigma^*$  orbital and the decrease in the four-electron interaction between this donor and the C3-C4  $\sigma$  orbital. Most substituents

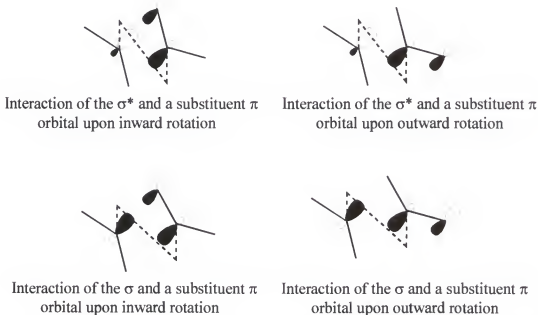


Figure 1-7 Schematic representation of frontier molecular orbital interactions for the cyclobutene/1,3-diene inter-conversion

prefer outward rotations because of either or both of these two electronic effects. When the substituent is an electron acceptor, inward rotation can be favorable because this motion permits a vacant  $\pi^*$  orbital of the substituent to overlap with the remote terminus of the breaking  $\sigma$  bond. Put another way, upon outward rotation, the substituent overlaps only with the orbital on the attached carbon.<sup>26,27</sup> Upon inward rotation, the substituent also overlaps with the orbital on the remote terminus of the breaking bond. When the substituent orbital is doubly occupied, outward rotation is favored. This minimizes the four electron repulsion of the substituent orbital with the HOMO (Highest Occupied Molecular Orbital) of the breaking bond and maximizes the two-electron stabilization of

the substituent with the LUMO (Lowest Unoccupied Molecular Orbital) of the breaking bond.<sup>28</sup> If the substituent orbital is vacant, then inward rotation is favored to maximize the two-electron stabilization arising from the interaction of the substituent orbital with the HOMO of the breaking bond. This stabilizing interaction can overcome the steric repulsion which occurs upon inward rotation only with powerful  $\pi$ -acceptors (such as formal<sup>27</sup> or dialkylboryl<sup>23</sup>). In 1985, Houk introduced the new term *torquoselectivity* (electronic selectivity of the rotation pathway)<sup>23</sup>, which symbolizes the primary occurrence of a reaction via one of the two possible conrotatory pathways for thermal opening of the cyclobutene ring.

The  $4\pi$  conrotatory process is ideally arranged to maximize the electronic difference between inward and outward rotation and to minimize the steric interactions involved in the transition structure. The study of torquoselectivity was extended to  $8\pi$  conrotatory electrocyclic processes.<sup>29</sup> The inter-conversion of *cis,cis*-1,3,5,7-octatetraene and *cis,cis,cis*-1,3,5-cyclooctatriene is thermally allowed according to Woodward-Hoffmann rules<sup>2</sup>. The studies from Houk's group showed that the transition structure has a helical geometry. Although the process is clearly conrotatory, the helical transition structure causes substituents on the inside or outside to experience essentially the same relationship to the breaking C-C bond, since the two termini of the partially formed  $\sigma$  bond are aligned nearly perfectly, not twisted (torqued) as in the conrotatory cyclobutene/butadiene inter-conversion. Therefore, the interaction of substituent p orbital with the breaking bond  $\sigma$  orbitals are essentially the same. Consequently, the electronic nature of the substituent does not play an important role in directing the rotational preference. Steric effects do cause a small preference for all substituents to

rotate outward, ranging from 0.8 kcal/mol for fluorine to 3.1 kcal/mol for a formyl group at the MP2/6-31G\*//RHF/3-21G + ZPE level, as shown in Table 1-1

Table 1-1 Activation energies and relative Energies of the Transition Structures for inward and Outward Rotation of the Substituent for the Ring Opening of 7-Substituted 1,3,5-Cyclooctatrienes,  $\Delta E_a = E_{in} - E_{out}$ , Energies in kcal/mol

substituent	basis set	Ea(in)	Ea(out)	$\Delta E_a$
F	MP2/6-31G*+ZPE	24.9	24.1	0.8
CH <sub>3</sub>	MP2/6-31G*+ZPE	23.6	20.7	2.9
CHO	MP2/6-31G*+ZPE	20.2	17.1	3.1

It is evident that one may also speak of the selectivity of the rotation pathway in the case of the realization of two *disrotatory* pathways in 6- $\pi$  systems, which leads to the author's primary and initial project.

Inspired by the thoroughly studied examples of the four-electron electrocyclic ring-openings, Houk's group has done computational studies, trying to apply this theory to disrotatory processes.<sup>30</sup> For comparison, Table 1-2 shows the calculated activation energies and relative energies of the transition structures for inward and outward rotation of the substituent for the ring openings of 5-substituted 1,3-cyclohexadienes, while the activation energies for the corresponding 3-substituted cyclobutenes are shown in Table 1-3. Similar to the 4- $\pi$  electron system, a preference for outward rotation is computed for electron-donors, while a preference for inward rotation is found for the electron acceptors. However, significant reduction of the activation energy differences are computed for the 1,3-hexadienes. For example, inward rotation is favored for the ring opening of 3-

borylcyclobutene by 18.7 kcal/mol at MP2/6-31G\*//RHF/3-21G + ZPE level of theory, but inward rotation in 5-borylcyclohexadiene is favored by only 9.2 kcal/mol. Outward rotation is favored by 15.1 kcal/mol for 3-fluorocyclobutene, but only 4.7 for 5-

Table 1-2 Activation energies and relative Energies of the Transition Structures for inward and Outward Rotation of the Substituent for the Ring Opening of 5-Substituted 1,3-Cyclohexadienes.<sup>30</sup>  $\Delta E_a = E_{in} - E_{out}$ . Energies in kcal/mol

substituent	basis set	$E_a(in)$	$E_a(out)$	$\Delta E_a$
F	MP2/6-31G*+ZPE	51.8	47.1	4.7
CH <sub>3</sub>	MP2/6-31G*+ZPE	52.0	48.1	3.9
CHO	MP2/6-31G*+ZPE	40.5	40.9	-0.4
BH <sub>2</sub>	MP2/6-31G*+ZPE	33.1	42.3	-9.2

Table 1-3 Activation energies and relative Energies of the Transition Structures for inward and Outward Rotation of the Substituent for the Ring Opening of 3-substituted Cyclobutenes.<sup>30</sup>  $\Delta E_a = E_{in} - E_{out}$ . Energies in kcal/mol

substituent	basis set	$E_a(in)$	$E_a(out)$	$\Delta E_a$
F	MP2/6-31G*+ZPE	44.3	29.2	15.1
CH <sub>3</sub>	MP2/6-31G*+ZPE	38.8	33.5	5.3
CHO	MP2/6-31G*+ZPE	26.5	31.2	-4.7
BH <sub>2</sub>	MP2/6-31G*+ZPE	10.8	29.5	-18.7

fluorocyclohexadiene. That is, the dependence of stereoselection on the electronic characteristics of substituents still exists in the disrotatory processes, but to a smaller degree.

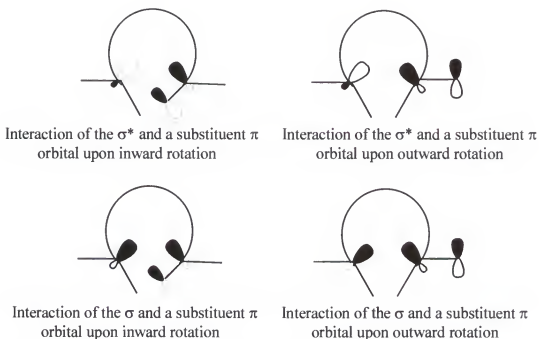
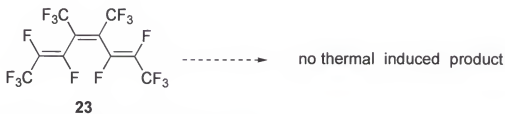


Figure 1-8. Schematic representation of frontier molecular orbital interactions of 1,3-cyclohexadiene/1,3,5-hexatriene inter-conversion. The loop represents the carbon atoms and bonds between the terminal carbons.

The predicted diminished electronic effect can be explained with the aid of the diagram shown in Figure 1-8, considering the interaction between either the HOMO or LUMO of the forming bond and a p or  $\pi$ -orbital of a substituent. As with the conrotatory case, a net stabilization occurs upon outward rotation of either electron-acceptors or electron-donors. This arises from two-electron interactions shown at the right: a donor  $\pi$  orbital interaction with  $\sigma^*$  LUMO, or an acceptor substituent vacant orbitals mixes with the  $\sigma$  HOMO. Stabilization upon inward rotation is predicted for an electron-acceptor substituent with a low-lying vacant orbital. The amount of overlap between substituent and  $\sigma$  HOMO orbitals of the inward transition structure is reduced compared to that in the conrotatory process. This reduces the amount of stabilization of an inward-rotating

electron-acceptor and the amount of destabilization of an inward-rotating electron-donor. The influence of electronic control upon selectivity is decreased.

While steric effects are not important in determining the stereoselectivity on conrotatory cyclobutene ring openings, the disrotatory motion leads to much *larger steric effects*, since the two inward hydrogens, the smallest substituents, of the terminal carbon atoms are separated by less than the sum of the van der Waals radii. (The distance of the two hydrogen is  $1.858\text{\AA}$ <sup>30</sup>, while the sum of van der Waals radii of two hydrogens is  $2.40\text{\AA}$ ) Substitution of any kind of substituent group for an inward hydrogen will cause larger steric interaction at the transition structures. Concrete evidence of this hypothesis was provided by Dolbier's group. They found that the normal boat-like transition state of a thermal  $6\pi$  electrocyclic reaction of 1,3,5-hexatriene has stringent steric requirements.<sup>31,32</sup> Perfluoro-*E,Z,E*-4,5-dimethyl-2,4,6-octatriene resists a  $6\pi$



perfluoro-*E,Z,E*-4,5-dimethyl-2,4,6-octatriene

Figure 1-9. Example of inhibited thermal electrocyclic process.

electrocyclic reaction even at temperatures of  $202^{\circ}\text{C}$  or higher (Figure 1-9). Terminal *cis*-substituents as small as fluorine are thus observed to be strongly inhibiting to the thermal electrocyclic process. Apparently, in spite of the enhanced thermodynamics of the reaction ( $19\text{--}20\text{ kcal/mol}$  exothermic would be expected for its cyclization), the boat-like

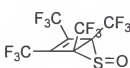
disrotatory thermal transition state is very steric demanding. In order to assess the torquoelectronic selectivity on the 6- $\pi$  system, an unconventional system needed to be developed to eliminate the steric impact.

## 1.2 Introducing Pseudo-Pericyclic Reactions

In 1970, Woodward and Hofmann defined pericyclic reactions as: “reactions in which all first-order changes in bonding relationships take place in concert on a closed curve”<sup>2</sup>. In addition, Lowry and Richardson<sup>33</sup> defined pericyclic reactions as: “processes characterized by bonding changes taking place through reorganization of electron pairs within a *closed loop* of interacting orbitals.” The bonding changes must be concerted in order for a reaction to fit into the pericyclic category; that is, bonds breaking and forming must do so simultaneously rather than in two or more steps. The number of  $\pi$ -electrons participating will (must) influence the “allowedness” of the reaction of the concerted reactions to conserve the orbital symmetry. For example, the 4- $\pi$  electron conrotatory inter-conversion of 1,3-butadiene/cyclobutene is thermally allowed, whereas a 6- $\pi$  electron conrotatory inter-conversion of 1,3,5-hexatriene/1,3-cyclohexadiene is thermally forbidden (disrotatory allowed). Such results have led to the well known rules and the familiar pattern of alternating forbidden and allowed reactions as the number of electrons is increased.

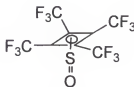
In 1976, Lemal<sup>34,35</sup> studied the automerization of the exo-S-oxide of perfluorotetramethyl thiophene (Dewar thiophene), shown in Figure 1-10a. Its <sup>19</sup>F NMR spectrum down to temperature as low as -95°C remains a narrow singlet. A combined analysis of Raman spectrum and infrared spectrum ruled out the unconventional, but

possible structure of Figure 1-10b. [1,3]-Sigmatropic rearrangements are orbital symmetry forbidden to occur suprafacially with respect to the migrating center, and the transition state geometry for allowed processes (antarafacial at sulfur) is very unfavorable. A diradical



24

Figure 1-10a



25

Figure 1-10b

Figure 1-10. Lemal's perfluorotetramethyl thiophene oxide.

pathway appears to be out of the question, given the extremely low activation energy barrier, since the activation parameters were found to be:  $\Delta H^\ddagger = 6.6 \pm 0.2$  kcal/mol,  $\Delta S^\ddagger = -0.5 \pm 0.6$  cal/mol-deg and  $\Delta G^\ddagger = 6.7 \pm 0.1$  kcal/mol at  $-135.8^\circ\text{C}$ .<sup>34</sup> Lemal proposed an automerization pathway for the degenerate thiophene, Figure 1-11.

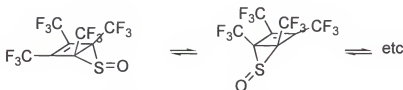


Figure 1-11 Automerization pathway of the Dewar thiophene oxide; an allowed [1,3] sigmatropic rearrangement.

Here the sulfur lone pair forms the new bond to carbon, and the electrons of the cleaving C-S bond become a new lone pair, as shown in Figure 1-12. The term *pseudopericyclic* reaction was proposed to describe this [1,3] sigmatropic pathway: such

a reaction is a concerted transformation whose primary changes in bonding compass a cyclic array of atoms, at one (or more) of which nonbonding and bonding atomic orbitals interchange roles. In a crucial sense, the role interchange means a “disconnection” in the

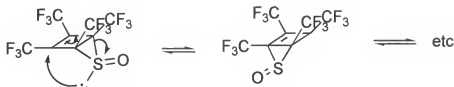


Figure 1-12. Pseudopericyclic [1,3] sigmatropic shift.

cyclic array of overlapping orbitals because the atomic orbitals switching functions are mutually orthogonal. Hence pseudopericyclic reactions *cannot be orbital symmetry forbidden*<sup>34</sup>, regardless of the number of electrons participating in the reaction.



Figure 1-13. Carbon Scrambling of Acylketene, Another [1,3] Sigmatropic Shift.

Another example was provided by Wentrup,<sup>36</sup> who observed that acylketenes could undergo carbon scrambling via 1,3-shift of a phenyl group, as shown in Figure 1-13. Although suprafacial thermal 1,3-shifts are forbidden by rules of symmetry, such shifts become possible in ketenes due to the presence of orthogonal orbitals. Some other examples of pseudopericyclic reactions are shown in Figure 1-14a and 1-14b.<sup>35</sup>

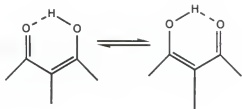


Figure 1-14a

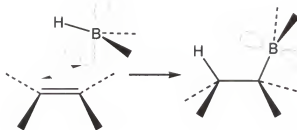


Figure 1-14b

Figure 1-14. Examples of pseudopericyclic precesses

Figure 1-14a shows the prototropy in internally hydrogen bonded enols of  $\beta$ -dicarbonyl compounds. As the proton tunnels between minima, lone pair and bonding orbitals formally interchange functions at both oxygens in the planar chelated ring. In olefin hydroboration (Figure 1-14b) the vacant boron orbital presumably switches roles with the orbital employed in bonding to hydrogen. By this device, a planar, four-center transition state, normally very high lying, becomes easily accessible.

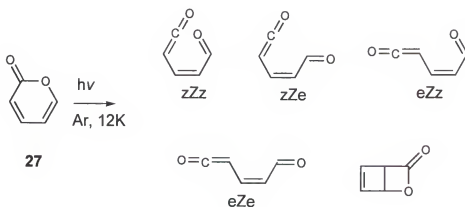


Figure 1-15 Photochemistry of pyran-2-one.

The potential importance of pseudopericyclic reactions, while being acknowledged occasionally since Lemal's invention<sup>37, 38, 39, 40</sup>, has been given new emphasis through a series of papers by Birney.<sup>41-46</sup> One typical example is the extensive study on matrix isolation<sup>41</sup> photochemistry of pyran-2-one, Figure 1-15.

*Ab initio* (MP4(full, SDQ)/D95\*\*//MP2/6-31G\*+ZPE) calculations were carried out on all the conformations. It was found that the possible conformation (zZz) does not exist, but closes without barrier, via a pseudopericyclic pathway to pyran-2-one.

Likewise, the transition state for the degenerate 1,5-sigmatropic hydrogen migration of zZe was anticipated to be planar, which may also be viewed as pseudopericyclic.<sup>41</sup>

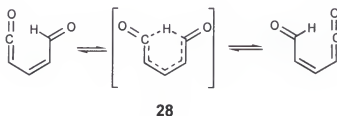


Figure 1-16 Degenerate 1,5-Sigmatropic hydrogen migration

In summary:<sup>43</sup> 1) a pseudopericyclic reaction may be orbital symmetry allowed via a pathway that involves orbital disconnections regardless of the number of electrons involved; 2) barriers to pseudopericyclic reactions can be very low or even non-existent; 3) pseudopericyclic reactions will have planar transition if possible.

### 1.3 A View On Rotational Kinetic Isotope Effects

Kinetic isotope effect (KIE) measurements are one of the few experimental probes for the transition state of the rate-limiting step of a reaction.<sup>47</sup> Consequently, the measurement of KIEs has found widespread use in mechanistic studies of various reaction types.<sup>48,49,50</sup> The analysis of primary and secondary isotope effects has been particularly valuable for the investigation of pericyclic reactions.<sup>51,52</sup> For example, experimental studies of secondary kinetic isotope effects (SKIEs) provide evidence that the Diels-Alder reaction proceeds in a concerted fashion<sup>53,54,55,56</sup> rather than by a stepwise mechanism.<sup>57</sup> It is generally accepted that changes in the out-of-plane bending of the hydrogen attached to the carbon that undergoes bonding change are largely responsible for the inverse secondary isotope effects.<sup>58,59</sup> According to this qualitative analysis, the change of an  $sp^2$  hybridized center with a low C-H bending frequency to a  $sp^3$ -hybridized center with high C-H bending frequency leads to an inverse ( $K_H/K_D < 1$ ) kinetic isotope effect, because during the reaction, the zero-point energy increases more for the C-H bond than for the C-D bond. As shown in Figure 1-17<sup>58</sup>, the force constant for the vibration in the transition state is greater than in the reactant; thus, the activation energy for the deuterium compound is smaller than that for the hydrogen compound, and the isotope effect is less than unity. For a hybridization change in the opposite direction, a normal SKIE ( $K_H/K_D > 1$ ) is predicted. From this point of view, hydrogens attached to the same carbon should have identical SKIEs.

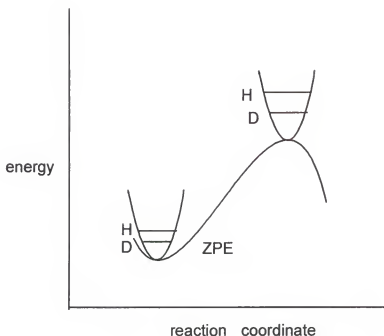


Figure 1-17. Reaction coordinate diagram illustrating the secondary isotope effect arising from a motion of hydrogen (deuterium) that undergoes a change of force constant in the reaction.

Another potential source of SKIEs was revealed for the first time when Crawford examined the thermal deazetation of the deuterated pyrazoline(Figure 1-18)<sup>60</sup>, and observed a dramatic normal kinetic isotopic effect ( $k_H/k_D = 1.37 \pm 0.05$ ) for the cyclization of the expected trimethylenemethene intermediate. Thus, a normal kinetic isotope effect was observed for product formation in the pyrolysis of 4-methylene-1-pyrazolin-3,3- $d_2$  to methylenecyclopropane.

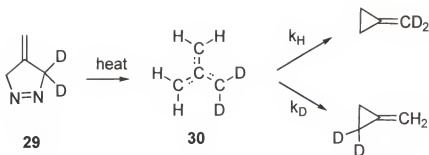


Figure 1-18.  $k_H/k_D = 1.37$ ,  $k_D$  and  $k_H$  are the rates for forming the product by rotating the dideuteriomethylene group and diprotiomethylene group respectively.

A similar normal secondary deuterium isotope effect was observed by Dolbier<sup>61,62</sup> in his studies of [2+2] cycloaddition of 1,1-dideuterio allene, as shown is Figure 1-19

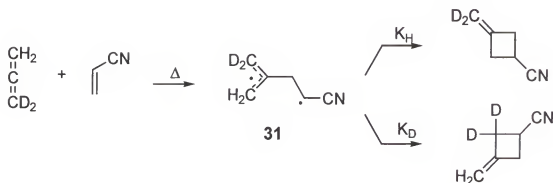


Figure 1-19. [2+2] Cycloaddition of allene and acrylonitrile, the kinetic secondary deuterium isotope effect is  $k_H/k_D = 1.21 \pm 0.02$

The proposed explanation for such a normal isotope effect in a process which converts an  $sp^2$  to  $sp^3$  carbon center was that in the product-determining step, the dideuteromethylene group is slower to rotate out of conjugation to a conformation where ring formation can occur than a diprotiomethylene group.<sup>61</sup> Recent experimental and theoretical examples contributed by Cadwell<sup>63</sup>, Gajewski and Houk<sup>64</sup> again revealed the importance of 'rotational' KIEs. *cis*-Stilbene, as shown in Figure 1-20, thermally isomerizes to *trans* isomer with a rotational kinetic isotope effect of  $1.47 \pm 0.13$ . Again it

is seen that the terminus of the rotating bond with the heavier substituents has less motion in the transition state.

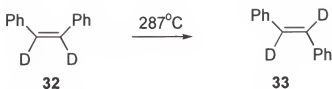


Figure 1-20. Isomerization of *cis*-stilbene.  $k_{\text{H}}/k_{\text{D}}=1.47$

Baldwin<sup>65</sup> studied secondary deuterium isotope effect in the electrocyclic ring closure of 1,3,5-hexatriene (Figure 1-21). He found a  $k_{\text{H}}/k_{\text{D}2} = 0.88 \pm 0.02$  for the two IN protons and  $1.05 \pm 0.03$  for the OUT protons. The difference in the KIEs for the IN and OUT protons in the electrocyclization of hexatriene was attributed by Baldwin to the close proximity of the IN protons in the transition state, resulting in an increase of the force constants due to nonbonding (steric) interactions. An increase in intramolecular nonbonding interactions on passage to the transition state may increase force constant of the IN hydrogens and give rise to the inverse  $k_{\text{H}}/k_{\text{D}}$  effect observed. Calculation at the RHF/6-31G\* level shows reasonable agreement with the experimental results.<sup>67</sup>

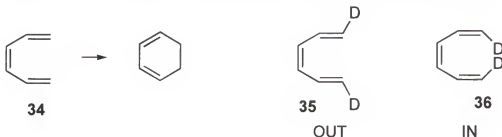


Figure 1-21. Thermal Isomerization Of Hexatriene To 1,3-Cyclohexadiene. Diastereotopically Distinct Secondary Kinetic Isotope Effects Were Found.  $(k_{\text{H}}/k_{\text{D}})_{\text{IN}} < 1$ ,  $(k_{\text{H}}/k_{\text{D}})_{\text{OUT}} > 1$ .

Conversely, normal isotope effects were found for cyclobutene ring opening as shown in Figure 1-22.<sup>66</sup> It was explained by a rehybridization process. Due to different mean bond lengths for hydrogen and deuterium, deuterium atom has a smaller “effective size” as compared to hydrogen. The diastereotopically distinct C3-H inner H and outer H are of different p-character. The overall change in hybridization associated with the reaction is different, which gives rise to different  $k_H/k_D$  values:  $\left(\frac{k_H}{k_D}\right)_{IN} = 1.04 \pm 0.03$  and  $\left(\frac{k_H}{k_D}\right)_{OUT} = 1.15 \pm 0.03$ . These were also confirmed by calculations at the MP2/6-31G\* level.<sup>67</sup>

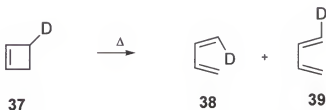


Figure 1-22. Deuterium substituted cyclobutene ring opening. Normal isotope effects were found for producing both isomers, however, they are in different magnitude.

Through this work, the author will discuss a system which will be promising to investigate toquoelectronics of  $6\pi$  electron system, rotational isotope effects, substituent polar effects and the pseudopericyclic phenomena.

## CHAPTER II

### THERMAL REARRANGEMENT OF *O*-VINYL-PHENYLISOCYANATES

#### 2.1 Introduction

The information about the energy and the structure of transition states is crucial to understanding a reaction mechanism. A transition state, according to the Hammond postulate<sup>68</sup>, is regarded as a configuration which lies on an energy profile between the reactants and the product, along a reaction coordinate which is composed of successive structures that change progressively from reactant-like to product-like. The geometry and charge distribution of the transition state (TS) are assumed to be a weighted average of the geometry and charge distribution of the reactant (R) and the product (P). That is, a transition state is situated at a free energy maximum along the reaction path that connects two energy minima. Therefore, an exothermic reaction will possess an "early" transition state which is reactant-like, as shown in Figure 2-1(a). Likewise, an endothermic reaction will possess a "late" transition state which is product-like as shown in Figure 2-1(c). The transition of an ergoneutral reaction should possess "intermediate" character, and lie near the midpoint of the reaction coordinate, Figure 2-1(b).

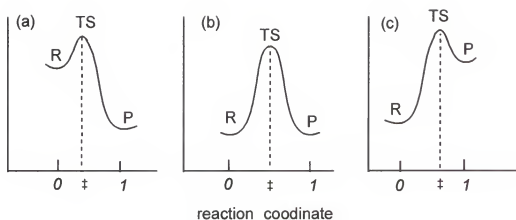


Figure 2-1 Examples of reactions that have reactant-like (“early”) (a), intermediate (“central”) (b) and product-like (“late”) (c) transition states.<sup>69</sup>

It is rather challenging to determine the experimental geometry of a transition state. However, modern quantum mechanical calculations offer the possibility of finding both minima and the transition state. GAUSSIAN and GAMESS programs<sup>70</sup>, guided by one’s chemical intuition, are used to calculate the first and second derivatives of the energy with respect to all geometrical variables; subsequently, the transition structure can be located. The shapes and binding present in transition state from the calculations then can give somewhat quantitative meaning to concepts of “late” or “early” transition states. And especially the energy change to the transition state with varying substitution could be informative to the substituent effects on a reaction.

A boat shaped transition structure was calculated for the thermal (disrotatory) ring closure of *cis*-1,3,5-hexatriene to form 1,3-cyclohexadiene as shown in Figure 2-2.<sup>65</sup> The partial single-bond length is 2.24Å and the double bond lengths are in the range of 1.39 to 1.40Å. Two hydrogen atoms are in close proximity at the bonding termini, which *destabilizes* the transition structure to some extent. The MP2/6-31G\* activation energy

of 26 kcal/mol<sup>71</sup> for the ring closure is in good agreement with experimental value of 29 kcal/mol.<sup>72</sup>

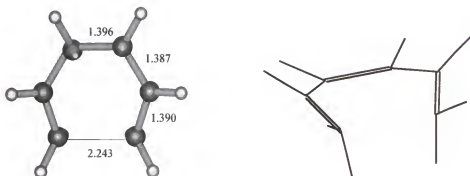


Figure 2-2. Boat-shaped transition structure for a 6- $\pi$  electron disrotatory electrocycization of hexatriene (RHF 6-31G\*)

Woodward and Hoffmann described the thermal 6- $\pi$  1,3,5-triene to 1,3-cyclohexadiene reaction as occurring through an orbital symmetry allowed, disrotatory pathway<sup>2</sup>. It was later demonstrated experimentally<sup>73</sup>. The cyclized products are formed in a stereospecific fashion with substituents at the terminal carbons of the triene rotating in opposite directions (disrotatory) as illustrated in Figure 2-3.

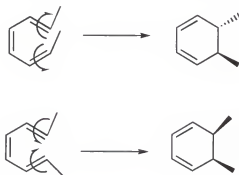


Figure 2-3. Stereo Specific Thermal Disrotatory 6- $\pi$  Electrocycization

The concept of torquoselectivity, which was developed by Houk to rationalize the strong electronic control of C3 and C4 substituents upon ring opening of cyclobutene, was well studied experimentally and theoretically.

Surprisingly, experimental probing of torquoelectronic effects on a 6- $\pi$  system had never been reported before our work. Its applicability has also been less explored theoretically. There might be two possible reasons that it is less investigated:

1) Observing torquoelectronics in thermal ring-opening of a "classic" 6 $\pi$  system is unlikely, since the thermodynamics for conversion of 1,3-cyclohexadiene to 1,3,5-hexatriene are unfavorable. As shown in Figure 2-4. Conversion of 1,3,5-hexatriene to 1,3-cyclohexadiene is 15 kcal/mol exothermic.<sup>74</sup>

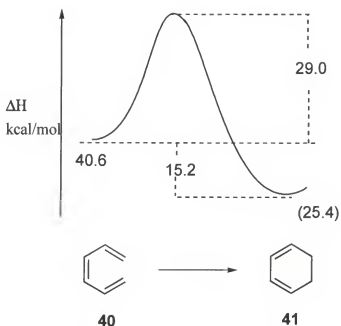


Figure 2-4. Enthalpy Diagram for Z-1,3,5-hexatriene and 1,3-cyclohexadiene.

2) In the transition state of the conversion of 1,3,5-hexatriene and 1,3-cyclohexadiene, the distance of the two hydrogen is  $1.858\text{\AA}^{30}$ , while the sum of van der Waals radii of two hydrogens is  $2.40\text{\AA}$ . The repulsion between the two atoms is so significant that steric effects overcome the electronic effects. It was also found that a single *cis*-methyl group at C1 was sufficient to increase the activation energy for electrocyclization by 3-4 kcal/mol,<sup>75</sup> while *cis*-methyl substituents at both C1 and C6 totally inhibited the thermal cyclization. Due to the steric demands in the transition state, terminal *cis*-substituents as small as fluorine are strongly inhibiting to the electrocyclic process (*vide supra*)<sup>31,32</sup>.

Thus, imperatively, an investigation of torquoelectronic selectivity demands a system which can minimize, if not eliminate, such steric interactions, so that purer electronic effects can be assessed.

### 2.1.1 Development of a suitable 6- $\pi$ electrocyclic system

In pursuit of an electrocyclization system which would allow unambiguous evaluation of torquoselectivity on a 6- $\pi$  electron system, we originally conceived of systems with a cumulene at one of the 6- $\pi$  system termini, as shown in Figure 2-5, in the hope that these precursors would be stable enough to be prepared but could be cyclized thermally at appropriate temperatures. By selecting an appropriate X group, the selectivity of *E*- vs *Z*-cyclization could then be observed. Unfortunately, such ketene and allene precursors proved to be synthetically inaccessible after brief exploratory efforts.

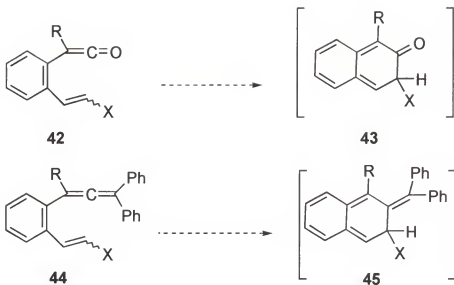


Figure 2-5. Two original systems, of which the precursors were synthetically challenging.

We then focused our attention on an alternative 6- $\pi$  system with the terminal cumulene function being an isocyanate group, as shown in Figure 2-6. The absence of *cis* (or *trans*) substituents at the carbonyl carbon of the isocyanate group could effectively minimize or eliminate the usual steric effects.

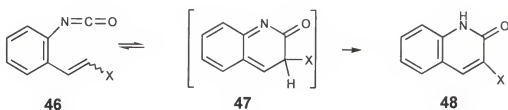


Figure 2-6 The 6- $\pi$  System which rearranged smoothly at *ca.* 110°C.

It was proposed that when the precursor rearranged, it would form a cyclized amide-type intermediate (in the bracket) which would tautomerize, perhaps by a [1,5] suprafacial hydrogen shift, to the fully aromatic product, 2-quinolinone.

It should be noted that the kinetic experiments would be done on the ring-formation instead of the ring-opening as in the  $4\pi$  torquoelectronic studies. By the laws of thermodynamics, every elementary reaction must be reversible; this concept is known as the *principle of microscopic reversibility*.<sup>76</sup> It asserts that the mechanism for any reaction is the same in both directions. This is logically the case: for if a lower-energy pathway were available for the reverse reaction, then it must also be a lower-energy pathway for the forward reaction, and it thus follows that both paths must traverse exactly identical routes via an identical transition state. Following this logic, the same selectivity should be exhibited in our isocyanate system whether we are studying the ring-opening or the cyclization process. Practically, it was more convenient to study the kinetic of the cyclization process. In a reverse ring-opening process, rotating the X group inwardly produces the *cis* isomer, while rotating the X group outwardly produces the *trans* isomer as presented in Figure 2-7.

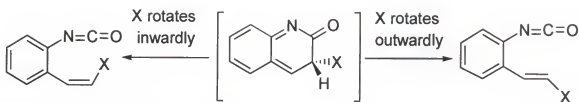
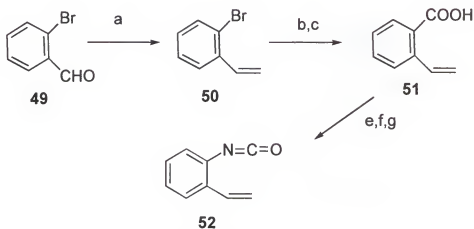


Figure 2-7. Two possible pathways when the ring 'opens', which are the reverse process of the ring-closure.

### 2.1.2 Thermal rearrangement of the parent system. A mechanistic approach



a)  $\text{PPh}_3\text{CH}_3\text{Br}/n\text{-BuLi}$  then  $\text{H}_2\text{O}$ ,<sup>77</sup> b)  $\text{Mg}/\text{ether}$ ,  $\text{CO}_2$  then  $\text{H}_2\text{O}$ ,<sup>78</sup> d)  $(\text{COCl})_2$  in  $\text{CH}_2\text{Cl}_2$ ,<sup>79</sup> e)  $\text{NaN}_3$  (sat, aq)  $0^\circ\text{C}$ ,<sup>80</sup> f)  $\text{C}_6\text{D}_6$ , RT

Figure 2-8. Synthesis of Parent System, 52

**Synthesis of *o*-vinyl-phenylisocyanate.** In order to test the feasibility of our proposal and to best understand this novel rearrangement, the parent system, *o*-vinyl phenyl isocyanate, was synthesized in 6 steps starting from a commercially available precursor, 2-bromobenzaldehyde. Performing a Wittig reaction on the aldehyde yielded 2-bromo styrene. This was followed by a Grignard reaction which was quenched with carbon dioxide to give 2-vinyl benzoic acid. (Attempts to exchange the bromide with lithium using *t*-butyllithium proved to be unsuccessful. The reaction mixture appeared to polymerize.) The acid was converted into the acid chloride by treating with oxalyl chloride in methylene chloride. The acid chloride was then dissolved in dry acetone and treated at zero degrees with saturated aqueous sodium azide to yield the acyl azide. (The

acid chloride reacts with azide anion rather than with water because this anion is more nucleophilic than water molecule.)

The idea of carrying out the Curtius rearrangement from the acyl azide to the isocyanate in refluxing benzene or toluene in the conventional way,<sup>81</sup> did not seem to be appropriate, since the isocyanate product would probably undergo cyclization during the course of thermal process. Fortuitously, the isocyanate substrate was able to be prepared at much lower temperature (room temperature) with a reasonably longer reaction time (10-12 hours) in  $C_6D_6$ .

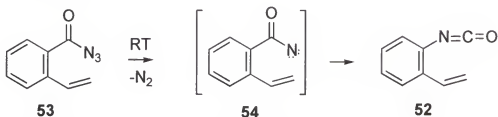
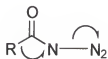


Figure 2-9. Curtius rearrangement of acyl azide to isocyanate.

The mechanism of the Curtius rearrangement, even though a thoroughly studied reaction, is still quite ambiguous.<sup>82</sup> After the departure of  $N_2$ , an electron deficient nitrene, in which the nitrogen has only a sextet of electrons, is believed to be formed, although nitrene intermediacy has not yet been unambiguously proven. Lwowski<sup>83,84</sup> argued that Curtius rearrangement does not involve a nitrene intermediate, but proceeds via a concerted mechanism, where rearrangement occurs simultaneous with the loss of nitrogen:



From our point of view, the exact nature of the mechanism is immaterial, as long as we get a smooth, clean and high yield reaction, which we did.

**Kinetic Study on electrocyclization of *o*-Vinyl Phenylisocyanate.**

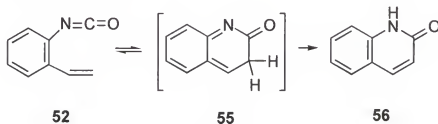


Figure 2-10. Thermal rearrangement of *o*-vinyl phenylisocyanate, an electrocyclization followed by a tautomerization.

We believe that the isocyanate precursor rearranges in two steps (Figure 2-10), the first being the reaction we are interested in, an electrocyclization to form an amide-type intermediate [55]. This step is apparently followed by a rapid prototropic tautomerization to form the quinolin-2-one [56]. The loss of aromaticity of the benzene ring in the first step and the regaining of the system's aromaticity in the second step make it likely that the first step (electrocyclization) should have the higher activation energy and therefore be the rate-determining step. This premise has been determined to be true by experimental studies which will be discussed later. Thus, as we had hoped, a kinetic study of this overall conversion should provide information only concerning the rate-determining electrocyclization step.

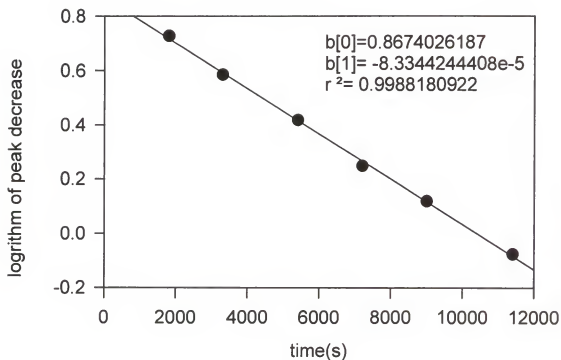


Figure 2-11 Determining the rate of rearrangement of **52** at 108.6 °C. The slope of the fitted line is  $-8.33(0.14) \times 10^{-5}$ , is tantamount to a rate constant of  $8.33(0.14) \times 10^{-5}$ ,  $r^2$  is the square of the regression.

The thermolysis of **52** was initially studied at 108.6°C in  $C_6D_6$ , and the cyclization reaction was found to behave very well as a unimolecular reaction. A plot of logarithm of the relative peak decrease, which is proportional to the consumption of the starting material, *versus* time, gave a straight line. (The plot being shown in Figure 2-11), which suggests a first order reaction mechanism.<sup>86</sup>



$$\text{rate} = \frac{d[A]}{dt} = k[A]^1 \quad (2-1)$$

$$\int \frac{d[A]}{[A]} = \int k dt$$

$$\ln\left(\frac{[A]_0}{[A]_t}\right) = kt$$

$$\ln[A]_t = -kt + \text{constant}$$

Thus, for a first order reaction, a plot of logarithm of the concentration at time  $t$  versus the time  $t$  fits a straight line. The slope of the line is  $-k$ , negative value of the rate constant.

Table 2-1. Rate Constants at different temperatures for the rearrangement of **52** to **56**.

T(°C)	103.1	106.8	109.5	112.6	115.7
k(s <sup>-1</sup> )	5.81(.13)×10 <sup>-5</sup>	8.33(.14)×10 <sup>-5</sup>	9.83(.37)×10 <sup>-5</sup>	1.27(.09)×10 <sup>-4</sup>	1.50(.02)×10 <sup>-4</sup>

The rate constants for the rearrangement of parent isocyanate (**52**) to (**56**) at various temperatures are listed at Table 2-1. The activation parameters for this reaction, which are listed in Figure 2-8, were obtained from the Arrhenius and Eyring equations<sup>45</sup>. The activation energy  $E_a$  and  $\log A$  value for the reaction were obtained from the Arrhenius equation (Equation 2-2).<sup>86</sup>

$$k = A \exp\left(-\frac{E_a}{RT}\right) \quad (2-2)$$

$$\ln(k) = 2.303 \log A - \frac{E_a}{RT}$$

Where  $k$  is the observed reaction rate constant,  $A$  is the preexponential factor. The value of the preexponential factor is related to the entropy change ( $\Delta S^\ddagger$ ) occurring during the activation process.  $R$  is the gas constant (8.31 J K<sup>-1</sup> mol<sup>-1</sup>) and  $T$  is the temperature in degrees Kelvin. The Arrhenius equation rearranges to  $\ln(k) = \ln 10 \times \log A -$

$E_a/RT$ . A linear least square regression plot of  $\ln(k)$  versus  $1/T$  yielded the  $E_a$  and  $\log A$  from the slope and intercept respectively of the fitted line. It should be noted that unimolecular reactions that occur by way of cyclic transition states, typically have negative entropies because of the loss of rotational degrees of freedom associated with the highly ordered transition state.<sup>46</sup> For such unimolecular reactions,  $\log A$  value typically lie between 12-14.<sup>47</sup>

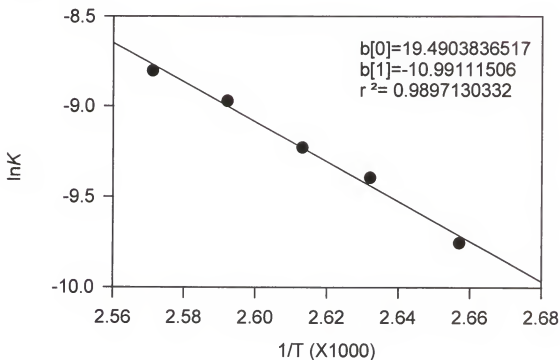


Figure 2 -12. Arrhenius Plot of **52** to **56**. Slope is -10.99 and the intercept is 19.49.  $E_a = 10.99 \times 1000R = 22$  kcal/mol,  $\log A = 19.49 \log(e) = 8.4$

The enthalpy of activation,  $\Delta H^\ddagger$ , and entropy of activation,  $\Delta S^\ddagger$ , of a reaction can be obtained from the Eyring equation (Equation 2-3)<sup>86</sup>.

$$k = \left( \frac{kT}{h} \right) \exp\left( -\frac{\Delta H^\ddagger}{RT} \right) \exp\left( \frac{\Delta S^\ddagger}{R} \right) \quad (2-3)$$

Where  $k$  is Boltzmann constant ( $1.38 \times 10^{-23} \text{ J K}^{-1}$ ),  $h$  is Planck's constant ( $6.63 \times 10^{-34} \text{ J s}$ ). The Eyring equation rearranges to Equation 2-4. A linear least squares regression plot of  $\ln(k/T)$  versus  $1/T$  yields  $\Delta H^\ddagger$  and  $\Delta S^\ddagger$  from the slope and the intercept respectively of the fitted line.

$$\ln\left(\frac{k}{T}\right) = \ln\left(\frac{k}{h}\right) + \frac{\Delta S^\ddagger}{R} - \frac{\Delta H^\ddagger}{R} \frac{1}{T} \quad (2-4)$$

$$\text{intercept} = \ln\left(\frac{k}{h}\right) + \frac{\Delta S^\ddagger}{R}, \quad \text{slope} = -\frac{\Delta H^\ddagger}{R}$$

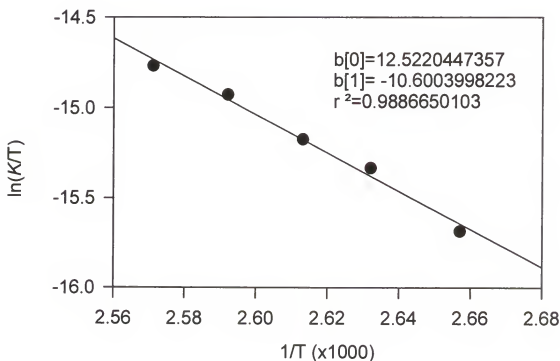


Figure 2-13. Eyring Plot of the parent system, **52** to **56**

We found no significant differences in the kinetic behavior of **52** when the kinetic studies were carried out in 10% pyridine (10% of pyridine with respect to the molar concentration of the substrate) as shown in Table 2-3. This was a solid indication that the

tautomerization step should *not* be the rate determining step (in that event, the base would certainly have sped up the proton transfer in the tautomerization step). The pyridine result also indicated that there must not be significant acid catalysis involved in the process. As one can see from Table 2-3, a better Arrhenius behavior was observed in the presence of pyridine.

Table 2-2 The rate constants obtained with 10% pyridine added

T(°C)	103.1	109.4	115.7
k(s <sup>-1</sup> )	$5.81(.68) \times 10^{-5}$	$9.77(.45) \times 10^{-5}$	$1.73(.09) \times 10^{-4}$

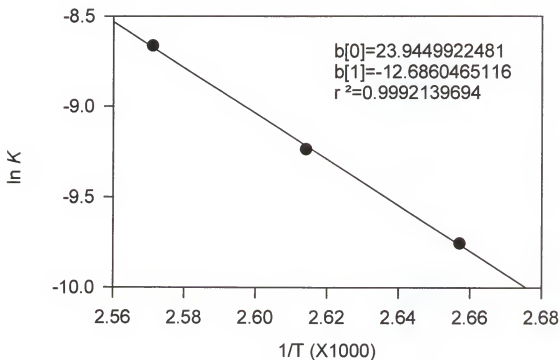


Figure 2-14. Arrhenius plot from the data run with pyridine

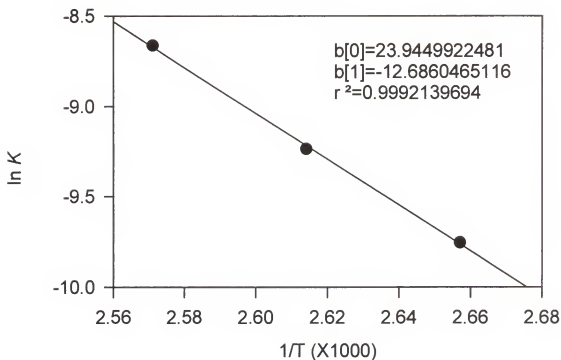


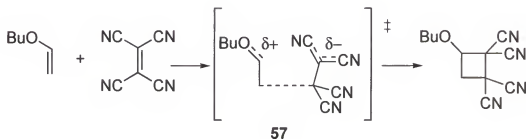
Figure 2-15. Eyring Plot from the data run with pyridine

Table 2-3. Comparison of activation parameters obtained for both without and with pyridine

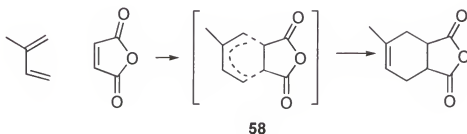
	logA (s <sup>-1</sup> )	Ea (kcal/mol)	$\Delta H^\ddagger$ (kcal/mol)	$\Delta S^\ddagger$ (cal/mol K)	$\Delta G^\ddagger$ (kcal/mol)
without pyridine	8.4 ± .7	23 ± 1	21 ± 1	-22 ± 1	29 ± 1
with pyridine	10.4 ± .2	25.2 ± .4	24.5 ± .5	-13 ± 1	29.6 ± .5

The kinetic experiment was repeated in deuterated acetonitrile (CD<sub>3</sub>CN with dielectric constant, 38), a much more polar solvent than deuterated benzene (C<sub>6</sub>D<sub>6</sub> with dielectric constant, 2.3). With acetonitrile as solvent, the observed rate constant at 109.7 °C is  $2.75 \times 10^{-4}$ , while the rate constant is  $9.83 \times 10^{-5}$  using C<sub>6</sub>D<sub>6</sub> as solvent. The rate acceleration in CD<sub>3</sub>CN with respect to C<sub>6</sub>D<sub>6</sub> is  $k_{\text{CD}_3\text{CN}}/k_{\text{C}_6\text{D}_6} = 2.7$ . The solvent effect is

rather small, which clearly points to a transition state in which solvation is not much different from that of the reagent. This result is consistent with a concerted process for the rearrangement, and rules out the participation of zwitterionic intermediates or highly polar transition states in the mechanism of the reaction. Typical examples of solvent effect are shown in Figure 2-16.



(a)  $\frac{k_{\text{MeCN}}}{k_{\text{C}_6\text{H}_{12}}} = 10,800$



(b)  $\frac{k_{\text{MeCN}}}{k_{\text{C}_6\text{H}_{12}}} = 1.5$

Figure 2-16. (a) Large solvent effect, highly polar transition state is involved.<sup>87</sup> (b) Nearly no solvent effect, a typical Diels-Alder reaction.<sup>88</sup>

The lack of dependence of rate on the presence of pyridine or the polarity of solvent indicates that the whole process is concerted.

In a concurrent computational investigation of the electrocyclozation of **52** to **55**, as shown in Figure 2-17, Bartberger and Dolbier<sup>89</sup> have calculated (at MP26-31G\*\*/RHF6-31G\* level of theory) the activation free energy for the cyclization process

to be 29.80 kcal/mol, a number which is in an excellent agreement with our observed experimental result of 29.6 kcal/mol (with pyridine added). Based on their calculations, it was found that the conversion of **52** to intermediate **55** is 19.2 kcal/mol endothermic.

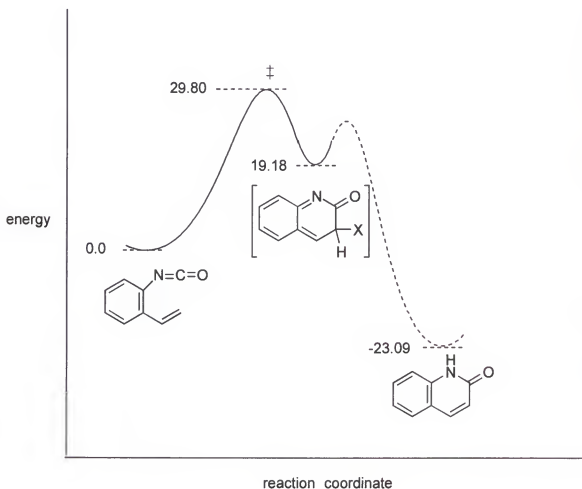


Figure 2-17. Energy diagram of the rearrangement. Energies are in kcal/mol at MP2/6-31G\*\*/RHF6.31G\* level, corrected by 0.8929 ZPE

The computational transition structure for the cyclization process is shown in Figure 2-18. It did not prove to be that of a classic, disrotatory, 6- $\pi$  electrocyclic process. Instead, the isocyanato function remained essentially coplanar with the benzene ring ( $-3.7^\circ$  out of plane) with the  $\text{N}=\text{C}=\text{O}$  bend angle being  $139.2^\circ$  in the transition state, and

the vinyl group being twisted ( $28.2^\circ$  out of plane). The terminal p-orbital appeared to be favorably oriented

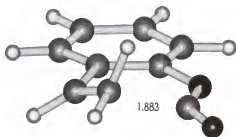


Figure 2-18. Transition Structure Of The Rearrangement

to overlap with the carbon p-orbital of the *carbonyl*  $\pi$ -bond, (Figure 2-18 and 2-19), rather than with that of the C=N  $\pi$ -bond, which would have been the case for the classic, disrotatory process. The overlapping orbitals are mutually *orthogonal*. Such a transition

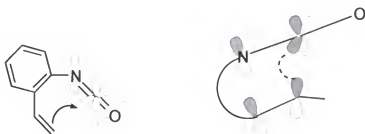


Figure 2-19. Alkenic p orbital interacting with orthogonal p orbital of carbonyl sp carbon. The plain loop represents the connection between isocyanate and the alkenyl group and the dashed line represents the interaction between the alkenic p orbital and the p orbital of the sp carbon.

structure permits the maintenance of conjugation within the phenyl isocyanate system, where one of the carbonyl non-bonded electron pairs becomes a bonding pair as the new  $\sigma$ -bond is formed. This description is consistent with Lemal's definition of a *pseudopericyclic* process (*vide supra*)<sup>34,35</sup> as one in which "nonbonding and bonding atomic orbitals interchange roles." The free energy of activation is 10.7kcal/mol for the

reverse ring-opening process. It is a value which is significantly lower than that of a classical pericyclic reaction (*ca.* 32-36 kcal/mol)<sup>2</sup>. That is, it is also energetically consistent with the *pseudopericyclic* character.

More interestingly, the “transition” from the starting material to the transition state requires only *one* terminus to rotate to reach the “*orthogonality*”, which in turn forms the C-C bond, a process which is very different from that of the classical pericyclic reactions. This *monorotation* should give rise to potential cleaner selectivity (*torquoelectronic*) when there is a substituent attached on the  $\beta$ -position of the vinyl group.

A normal C-C single bond length range is 1.46-1.62Å<sup>90</sup> and it is found to be 1.524Å for the formed C-C bond of the intermediate, shown in Figure 2-20. A partially formed broken (or forming) C-C single bond length ranges from 2.1-2.3Å<sup>90</sup> for an ordinary pericyclic reaction. The partial C-C bond (1.881Å) in the transition state of this isocyanate system is shorter than that of the typical pericyclic cyclization of *o*-divinylbenzene (2.118Å)<sup>89</sup>, and it is shorter still than that of 1,3,5-hexatriene ring-closure (2.24Å)<sup>65</sup>. This is an indication of the lateness of the transition state which is unsurprisingly consistent with the endothermicity of the reaction (calculated  $E_{a(rxn)}$ =19.18kca/mol).

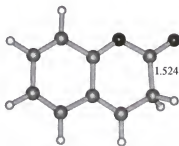


Figure 2-20. Geometry of the intermediate product (2) (strictly planar)

For a comparison, the transition structure of the “classical” pericyclic cyclization of *o*-divinylbenzene is shown in Figure 2-21<sup>89</sup>. The calculated partial single-bond length is 2.118Å and the dihedral angles for both vinyl groups are 33.0°. Rotation of *both* vinyl groups and their twisting out of plane of the phenyl ring allow the terminal p-orbitals to be favorably oriented to overlap with each other, resembling a boat-like transition state. In this transition state, there is congruence between orbital symmetry characteristics of reactant and product, or, to put it in a prosaic way, there is cyclic orbital overlap around the ring of interacting atoms.

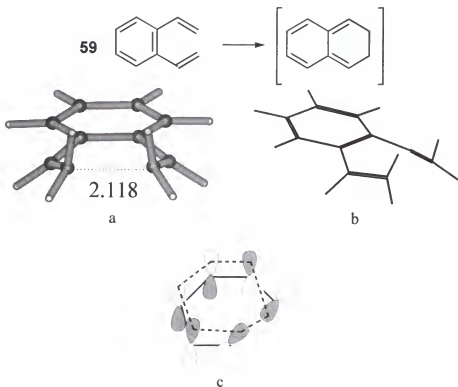


Figure 2-21. a) Transition structure of pericyclization of *o*-divinylbenzene calculated at MP2/6-31G\*\*/RHF6-31G\* level.  $E_a=37.16$  kcal/mol, a) Simplified transition state with carbon and hydrogen skeleton, and c) More simplified transition state of showing the *cyclic* orbital interaction (the benzene ring is arbitrarily omitted)<sup>2</sup>.

### 2.1.3 Conclusions

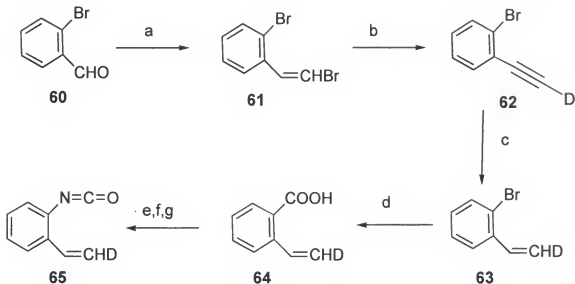
It appears that a promising system has been developed for evaluating substituent effects on pericyclic reactions. The steric repulsion which was found in classic 1,3,5-hexatriene to 1,3-cyclohexadiene electrocyclization process should be minimized due to the absence of the substituent at the isocyanate terminus. That is, this system should be free of the usual steric effects which have impeded past efforts to examine  $6\pi$  electron torquoselectivity.

From the geometry of the transition state, there is a mutually orthogonal interaction between the alkenic  $p$  orbital and the  $p$  orbital of the  $sp$  carbon of the isocyanate. A pseudopericyclic phenomenon was then recognized. The fact that the low activation barrier for the reverse (ring opening) reaction has only 10.7 kcal/mol (Figure 2-17), a number which is much lower than that for a normal pericyclic reaction (in the neighborhood of 30 kcal/mol), should not be surprising in light of the pseudopericyclic character.<sup>43</sup> There is *no closed loop* of interacting orbitals because there is a "disconnection" in the orbital overlap around the complete ring of forming(breaking) bond due to orthogonal orbitals. The relative low barrier is attributable to the pseudopericyclic nature of the transition state, in which the lack of cyclic orbital overlap minimizes electron-electron repulsion.

## 2.2 Investigating the Isotope Effects at the $\beta$ -Position

The replacement of one or more atoms in a reacting system by others of their respective isotopes is one of the most subtle structure perturbations which may be made. To a good approximation, isotope substitution does not affect the potential energy surface of the molecule, nor does it perturb the electronic energy levels. It is only those properties that are dependent upon atomic masses which are affected. For chemical purposes, the most recognized perturbation can be considered to be the vibrational frequencies. Each vibrational frequency, and hence the energy, depends on the masses of the atoms vibrating, and this will vary with the isotopic species. Vibrational energy will usually change during the course of reaction, or between reagent and transition states, since some bonds are in course of being broken or made, and their associated frequencies will be affected. Isotopic substitution should therefore affect reaction rate<sup>91</sup>. The most common isotopic substitution is D for H, in which case the relative mass change is the greatest. Another somewhat less recognized source which would affect reaction rate is the rotation about the C-C bond<sup>60,61,63</sup>. When the carbon which rotates is substituted by H or D, the rotational motion could be affected. Isotopic substitution should therefore also affect the reaction rate. Changes of reaction rate which are brought about by isotopic substitution are known as kinetic isotope effects and carry mechanistic information. The latter case, the rotational isotope effects, will be examined and used as a tool to test the mechanism of the newly developed rearrangement.

## Preparation of the Precursor.



a)  $\text{Ph}_3\text{P}^+\text{CH}_2\text{BrBr}^-/\text{KO}^t\text{Bu}/\text{THF}$ <sup>92</sup>, b)  $\text{KO}^t\text{Bu}$  (2eq)/THF then  $\text{D}_2\text{O}$ <sup>93</sup>, c) Pd on calcium carbonate/methanol,  $\text{H}_2$ <sup>94</sup>, (*cis* : *trans* : non-deuterated = 50 : 20 : 30), d) Mg/ether,  $\text{CO}_2$  then  $\text{H}_2\text{O}$ , e)  $(\text{COCl})_2$  in  $\text{CH}_2\text{Cl}_2$ , f)  $\text{NaN}_3$  (sat, aq),  $0^\circ\text{C}$ , g)  $\text{C}_6\text{D}_6$ , RT.

Figure 2-22. Preparation of  $\beta$ - $d_1$ -vinyl phenylisocyanate.

The precursor was synthesized in 7 steps with a Wittig reaction as the first step.

A mixture of triphenyl phosphine ( $\text{Ph}_3\text{P}$ ) and dibromomethane in refluxing toluene produced the ylid precursor (bromo-methyl) triphenylphosphonium bromide ( $\text{Ph}_3\text{P}^+\text{CH}_2\text{BrBr}^-$ )<sup>95</sup> in 63.4% yield. 2-Bromo benzaldehyde underwent a Wittig reaction using potassium *t*-butoxide as the base to give 2-bromo- $\beta$ -bromostyrene, which was treated with potassium *t*-butoxide to form 2-bromo phenylacetylene by eliminating HBr. The elimination reaction was carried out with two equivalents potassium *t*-butoxide, and was quenched with deuterated water ( $\text{D}_2\text{O}$ ) to yield 2-bromo phenylacetylene- $d_1$ . Deuterium was incorporated into 92% of the product. This acetylene was reduced under Lindlar conditions to yield a 50 : 20 : 30 ratio of *cis* : *trans* : non-deuterated styrene. The

unexpected formation of *trans* deuterated product and the increase of non-deuterated percentage in the product could be rationalized by the mechanistic depiction in Figure 2-23<sup>96</sup>. It is rationalized that both the phenyl and alkenic groups are coordinated to the catalyst after the Lindlar hydrogenation. There is a reversible equilibrium between the olefin substrate complex and the alkyl complex, during which the exchange of the terminal proton occurs.

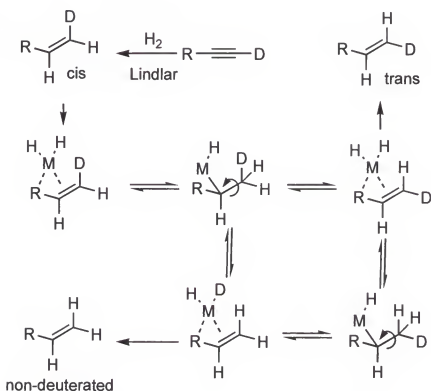


Figure 2-23. Mechanistic rationale for deuterium exchange at the terminal position<sup>96</sup>.

Initially, there were two other approaches attempted to build up the deuterated system. Neither of them proved to be synthetically viable, as briefly illustrated in Figure 2-24a and Figure 2-24c.

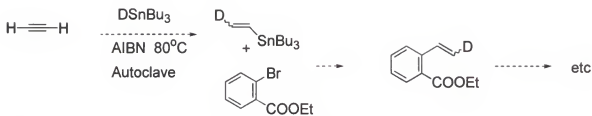


Figure 2-24a One of the attempts to the deuterated system.

In which case, vinylation of tri-*n*-butyltin deuteride was not successful, even though under the same conditions, tri-*n*-butyltin hydride worked<sup>97</sup>. To account for the frustrating results, it was proposed that the stronger Sn-D bond than Sn-H inhibits the chain transfer in the last step as shown in Figure 2-24b.

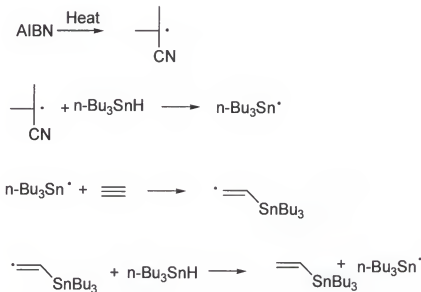


Figure 2-24b. The mechanism of vinylation.

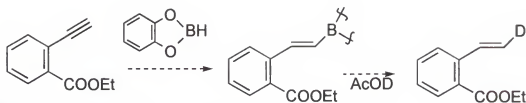


Figure 2-24c Hydroboration, another unsuccessful attempt.

The above reaction (Figure 2-24c) did not work as expected possibly due to the presence of the Lewis base, the electron withdrawing ester group at the *ortho* position. This group makes the acetylene electron deficient, which in turn could make the electrophilic addition of catecholborane improbable.

#### Kinetic Isotope Effect Study Of The Deuterated System.

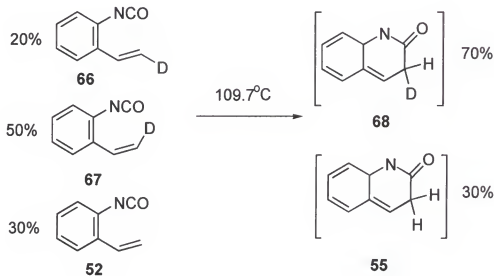


Figure 2-25. Electrocyclization Step of the Rearrangement.

With the unequal mixture of labeled isocyanates, their rearrangements were run all together so that the kinetics conditions were identical for all the isomers. The kinetics

were run at 109.7 °C in C<sub>6</sub>D<sub>6</sub>. The reaction conditions for three isomers were identical since they were in one-pot vessel.  $k_{\text{cis-D}} = 9.2(0.4) \times 10^{-5}$ ,  $k_{\text{trans-D}} = 9.5(0.6) \times 10^{-5}$  and  $k_{\text{non-D}} = 1.02(0.05) \times 10^{-5}$ ,  $\frac{k_H}{k_{\text{cis-D}}} = 1.11 \pm 0.07$  and  $\frac{k_H}{k_{\text{trans-D}}} = 1.07 \pm 0.08$ . Normal secondary deuterium kinetic isotope effects were observed for both the *cis* and the *trans* isomers.

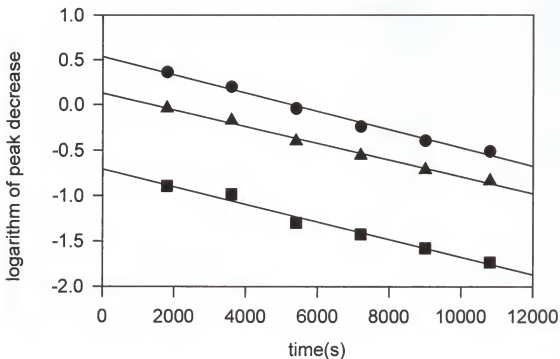


Figure 2-26. Determining the isotope effect of the rearrangement. ● The non-deuterated substrate, intercept 0.533, slope  $-1.01(0.05) \times 10^{-4}$ ,  $r^2=0.989$ ; ■ the *trans*-deuterated substrate, intercept -0.709, slope  $-9.51(0.60) \times 10^{-5}$ ,  $r^2=0.979$ ; ▲ the *cis*-deuterated substrate, intercept 0.126, slope  $-9.19(0.40) \times 10^{-5}$ ,  $r^2=0.993$

The H/D ratios of the starting material (70% deuterated) and the product (50% deuterated) were determined by <sup>1</sup>HNMR (Unity-500). Based on the NMR analysis, an

isotope effect of  $\frac{k_H}{k_D} = 2.5$  (refer to Figure 2-27) was found for the tautomerization step.

The marked difference of the kinetic isotope effect for the cyclization step

$$\left( \frac{k_H}{k_{cis-D}} = 1.11 \pm 0.07 \text{ and } \frac{k_H}{k_{trans-D}} = 1.07 \pm 0.08 \right) \text{ and the isotope effect for the}$$

tautomerization step ( $\frac{k_H}{k_D} = 2.5$ ) clearly indicated that the rate determining step and the

product determining step were different<sup>98</sup>, and this is another indication that the

electrocyclization is the rate determining step. Moreover, if the second step *was* the rate

determining step, identical isotope effects should be observed for both *cis* and *trans*

isomers and it should give rise to an appreciably larger isotope effect since the carbon-

hydrogen bond is ruptured at this stage. The first step of the reaction could not be

expected to give large isotope effect because although the carbon-hydrogen bond is

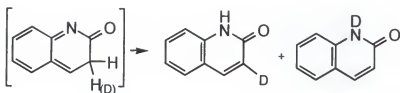
certainly changed, it is not ruptured. The observed KIE's suggested that the two step

mechanism is real and first step is rate-determining, with the overall reaction having a

weak kinetic isotope effect.

Assuming that  $x$  percent of the deuterated precursor goes to the "non-deuterated"

product,



$$\frac{H}{D} = \frac{30\%}{70\%}$$

$$70\%(1-x)$$

$$70\%x + 30\%$$

$$\frac{70\%x + 30\%}{70\%(1-x)} = \frac{50\%}{50\%}$$

$$x = 0.286$$

$$\frac{k_H}{k_D} = \frac{1-x}{x} \approx \frac{2.5}{1}$$

Figure 2-27. Determining the isotope effect of the second step. Starting from a 50:20:30 mixture of *cis*, *trans* and non-deuterated isocyanates, the amide-type intermediate should be a 70:30 mixture deuterated and non-deuterated. <sup>1</sup>HNMR showed that when the intensity of proton from non-deuterated product is 0.36(86.74, d), that from the deuterated was 0.35(87.82, s). That is, 50% of the product was deuterated.

In conclusion, the cyclization is the rate determining step and the tautomerization is a fast and product determining step.

According to the analysis by Streitweiser<sup>59</sup>, it is generally accepted the change of an sp<sup>2</sup>-hybridized center with a low C-H bending frequency to an sp<sup>3</sup>-hybridized center with high C-H bending frequency leads to an inverse kinetic isotope effect ( $k_H/k_D < 1$ ). This analysis falls apart in the electrocyclizations where more than a simple change in hybridization is involved, as in Baldwin's kinetic study on hexatriene cyclization. The protons attached to the same carbon, but in different environments, gave distinct SKIEs. This isotope effect was explained in terms of a "steric deuterium isotope" (*vide supra*)<sup>65</sup>.

When there is no substituent attached on the other terminus, the nonbonding interactions which were observed by Baldwin should be minimized. The smaller "effective size" of deuterium which is responsible for a "steric deuterium isotope" effect should play no role in the observed kinetic isotope effect for this isocyanate rearrangement. During the course of the reaction (or, between the reagent and transition state), the terminal methylene group changes from coplanar with the methine, to virtually orthogonal to it. Thus, similar mass effects to those observed in Crawford's and Dolbier's studies should be seen<sup>60,61,62</sup>. It was not surprising that an inverse isotope effect which would be attributable to sp<sup>2</sup> to sp<sup>3</sup> rehybridization, was not observed. Instead,

normal secondary deuterium kinetic isotope effects, which were interpreted as arising mainly from *rotational* motions of isotopic substituents, were observed. The terminus of the rotating bond with the *heavier substituent has less motion in the transition state*. For this reason, both *cis* and *trans* hydrogens led to normal kinetic isotope effects ( $k_H/k_D > 1$ ).

The kinetic study on the deuterated system also proved that the equilibrium between the *cis* and *trans* deuterated isomer via the cyclized intermediate did not exist. The ratio of the two isomers stayed appreciably constant (*cis* : *trans* = 50:20) during the course of the study. Since there is nearly zero difference in the ground state stabilities between the two deuterated isomers, if there *was* an observable reversibility (Figure 2-28), the ratio of the two should reach to 1:1, and very nice first order kinetic behaviors (as shown in Figure 2-26) for all the isomers would not have been observed.

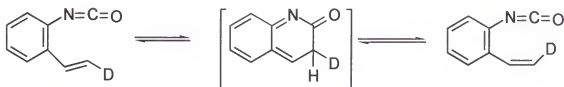


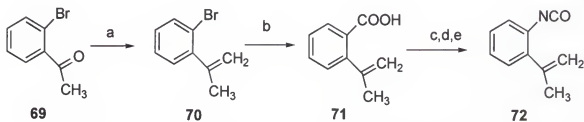
Figure 2-28. The non-existent "equilibrium" between two isomers.

### 2.3 Polar Effects of the $\alpha$ -Substitutions

It was not surprising to obtain a small solvent effect on this pseudopericyclic reaction. The reaction is insensitive to the solvent polarity because there is little separation of charge from the reactant to the transition state. However, the intrinsic polar effect of a substituent could be substantial. Since an electron donor-acceptor arrangement in the reactant will affect the polarity of a transition state, polarity of a substituent can be regarded as one of the important factors in forming/breaking the C-C bond<sup>99</sup>. It was therefore of great curiosity to observe the substituent polar effects on this rearrangement.

#### 2.3.1 Thermal rearrangement of iso-propenyl phenylisocyanate

##### Synthesis of the precursor.



a)  $\text{PPh}_3\text{CH}_3\text{Br}/n\text{-BuLi}$  then  $\text{H}_2\text{O}$ <sup>77</sup>, b)  $\text{Mg}/\text{ether}$ ,  $\text{CO}_2$  then  $\text{H}_2\text{O}$ <sup>78</sup>, d)  $(\text{COCl})_2$  in  $\text{CH}_2\text{Cl}_2$ , e)  $\text{NaN}_3$  (sat, aq),  $0^\circ\text{C}$ , f)  $\text{C}_6\text{D}_6$ , RT

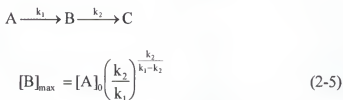
Figure 2-29. Preparation of the  $\alpha$ -methyl Precursor

With the methodology of synthesizing the parent precursor in hand, building up the *o*-isopropenyl phenylisocyanate became straight forward. By performing a Wittig reaction with commercially available 2-bromo acetophenone, 1-bromo-2-isopropenyl

benzene was made in 65% yield. The bromide was converted to 2-isopropenyl benzoic acid via a Grignard reaction with Mg/ether and quenching with carbon dioxide to give 71% yield of product. The acid was converted to the isocyanate using the same method used for the parent system.

**Kinetic Study on Electrocyclization of 2-iso-propenyl Phenylisocyanate.** It was found that the rearrangement of the isocyanate occurred at room temperature, which is competitive with that of the Curtius rearrangement. The generation of the isocyanate from the azide at lower temperature, via irradiation, proved to be impractical. Cyclization product was observed at a temperature as low as  $-15^{\circ}\text{C}$  (dry ice in ethylene glycol) under irradiation. Once generated, the isocyanate appeared to cyclize under photochemical conditions. Therefore, an indirect method of measurement was necessary in order to conduct the kinetic study.

Fortunately, for a consecutive two-step reaction, where  $k_1$  and  $k_2$  are competitive,  $k_2$  can be estimated from following analysis<sup>100, 101</sup>:



$$\frac{[B]_{\max}}{[A]_0} \approx \frac{1}{4}$$

$$k_2 \approx 2k_1 = (2.44 \pm 0.02) \times 10^{-4} \text{ s}^{-1}$$

$$\text{Since } \ln k = -\frac{\Delta G^\ddagger}{RT} + \ln \frac{kT}{h}$$

$$\Delta G^\ddagger = 23.16 \text{ kcal/mol}$$

The kinetic experiment was run inside the Unity-500 Varian NMR. The temperature was set to 35°C (and later was calibrated with proton signals of standard methanol). The spectrometer was set for an acquisition array for each 10 minutes and 9 consecutive FIDs (Free Induction Decay) were collected for NMR analysis.<sup>102</sup> A plot of the logarithm of the

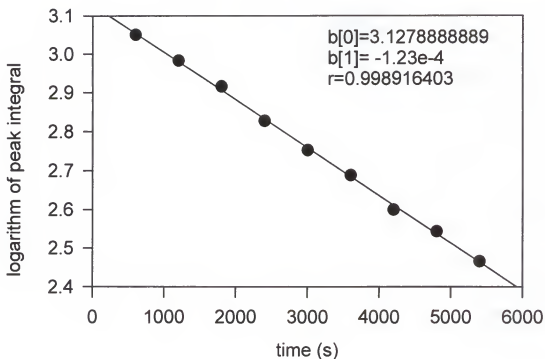


Figure 2-30. Determining the rate of Rearrangement of  $\alpha$ -methyl system. The plot of peak decrease of acyl azide versus time was used to estimate the rate of the cyclization of isocyanate system.  $k=1.23(0.02)\times 10^{-4}\text{s}^{-1}$

peak decrease of the acyl azide versus time was shown in Figure 2-34. The ratio  $[B]_{\text{max}}$  to  $[A]_0$  was estimated from their peak intensities of the NMR spectra. (The initial intensity of the peak of vinyl proton of acyl azide was 38.76 and that of the isocyanate

was 10.50. The ratio of  $[B]_{\max}$  to  $[A]_0$  was rounded off to 1 : 4 and the rate was determined as indicated in Equation 2-5.)

An  $\alpha$ -methyl group is seen to significantly enhance the reactivity of the electrocyclization process. From an MP2 calculation,  $\Delta\Delta G^\ddagger = 26.11$  kcal/mol, which is 3.7 kcal/mol lower than that of the parent system. Here again, the computational study and experimental results are in reasonable agreement. Thus, an electron donor at the  $\alpha$ -position is then proven by experimental results and supported by theoretical calculations, to enhance the reactivity of the electrocyclization. This hypothesis will be evaluated further in the next section by putting an electron acceptor ( $\text{CF}_3$ ) at the  $\alpha$ -position.

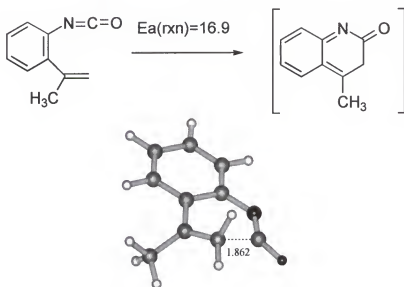
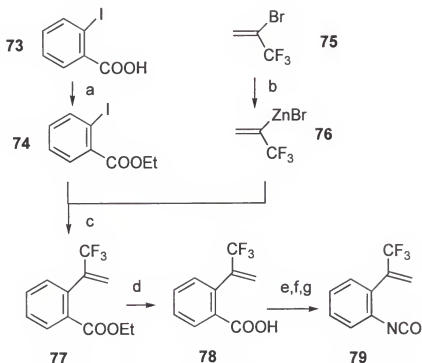


Figure 2-31. Transition structure of  $\alpha$ -methyl system(MP2/6-31G\*//RHF/6-31G\*)<sup>89</sup>.

As shown in Figure 2-35, at the transition state of this rearrangement the forming C-C bond is 1.862Å, about 20% shorter than a typical pericyclic reaction (2.1-2.3Å)<sup>90</sup>. The reaction is endothermic (16.9kcal/mol) based on calculations done at MP2/6-31G\*//RHF/6-31G\* level.

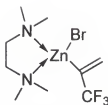
### 2.3.2 Thermal rearrangement of $\alpha$ -trifluoromethyl system



a) ethanol/ $\text{SOCl}_2$ <sup>103</sup>, b)  $\text{Zn}(\text{Ag})$ <sup>105</sup>,  $(\text{CH}_3)_3\text{SiCl}$ , TMEDA/THF<sup>104</sup>, c) THF,  $\text{Pd}(\text{PPh}_3)_4$ <sup>104</sup>, d)  $\text{NaOH}$  (20% aq) ethanol, e)  $(\text{COCl})_2$  in  $\text{CH}_2\text{Cl}_2$ , f)  $\text{NaN}_3$  (sat., aq),  $0^\circ\text{C}$ , g)  $\text{C}_6\text{D}_6$ , RT

Figure 2-32. Synthesis of  $\alpha$ -trifluoromethyl system.

**Synthesis of 3,3,3-trifluoro-*iso*-propenyl phenyl isocyanate.** The 3,3,3-trifluoro-*iso*-propenyl phenyl isocyanate was synthesized in a concurrent way. Esterification of the iodobenzoic acid gave a quantitative yield of ethyl 2-iodobenzoate. The esterification was necessary because the acid would impede the following coupling reaction. The trifluoroisopropenylzinc reagent was prepared from 2-bromotrifluoropropene and  $\text{Zn}(\text{Ag})$  with trimethylchlorosilane as an activating reagent and TMEDA (tetramethylethylenediamine) as a chelating reagent<sup>106</sup>. (Figure 2-33)



80

Figure 2-33. Complex of 3,3,3-trifluoroisopropenyl zinc reagent with TMEDA. The chelation makes carbon-Zinc bond more covalently characterized, which retards the elimination of fluoride anion to form the  $\text{CF}_3$  form 1,1-difluoro allene.

This zinc reagent was not isolated and was used directly for a palladium catalyzed coupling reaction with the aryl iodide which gave the product in 67% yield. Hydrolysis of the ester regenerated the acid, which was transformed to the isocyanate precursor as before.

**Kinetic study on electrocyclization of the  $\alpha$ -trifluoro system.** The kinetic experiment was done at 149.3 °C. The observed rate constant of the rearrangement reaction was close to that of the parent hydrocarbon system at 103°C. It is obvious that the reactivity of the cyclization is inhibited by applying a  $\text{CF}_3$  group (with  $\sigma_{\text{R}}^0 = 0.09$ , a weak electron acceptor) at the  $\alpha$ -position. In other words, an acceptor at the  $\alpha$ -position raises the activation barrier. Therefore, a higher temperature is required for the rearrangement.

Again, a late-transition state (partial C-C bond length is 1.866Å) is observed (Figure 2-35). At MP2/6-31G\*\*/RHF/6-31G\* level of theory, the reaction is 22.2 kcal/mol endothermic and calculated activation barrier is 31.94kcal/mol, *i.e.* 2.14 kcal/mol uphill from the parent system. Demand of a higher temperature for the isomerization is consistent with the theoretical estimation.

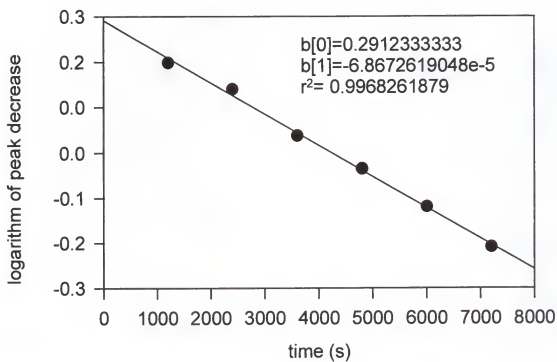


Figure 2-34. Determining the rate constant of the  $\alpha$ -CF<sub>3</sub> system.  $k=6.9(0.2) \times 10^{-5} \text{ s}^{-1}$ .

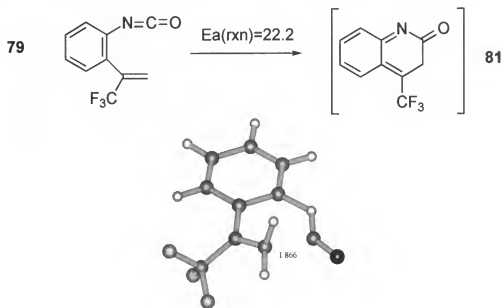


Figure 2-35. Transition structure of  $\alpha$ -trifluoromethyl system<sup>89</sup>.

### 2.3.3 Conclusions

It was also found in theory (MP2/6-31G\*//RHF/6-31G\* level)<sup>89</sup> that an  $\alpha$ -methoxy system will have a transition structure shown in Figure 2-36. The reaction would be 16.3 kcal/mol endothermic (partial C-C is 1.896Å) and the free energy of activation would be 21.9 kcal/mol, which is 7.9 kcal/mol lower than that of the parent system.

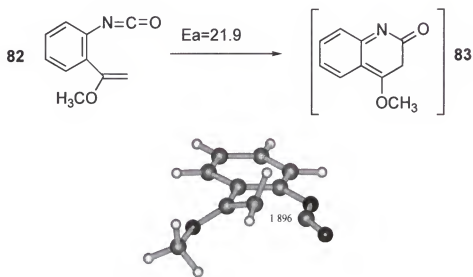
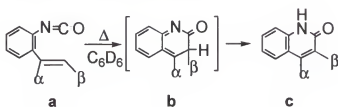


Figure 2-36. Transition structure of an  $\alpha$ -methoxy system (MP2/6-31G\*//RHF/6-31G\* level.)

Listed in Table 3-3 are the kinetic parameters from experimental results and computational results. It is believed that the substitution of polar substituents can give rise to strong kinetic effects which can largely be attributed to polar influences on the thermodynamics of the endothermic, rate-determining step of these processes. The polar effect on these electrocyclic reactions could be understood in terms of favorable *nucleophilic/electrophilic* interactions. The carbonyl carbon of the isocyanate acts as an electron acceptor, which could accommodate additional electron density. The vinyl group is acting as a donor group. Therefore, when there was an electron acceptor at the  $\alpha$ -

position, the reaction was retarded; when there was an electron donor at the  $\alpha$ -position, the reactivity was enhanced.

Table 3-3. Comparison of the reactivities of the substrates. Energies are in kcal/mol; calculations are done at the level of MP2/6-31G\*/RHF/6-31G\* + ZPE. Some of the experimental data will be discussed in later sections.



Substituent					Calculated		
$\alpha$	$\beta$	$T, ^\circ\text{C}$	$k(\text{s}^{-1})$	$\Delta G^\ddagger$	$E_{\text{a(a} \rightarrow \text{b})}$	$E_{\text{rxn(a} \rightarrow \text{b})}$	$E_{\text{rxn(a} \rightarrow \text{c})}$
H	H	109.4	$9.8(0.5) \times 10^{-5}$	29.6	29.8	19.2	-23.1
H	CH <sub>3</sub>	112.6	$7.3(0.5) \times 10^{-5}$	30.1	29.1	20.8	-25.3
H	F	178.9	$2.0(0.3) \times 10^{-4}$	34.5	32.7	25.5	-21.1
H	CF <sub>3</sub>	182.3	$9.0(0.5) \times 10^{-5}$	35.5	32.8	22.2	-24.4
CH <sub>3</sub>	H	35	$2.4 \times 10^{-4}$	23.2	26.1	16.9	-24.3
CF <sub>3</sub>	H	149.3	$6.9(0.2) \times 10^{-5}$	33.0	31.9	22.8	-21.3
CH <sub>3</sub>	F	101.6	$3.80(0.01) \times 10^{-4}$	28.0	29.0	23.0	-22.0
H	CN				34.7	27.2	-20.8
H	CHO				32.3	23.5	-23.1
OCH <sub>3</sub>	H				21.9	16.3	-23.5

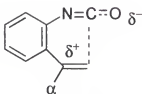


Figure 2-37. Polar effect on the rearrangement.

## 2.4. Investigation of Torquoelectronic Selectivity on $6\pi$ System

After exploring and understanding the kinetic behavior of the parent system and the substituent polar effects on the rearrangement of the isocyanate system, torquoelectronics were then investigated. In selecting the substituents, the important considerations are their steric and electronic properties. Ideally, the substituents selected possess distinct electronics and sterics.

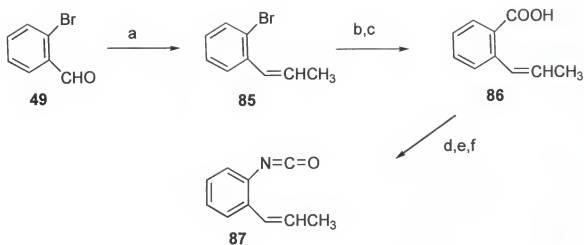
Quantitative models of steric effects of substituents indicate that the size decreases in the order:  $\text{CF}_3 > \text{CH}_3 > \text{F}$ . For example, Taft  $E_s$  values<sup>107</sup> are -2.4, -1.24 and -0.46 for  $\text{CF}_3$ ,  $\text{CH}_3$  and  $\text{F}$ , respectively. ( $E_s = \log \left( \frac{k}{k_0} \right)_A$ , in which  $k$  and  $k_0$  are the rate constants for hydrolysis of  $\text{XCOOR}$  and  $\text{CH}_3\text{COOR}$ , respectively, and in which the subscript  $A$  denotes acid-catalyzed hydrolysis.  $\text{CH}_3$  was originally set at  $E_s=0$ . This value is often reset to  $E_s=0$  for hydrogen atom, which makes  $\text{CH}_3$  at  $E_s = -1.24$ ) By this measure,  $\text{CF}_3$  is nearly as large as *t*-butyl ( $E_s$ , -2.78). From another aspect, "A" values for these groups are 2.4-2.5<sup>109,110</sup>, 1.7 and 0.24<sup>108,109,111</sup> for  $\text{CF}_3$ ,  $\text{CH}_3$  and  $\text{F}$ , respectively. ("A" values are defined as the conformational free-energy differences between axial and equatorial conformations of monosubstituted cyclohexanes. The bulkier the group, the stronger the tendency for it to be equatorial, therefore the bigger the "A" value.) The bulkiness of the substituents can also be evaluated by their calculated van der Waals volume. The van der Waals radius of 2.7 Å for trifluoromethyl group can be compared to 2.0 Å for methyl, while its van der Waals volume (hemisphere)<sup>112</sup> of 42.5 Å<sup>3</sup> to that 16.8 Å<sup>3</sup> for the methyl group. Following this analysis, fluorine atom with Van der Waals

radius 1.47 Å bears *ca.* 6.65 Å<sup>3</sup> van der Waals volume (hemisphere). The size of the trifluoromethyl group is about 2.5 times the volume of the methyl group and is 6.4 times the volume of the monofluoro group. From the electronic property point of view,  $\sigma_R^0$  for CF<sub>3</sub>, CH<sub>3</sub>, and F are 0.09, -0.11, and -0.33, respectively<sup>113</sup>. ( $\sigma_R^0$  is an experimentally determined measure of the resonance contribution to the net electron-donating or withdrawing character of the substituents with the denotation of “+” for electron acceptor and “-” for electron donors.) Therefore, the  $\pi$  electron delocalization abilities are in the order: CF<sub>3</sub> < CH<sub>3</sub> < F, which is in the exactly opposite for the order of bulkiness of these substituents.

It became obvious that by comparing the different kinetic behaviors of the substrates containing CF<sub>3</sub>, CH<sub>3</sub> and F as a substituent at the  $\beta$ -position, one could unambiguously determine whether electronics or sterics is the major contributor to the electrocyclization process. With this premise in mind, CH<sub>3</sub>, F and CF<sub>3</sub>  $\beta$ -substituted precursors were synthesized and the kinetic studies were conducted.

#### 2.4.1 Thermal rearrangement of *o*-(*E/Z*) propenyl phenylisocyanate

**Synthesis of *o*-(*E/Z*) propenyl phenylisocyanate.** Similar to the parent precursor, the  $\beta$ -methyl system was synthesized in 6 steps. Again, starting with commercially available 2-bromobenzaldehyde via a Wittig reaction (PPh<sub>3</sub>CH<sub>2</sub>CH<sub>3</sub>Br with *n*-butyl lithium as the base), 1-bromo-2-(1-propenyl)benzene was made in 91.8% yield. The bromide was transformed to the carboxylic acid with lithium exchange (*t*-butyl



a)  $\text{Ph}_3\text{PCH}_2\text{CH}_3\text{Br}/n\text{-BuLi}$ , then  $\text{H}_2\text{O}$ , b)  $t\text{-BuLi}/\text{THF}$ ,  $-78^\circ\text{C}$ , c)  $\text{CO}_2$  then  $\text{H}_2\text{O}$ , d)  $(\text{COCl})_2/\text{CH}_2\text{Cl}_2$ , e)  $\text{NaN}_3(\text{sat, aq})$ ,  $0^\circ\text{C}$ , f)  $\text{C}_6\text{D}_6$  RT.

Figure 2-38. Preparation of the  $\beta$ -Methyl System

Lithium) and quenched with carbon dioxide in 89.5% yield (*cis* : *trans* = 56:44). The stereochemistry was determined by the through-bond couplings: *cis*  $^3\text{J}(\text{CH}_3\text{-CH=}) = 7.14\text{Hz}$ , *cis*  $^3\text{J}(\text{CH=CH}) = 11.54\text{Hz}$ ; *trans*  $^3\text{J}(\text{CH}_3\text{-CH=}) = 6.87\text{Hz}$ , *trans*  $^3\text{J}(\text{CH=CH}) = 15.66\text{Hz}$ <sup>114</sup>. The 2-(1-propenyl) benzoic acid was then converted to the isocyanate using the same method used for the parent system.

#### Kinetic study on electrocyclization of *o*-(*E/Z*) propenyl phenylisocyanate.

This isocyanate precursor was cyclized at  $112.6^\circ\text{C}$  in  $\text{C}_6\text{D}_6$ . Based on Equation 2-5, at  $112.6^\circ\text{C}$ ,  $\Delta G^\ddagger(\text{cis-exp}) = 32.0\text{ kcal/mol}$ , and  $\Delta G^\ddagger(\text{trans-exp}) = 30.1\text{ kcal/mol}$ ,  $\Delta\Delta G^\ddagger(\text{cis-trans}) = 1.9\text{ kcal/mol}$ . That is, experimentally, at this temperature, the *trans* isomer is 1.9 kcal/mol favored for this 6- $\pi$  electrocyclization. The relative reactivity of the *trans* isomer with respect to the *cis* isomer at  $112.6^\circ\text{C}$  is  $k_{\text{trans}}/k_{\text{cis}} = 11.7$ .

$$\ln k = -\frac{\Delta G^\ddagger}{RT} + \ln \frac{kT}{h} \quad (2-5)$$

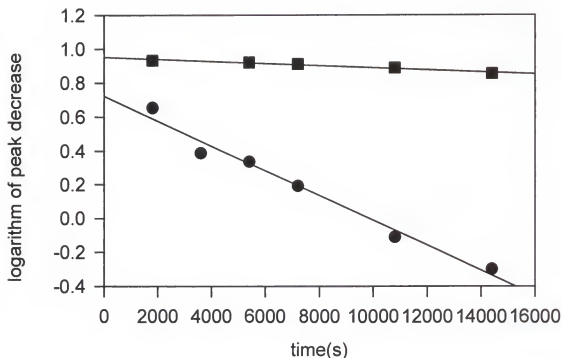


Figure 2-39. Determining the rate of the rearrangement of  $\beta$ -methyl system. ● the *trans* isomer,  $k=7.34(0.50)\times 10^{-5} \text{ s}^{-1}$ ,  $r^2=0.980$ ; ■ the *cis* isomer,  $k=6.24(0.75)\times 10^{-6} \text{ s}^{-1}$ ,  $r^2=0.957$ .

At MP2/6-31G\*\*/RHF/6-31G\* + ZPE level of theory, the calculated activation free energies for the electrocyclization of the *cis* and the *trans* isomers are  $\Delta G^\ddagger(\text{cis-calc}) = 31.14 \text{ kcal/mol}$ ;  $\Delta G^\ddagger(\text{trans-calc}) = 29.12 \text{ kcal/mol}$ , respectively, and the difference is  $\Delta\Delta G^\ddagger(\text{cis-trans}) = 2.0 \text{ kcal/mol}$ . At the same level of calculation, the *trans* isomer is energetically 1.9 kcal/mol more stable than the *cis* isomer at ground state, as shown in Figure 2-40, while the transition state for the *cis* isomer is 3.93 kcal/mol less stable than that for the *trans* isomer. Thus, the rearrangement of the *trans* isomer by this

computational analysis, should be favored by 2.0 kcal/mol. That is, mathematically according to Equation 2-5, the preference of the *trans* isomer to the *cis* isomer is

$$\left( \frac{k_{trans}}{k_{cis}} \right)_{calc} = 13.8, \text{ a number which agrees remarkably well with the experimental data.}$$

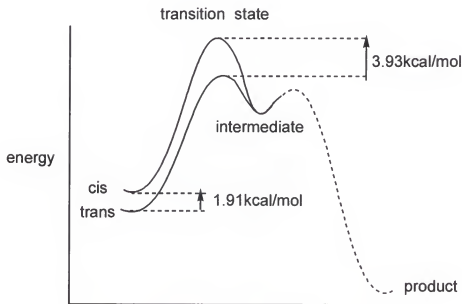


Figure 2-40. Approximate energy diagram for cyclization of the  $\beta$ -methyl system. Energies at level of MP2/6-31G\*//RHF/6.31G\*; The difference of the activation barrier is 2.0 kcal/mol

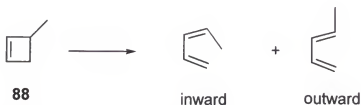


Figure 2-41. The influence of 3-methyl upon activation energies for conrotatory electrocyclic reaction of cyclobutene. Relating to the unsubstituted cyclobutene opening,  $\Delta E_a(\text{in}) = +3$  kcal/mol and  $\Delta E_a(\text{out}) = -1$  kcal/mol.

As a comparison, it was estimated that for the ring opening of 3-methylcyclobutene (Figure 2-41)<sup>24</sup>,  $\Delta E_a(\text{inward-outward})$  was 4 kcal/mol. It can be postulated that at 112.6 °C, the preference of ring-opening outwardly over inwardly is  $\frac{k_{\text{trans}}}{k_{\text{cis}}} = 183$ . That is a methyl-group rotating outwardly is much more favorable over inwardly in the cyclobutene ring-openings than a methyl in this 6 $\pi$  electron isocyanate system.

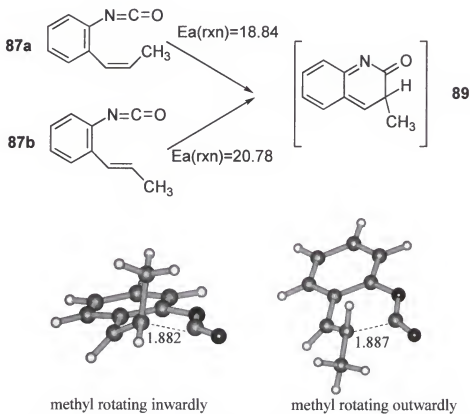


Figure 2-42. MP2/6-31G\*\*/RHF/6-31G\* transition structures of  $\beta$ -methyl system.

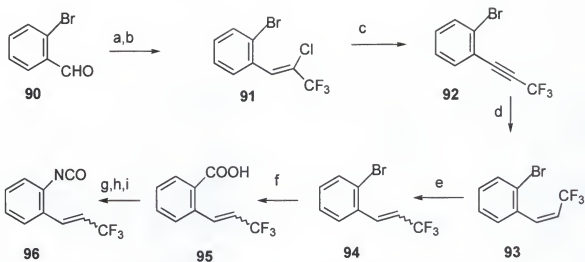
At MP26-31G\*\*/RHF6-31G\* level of theory (Bartberger and Dolbier)<sup>89</sup> the transition structures for the rearrangement of the *cis* and the *trans* isomers are shown in Figure 2-42. The forming C-C single bond length is 1.882Å for the *cis* and 1.887Å for the *trans*. It is again found to be shorter than that of a typical pericyclic reaction(2.1-

2.3Å)<sup>90</sup>. The reaction is endothermic by 18.8 kcal/mol and 20.8 kcal/mol for the *cis* and the *trans* isomers, respectively.

The absence of a substituent at the carbonyl carbon should eliminate the steric difference between the *cis*-methyl and *trans*-methyl isomers upon the electrocyclization. A methyl group, which is capable of releasing electrons by hyperconjugation, is a weak electron donor. (Taft <sup>113</sup>  $\sigma_R^0 = -0.11$  for methyl,  $\sigma_R^0 = -0.34$  for fluoro,  $\sigma_R^0 = -0.48$  for amino group.) The weak electron donating property of the methyl group *should* be the origin of the discrepancy of the energy of activation. Thus, it prompted us to investigate if the concept of torquoelectronic selectivity was applicable to this 6- $\pi$  electronic cyclization. The argument at this point was still somewhat weak, because the sterics *could* be the contributor to the different reactivities of the *cis*-methyl and the *trans*-methyl isomers. It was intuitively true that the ambiguity could be cleared up by experiments on the bulkier (or smaller) substituents.

#### 2.4.2 Thermal rearrangement of *o*-(E/Z)-3,3,3-trifluoropropenyl phenylisocyanate

**Synthesis of the precursor.** *o*-Bromo benzaldehyde was readily transformed to the olefin by a one-pot reaction which employed 1,1,1-trichloro-2,2,2-trifluoroethane, zinc powder and acetic anhydride. Dehydrochlorination of the olefin using sodium *t*-butoxide (derived from sodium amide and *t*-butyl alcohol) gave rise to the desired acetylene in 71% isolated yield. Potassium *t*-butoxide was totally ineffective to the elimination reaction. The hydrogenation of the acetylene to olefin under Lindlar conditions proved to be very slow (the reaction proceeded at *ca.* 5% per day) with various solvents. Activated Zn(Ag) in methanol was found very effective method of the



a) Zn,  $\text{CCl}_3\text{CF}_3/\text{THF}$ ,  $50^\circ\text{C}$ , b)  $\text{AcOH}$ , Zn,  $50^\circ\text{C}$ <sup>115</sup>, c)  $\text{NaNH}_2/\text{t-butanol}/\text{PhH}$ ,<sup>115</sup> d)  $\text{Zn}(\text{Ag})$ <sup>105,116</sup>, methanol reflux, 100% *cis*, e) irradiation<sup>37</sup> in  $\text{CHCl}_3$ , overnight, 1:1.2 *cis* vs *trans*. f)  $\text{t-BuLi}/\text{THF}$ , then  $\text{CO}_2$  then  $\text{H}_2\text{O}$ , g)  $(\text{COCl})_2/\text{CH}_2\text{Cl}_2$ , h)  $\text{NaN}_3$  (sat, aq)  $0^\circ\text{C}$ , i)  $\text{C}_6\text{D}_6$ , RT

Figure 2-43. Preparation of  $\beta$ -trifluoromethyl system

hydrogenation giving clean *Z*-isomer (89% yield). However, the reaction mechanism is still baffling. Irradiation of the *Z*-isomer in chloroform gave a *ca.* 1:1.4 *cis* and *trans* mixture. The obtained bromide was transformed to the isocyanate in the same way as for the  $\beta$ -methyl system.

There are numerous examples<sup>118-123</sup> in the literature of radical addition reactions of perfluoroalkyl iodides to carbon carbon double bonds and the elimination of iodo-adduct to produce a fluorinated alkene. Following these known procedures, several attempts were made to perform a radical addition of trifluoromethyl radical (generated from trifluoromethyl iodide) to 2-bromo-styrene followed by an elimination of hydrogen iodide to yield a precursor for the studies. Shown in Figure 2-44 are two of the unsuccessful examples. The reactions produced either no product or numerous products

which could not be successfully isolated. It is still curious while trifluoromethyl radical add easily to aliphatic C-C double bonds, but will not react cleanly with the styrene.

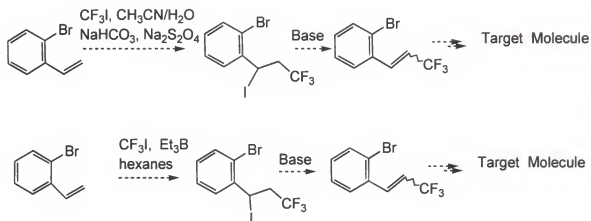


Figure 2-44. Two of the attempts to add  $\text{CF}_3\text{I}$  onto styrene. All the conditions that works for normal olefin failed on the styrene.

### Kinetic study on electrocyclization of the $\beta$ -trifluoromethyl system.

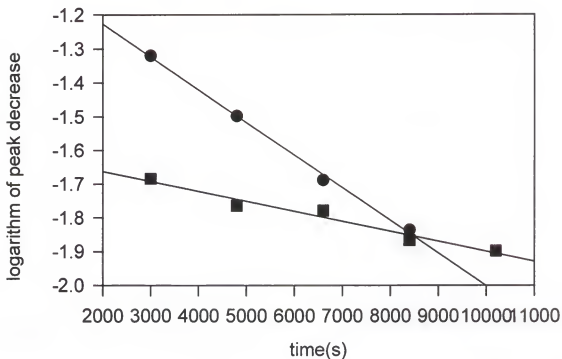


Figure 2-45. Determining the rate constant of rearrangement of  $\beta$ -trifluoromethyl system. ■ the *cis* isomer,  $k=2.82 \times 10^{-5}$ ,  $r^2=0.952$ ; ● the *trans* isomer,  $k=8.95 \times 10^{-5}$ ,  $r^2=0.992$ .

The kinetic experiment was conducted at 182.3 °C. The observed rate constants for the *cis* isomer and the *trans* isomer are  $k_{\text{cis}}=2.82 \times 10^{-5}$  and  $k_{\text{trans}}=8.95 \times 10^{-5}$ , respectively, that is  $\frac{k_{\text{trans}}}{k_{\text{cis}}} = 3.2$ .  $\Delta G^\ddagger$  from the experimental data is 36.5kcal/mol and 35.5kcal/mol for the *cis* and the *trans* isomers, respectively ( $\Delta\Delta G^\ddagger(\text{cis-trans})=1.0$  kcal/mol). The activation free energies from the calculation is 33.69kcal/mol and 32.77 kcal/mol for the *cis* and the *trans* isomers, respectively. The difference of the activation barrier is 0.92 kcal/mol. It was incredibly consistent with the experimental results.

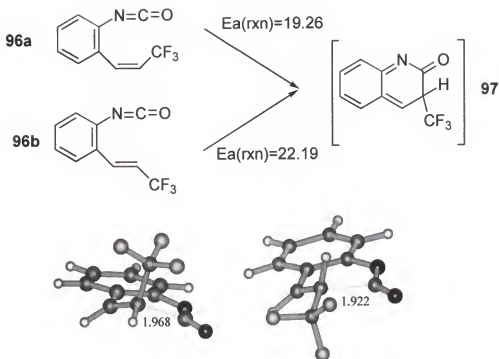


Figure 2-46. MP2/6-31G\*//RHF/6-31G\* (Bartberger and Dolbier)<sup>89</sup> transition structures of  $\beta$ -trifluoromethyl system.

From the transition geometries of both isomers, one can again conclude a late transition state for both isomers. The forming C-C bond lengths (1.968 Å and 1.922 Å for *cis* and *trans* isomers, respectively) are both about 0.1 Å longer than that of the parent system, but they are still shorter than that of a typical pericyclic reaction (2.1-2.3 Å)<sup>90</sup>. The reaction is 19.26 kcal/mol endothermic for the *cis* isomer and is 22.19 kcal/mol for the *trans* isomer.

Conclusively, the rearrangement preference of the *trans* isomer over the *cis* isomer is 3.2, a number which is much smaller than that of the  $\beta$ -methyl system. From the steric point of view, a bulkier substitution ( $E_s$  is -2.4 for  $\text{CF}_3$ , -1.24 for  $\text{CH}_3$ ) gives rise to a smaller impact on the selectivity! Therefore, steric contribution to the preferences of the rearrangements can be discredited. The final nail in the coffin could be delivered if the kinetics could be examined on a substitution, which is smaller in size, but more

electronically demanding. The ideal candidate is a fluorine substituent, which is the smallest of all nonhydrogen substituents with Es of -0.46 as compared to CH<sub>3</sub> (-1.24) and CF<sub>3</sub> (-2.4); it is also one of the best  $\pi$ -donors, due to the fact that fluorine is a second-period element, and thus its atomic orbitals are an ideal size for effective overlap with carbon orbitals both in forming  $\sigma$ -bonds and in  $\pi$ -conjugative interaction with contiguous carbon  $\pi$  system<sup>14</sup>.

### 2.4.3 Thermal rearrangement of o-iso-(1-fluoro)-propenyl phenylisocyanate

**Synthesis of the  $\alpha$ -methyl- $\beta$ -fluoro system.** As will be discussed in Section 2.4.4, despite the high temperature required for the  $\beta$ -fluoro system, the *trans* isomer was notably more reactive than the *cis* isomer. The experimental result however, was in disagreement with computational theory. The demanding high temperature for the reaction might be responsible for the discrepancy. The polar effect studies (Section 2.3) opened an avenue which could lower the activation barrier by applying methyl group (an electron donor) at the  $\alpha$ -position. Thus, an  $\alpha$ -methyl- $\beta$ -fluoro system was proposed, in the hope that the electrocyclization would occur at a much lower temperature.

Burton had developed a method to synthesize monofluoro-olefins from ketones as shown in Figure 2-47. Even though they were effective approaches to the desired monofluoro-olefins, the availability, cost of reagent, and more unfortunately, poor reproducibility of these reactions, limit the utility of the reactions. The author also tried to use another approach to synthesize *gem*-difluoro-olefin, with the hope that it would be reduced to the monofluoro-olefin, shown in Figure 2-48. The method practically failed

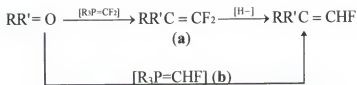
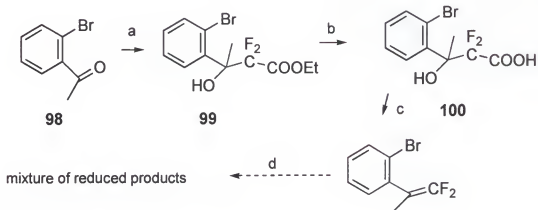


Figure 2-47. Burton's strategies to make monofluoroolefin. (a)<sup>124</sup> the Difluoromethylenation requires extremely dry solvents to obtain satisfactory yields, in the case of (b)<sup>125,126</sup> requires the use of the expensive  $\text{CH}_2\text{F}_2$  or  $\text{CHF}_3$  for the monofluoromethylenation.

because of the presence of bromide at the benzene ring. The reduction reaction upon the bromide and the fluoride are compatible. Several products were formed concurrently.

The reaction mixture was very messy and hence, inefficient.

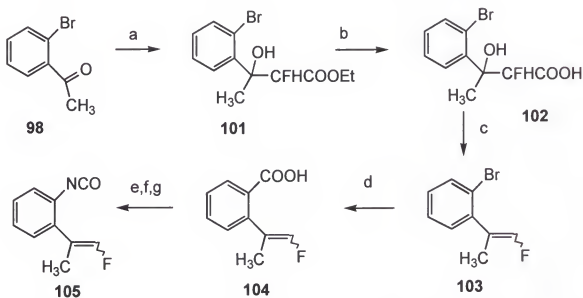


a)  $\text{Zn}/\text{BrCF}_2\text{COOEt}/\text{THF}$ , b)  $\text{NaOH}$  (10%, aq), c)  $\text{TsCl}$ ,  $\text{Pyr}$ ,  $\text{CHCl}_3$ <sup>127,128,129</sup>, d)  $\text{red-Al}$ <sup>124</sup> (sodium bis(2-methoxyethoxy)aluminum hydride)

Figure 2-48. Initial attempt to precursor. The reduction (d) reaction was a mess.

A new approach was developed by using ethyl bromodifluoroacetate as one of starting materials. (Figure 2-49) The Reformatsky reaction was carried out in THF with  $\text{CeCl}_3$ <sup>130,131</sup> as catalyst in 50% yield. The obtained acetate was hydrolyzed to carboxylic acid with one equivalent of  $\text{NaOH}$  in ethanol (95%). The  $\beta$ -hydroxy carboxylic acid was

converted to monofluoroolefin in one-pot by treating it with TsCl (1eq) and pyridine (2eq) in chloroform, presumably via a decarboxylation of the  $\beta$ -lactone at 170-180°C. This bromide was then transformed to the carboxylic acid via lithium exchange (*t*-butyllithium) and quenching with carbon dioxide. (*cis* : *trans* = 44:56). The carboxylic acid was then transformed to the isocyanate as in the previous cases.



a)  $\text{BrCHFCOOEt}/\text{Zn}/\text{THF}$ ,  $\text{CeCl}_3$ , b)  $\text{NaOH}$  (1 eq, 1M in ethanol), c)  $\text{TsCl}$  (1eq), pyridine (2eq)/ $\text{CH}_3\text{Cl}$ , 180°C, d)  $t\text{-BuLi}/\text{THF}$ , -78°C,  $\text{CO}_2$  then  $\text{H}_2\text{O}$ , e)  $(\text{COCl})_2/\text{CH}_2\text{Cl}_2$ , f)  $\text{NaN}_3$ (sat, aq), 0°C, g)  $\text{C}_6\text{D}_6$  RT.

Figure 2-49. Preparation of precursor of the  $\alpha$ -Methyl- $\beta$ -Fluoro System

Determining the stereo chemistry with J-coupling phenomena which involve scalar (or through-bond) coupling was not convincing, as seen in Figure 2-50a. The spin constants are too close to distinguish the stereo chemistry.

The stereo chemistry was then determined by the nuclear Overhauser effect (nOe)

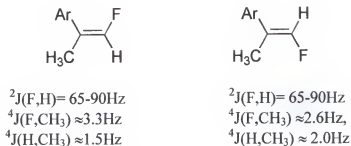


Figure 2-50a. Comparison of spin-spin coupling of the *cis* and *trans* isomers. The  $J$  values are too close to distinguish the stereochemistry<sup>114</sup>.

difference. Besides the through-bond couplings, the nuclei also interact through space, involving direct dipole (or magnetic) couplings. The information gained through such direct coupling interactions can be recorded in the form of nOe, providing valuable insight into the internuclear distances and molecular motion. The nuclear Overhauser effect is the change of intensity of the resonance of one nuclear when the transitions of another nucleus (lying close to the first nucleus in space) are perturbed by irradiation. As presented in Figure 2-50b, by irradiating the protons on the indicated methyl group, only the *trans* isomer will show positive nOe on the vinyl proton. (Of course, the proton on the phenyl ring, which is *ortho* to the vinyl group, also gives positive nOe)<sup>132</sup>. And because the vinyl proton in the *cis* isomer is farther away in space from the methyl group, there is no nOe observed for that proton.

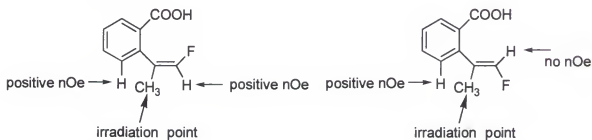


Figure 2-50b. Determining the stereo-chemistry of the isomers by nOe technique.

**Kinetic study on electrocyclicization of the  $\alpha$ -methyl- $\beta$ -fluoro system.** This was one of the examples that the results turned out to be just as good as the prediction. 2-((*E/Z*)-2-Fluoro-1-methyl-1-ethenyl) phenylisocyanate with an electron donating methyl group at the  $\alpha$ -position did lower the activation barrier so that the kinetic study could be conducted at a much lower temperature than the  $\beta$ -fluoro system. The rearrangement went smoothly at 101.6°C and a better kinetic influence of the fluorine substituent on the electrocyclicization was observed. Furthermore, due to the distance

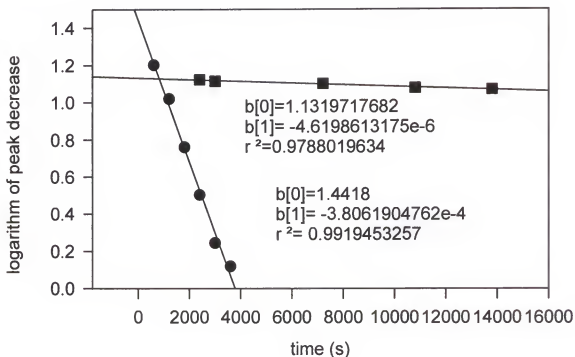


Figure 2-51. Determining the rate of rearrangement of the  $\alpha$ -methyl  $\beta$ -fluoro system. ■ the *cis* isomer,  $k=4.62(0.39)\times 10^{-6}\text{ s}^{-1}$ ,  $r^2=0.979$ ; ● the *trans* isomer,  $k=3.81(0.01)\times 10^{-4}\text{ s}^{-1}$ ,  $r^2=0.992$ .

between the methyl group and the breaking (forming) C-C bond, there is no direct interaction between molecular orbital of the forming (breaking) C-C bond and the

molecular orbital of that methyl group. Thus, a methyl group at the  $\alpha$ -position would *only* enhance the reactivity of the reaction however, it should not influence the investigation of torquoelectronic selectivity of fluorine atom at the terminal carbon.

The observed rate constant for the rearrangement is  $4.62 \times 10^{-6} \text{ s}^{-1}$  for the *cis* isomer and  $3.81 \times 10^{-4} \text{ s}^{-1}$  for the *trans* isomer. That is, the preference of the *trans*-fluoro isomer over the *cis*-fluoro isomer is  $\frac{k_{trans}}{k_{cis}} = 82.4$ . The free energy of activation ( $\Delta G^\ddagger$ ) from the experimental data is 31.28 kcal/mol for the *cis* isomer and 27.99 kcal/mol for the *trans*. The difference is  $\Delta\Delta G^\ddagger(cis-trans) = 3.3$  kcal/mol. While the free energy of activation from the theoretical calculation (MP2/6-31G\*\*//RHF/6-31G\*)<sup>89</sup> is 36.40 kcal/mol for the *cis* isomer and 28.96 kcal/mol for the *trans*. The difference is 7.4 kcal/mol. From this energetic difference, one can estimate that the preference of the *trans* isomer over the *cis* would be  $\frac{k_{trans}}{k_{cis}} = 20537$  at 101.6°C. As a sense of comparison, the theoretical results somewhat overestimated the preference of the *trans* isomer.

At any rate, fluorine, as the smallest group, exhibited the greatest different reactivities between the two isomers. It becomes more obvious that for this isocyanate system, the major contributing factor to the selectivity of the rearrangement is not the *sterics* of the substituent but the *electronics*, that is playing the important role. Thus, torquoelectronic control on the rearrangement was demonstrated unambiguously.

The calculated transition structures for both the *cis* and *trans* isomers are shown in Figure 2-52. The forming single bond length is 1.853 Å for the *cis* isomer and 1.867 Å for

the *trans*. The reaction is endothermic by 22.5 kcal/mol and 23.1 kcal/mol for the *cis* and *trans* isomers, respectively.

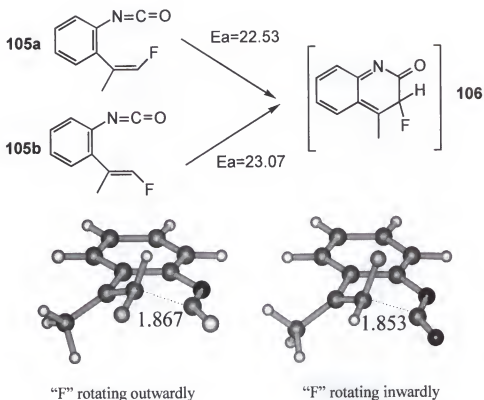
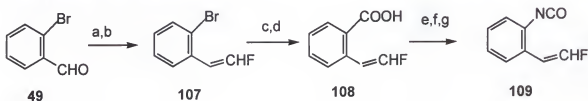


Figure 2-52. Transition Structure of rearrangement of  $\alpha$ -methyl- $\beta$ -fluoro system (MP2/6-31G\*/RHF/6-31G\* (Bartberger and Dolbier)<sup>89</sup>

#### 2.4.4 Thermal rearrangement of *o*-(*E*/*Z*) $\beta$ -fluorovinyl phenylisocyanate



a)  $n\text{-Bu}_3\text{P}/\text{CH}_2\text{Cl}_2/\text{CFCl}_3$  (24 hours), then  $\text{NaOH}$  (10%, aq)<sup>133</sup>, (95% *trans*, 5% *cis*), b) Irradiation<sup>37</sup> with  $\text{Ph}_2\text{CO}$  in  $\text{CHCl}_3$ , 1:1 *trans* and *cis*, c)  $t\text{-BuLi}/\text{THF}$ , d)  $\text{CO}_2$  then  $\text{H}_2\text{O}$ , e)  $(\text{COCl})_2/\text{CH}_2\text{Cl}_2$ , f)  $\text{NaN}_3$  (sat, aq)  $0^\circ\text{C}$ , g)  $\text{C}_6\text{D}_6$ , RT

Figure 2-53. Preparation of  $\beta$ -Fluoro Vinyl Phenylisocyanate

**Synthesis of the precursor.** The  $\beta$ -monofluoro styrene was synthesized from 2-bromo benzaldehyde by a Wittig-type monofluoroolefination and was isolated in 42% yield, in which 95% was the *Z*-isomer ( $trans\ ^3J(F,H) = 46.5\text{ Hz}$ ,  $cis\ ^3J(F,H) = 21.0\text{ Hz}$ )<sup>114</sup>. To best serve the purpose of the project, a nearly equal amount of both isomers was necessary for convenience and accuracy of the measurement. Irradiating of the 95% mixture (wave length 254nm) with *ca.* 2% benzophenone as sensitizer in chloroform in a quartz vessel for 4 hours gave a 50:50 mixture of *Z* and *E* isomers. Unlike the parent system, the bromide was unreactive under Grignard reaction conditions; however, it underwent lithium exchange when *t*-butyllithium in THF was used at -78°C. The formed anion was then quenched with carbon dioxide to yield the acid (70.9%), which was transformed to the isocyanate in the same way as the parent hydrocarbon system.

# Kinetic study on electrocyclization of *o*-(*E/Z*) $\beta$ - fluorovinyl phenylisocyanate.

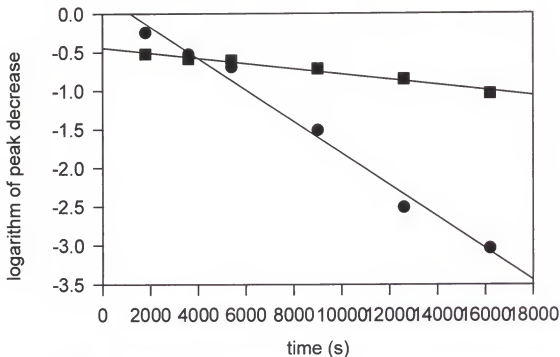


Figure 2-54 Determining the rate constant for the  $\beta$ -fluoro system. ■ the *cis* isomer,  $k=3.43 \times 10^{-5}$ ,  $r^2=0.974$ , ● the *trans* isomer,  $k=2.04 \times 10^{-4}$ ,  $r^2=0.987$ .

At 178.9 °C the observed rate constants for the rearrangements of the fluorovinyl phenylisocyanates were:  $k_{cis}=3.43(.27) \times 10^{-5} \text{ s}^{-1}$  and  $k_{trans}=2.04(.12) \times 10^{-4} \text{ s}^{-1}$ . From this experimental data and the Equation 2-5,  $\Delta G^\ddagger_{cis} = 36.1 \text{ kcal/mol}$ ,  $\Delta G^\ddagger_{trans} = 34.5 \text{ kcal/mol}$ .

That is  $\Delta \Delta G^\ddagger(\text{cis-trans}) = 1.6 \text{ kcal/mol}$ . The preference of the *trans* isomer over the *cis*

isomer for this electrocyclization is  $\frac{k_{trans}}{k_{cis}} = 6.0$  at this high temperature (178.9°C). When

the kinetic study was repeated at different temperatures, it was found that the results did

not fit well into an Arrhenius plot. The ratio  $\frac{k_{trans}}{k_{cis}}$ , however was appreciably of the

same magnitude at different temperatures. At 182.1°C,  $\frac{k_{trans}}{k_{cis}} = 3.4$  ( $k_{trans} = 9.35 \times 10^{-5} \text{ s}^{-1}$ ,  $k_{cis} = 2.78 \times 10^{-5} \text{ s}^{-1}$ ).

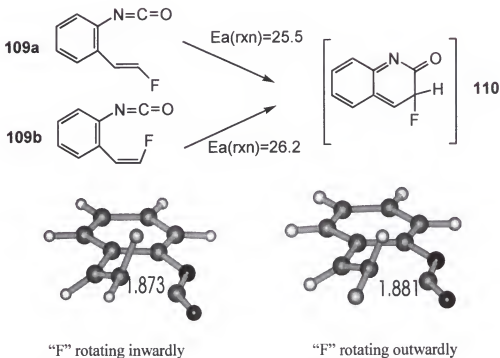


Figure 2-55. MP2/6-31G\*\*/RHF/6-31G\* transition structure<sup>89</sup> of rotating fluorine inwardly and outwardly.

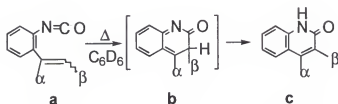
Figure 2-55 shows the transition structures (MP2/6-31G\*\*/RHF/6-31G\* level of theory) for the electrocyclizations of the *trans* and the *cis*  $\beta$ -monofluoro system. The partial C-C bond length is 1.873 Å for the *trans* isomer and 1.881 Å for the *cis* isomer, both resembling late transition states. At the same level of theory, the reaction is endothermic, 26.24 kcal/mol for the *cis* isomer and 25.55 kcal/mol for the *trans* isomer. The calculated free energy of activation at MP2/6-31G\*\*/RHF/6-31G\* + ZPE levels are 40.93 kcal/mol for *cis* isomer and 32.73 kcal/mol for the *trans* isomer, *i.e.*  $\Delta\Delta G^\ddagger(\text{cis-}$

trans) = 8.2 kcal/mol, a number which is not in good agreement with the experimental results. The computational study did predict that the electrocyclization would be slower than the parent hydrocarbon system. The activation barrier was calculated to be 11 kcal/mol higher for the *trans*-isomer and 3 kcal/mol higher for the *cis*-isomer than for the parent hydrocarbon system. The experimental results showed that the temperature for the rearrangement needed to be nearly 70 °C higher for the fluoro system to have a similar rate constant as the parent hydrocarbon system.

There are two reasons we were reluctant to accept these results as being reliable. First, the Arrhenius behavior of the  $\beta$ -fluoro system was poor (indeed the rates at 182°C were measured to be greater than that at 178°C). Second, unlike the situation for the parent system, addition of small amount of pyridine (or for that matter, any base) did not improve the kinetic situation. On the contrary, addition of pyridine, DBU or N,N-dimethylaniline led to destruction of the starting material. Therefore, for undefined reasons, we considered the data from the  $\beta$ -fluoro system not to be reliable.

#### 2.4.5 Conclusions

The substituent effects on the rearrangements (pseudopericyclic processes) were seen from these results. The different reactivities of the *E* and *Z* isomers can be attributed to the electronic properties the substitution. Fluorine, the smallest group however one of the best  $\pi$ -donors, must have a significant kinetic propensity for the *Z* isomer to react much faster than the *E* isomer. The results and comparison of their properties are presented in Tables 2-4 and 2-5.

Table 2-4 Comparison of the rate constants for the *cis* and the *trans* isomers.

Substituent		T (°C)	$k_E/k_Z$	$\Delta\Delta G^\ddagger$	Calculated	
$\alpha$	$\beta$			(kcal/mol)	$\Delta\Delta E_a$	$\Delta\Delta E_{rxn(a \rightarrow b)}$
H	CH <sub>3</sub>	112.6	11.7	-1.9	-2.0	+2.0
H	CF <sub>3</sub>	182.3	3.2	-1.0	-0.9	+2.9
CH <sub>3</sub>	F	101.6	82.4	-3.3	-7.4	+0.6
H	CHO				+2.2	+3.2

Table 2-5 Comparison of steric and electronic properties of the substituents.

	A value	E <sub>s</sub>	$\sigma_R^0$
F	0.24	-0.46	-0.33
CH <sub>3</sub>	1.7	-1.24	-0.11
CF <sub>3</sub>	2.4-2.5	-2.4	0.09

The smallest substituent (F with  $E_s = -0.46$ ) gives rise to the largest, whereas the largest (CF<sub>3</sub> with  $E_s = -2.4$ ) gives rise to the smallest kinetic effect! It is starkly clear that the  $k_E/k_Z$  ratios are not *steric* in origin. Being the best  $\pi$ -donor among the three substituents, fluorine exerted the biggest influence on the selectivity of the reactions. Compared to the influence of the electronics, the impact of the sterics on the kinetic preference becomes unimportant. Therefore, the major contributing factor to selectivity of this isocyanate system is the electronic properties of the substituents. Thus,

*torquoelectronic* selectivity on 6- $\pi$  electron system was successfully demonstrated experimentally.

As illustrated in Figure 1-8, the molecular orbital interaction in a disrotatory reaction is not as significant as in a conrotatory. It was not surprising to observe — and was confirmed by theoretical calculations — the diminished torquoselectivity on the 6- $\pi$  electron system. The overall experimental results prompted us to the electronic consideration. The monorotation and the pseudopericyclic characteristic of the novel rearrangement furnishes similar molecular orbital interactions as disrotatory process. Figure 2-56 shows the different MO interactions for conrotatory, disrotatory and monorotatory processes. When the C-C  $\sigma$  bond breaks (or forms), the “*torque*” about this bond will influence the magnitude of donor and acceptor substituent interactions. Here, a net stabilization occurs upon outward rotation of either electron-acceptors or electron-donors. The amount of overlap between substituent and  $\sigma$  HOMO orbitals of the inward transition structure is reduced compared to that in the conrotatory process. This reduces the amount of stabilization of an inward-rotating electron-acceptor and the amount of destabilization of an inward-rotating electron-donor. Though the molecular interactions of the studied pseudopericyclic reaction are not as dramatic as those in the cyclobutene openings, the influence of the substituent is similar however, the influence of electronic control upon selectivity is decreased.

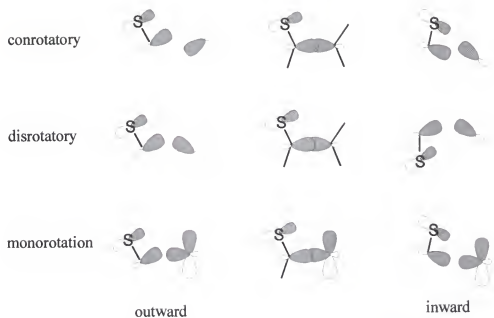
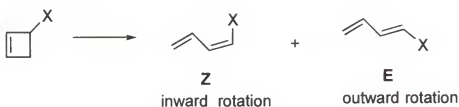


Figure 2-56. Comparison of orbital interactions among 4- $\pi$  conrotatory process, 6- $\pi$  disrotatory process and the pseudopericyclic monorotation process.



substituent	T(°C)	E : Z	reference
F	68-103	100 : 0	20
CH <sub>3</sub>	112.6	183 : 1	24
CF <sub>3</sub>	200	49 : 1	20

Figure 2-57. Product Distribution of the Ring-Opening of 3-Substituted Cyclobutenes.

The effects of the same three groups on the 3-substituted cyclobutene ring opening is illustrated in Figure 2-57. The electronic controls are much more significant than the ones found in this isocyanate system. That is, the magnitude of torquoelectronic

selectivity for a  $4\pi$  electron system is much more significant than that for a  $6\pi$  electron system. This is consistent with Houk's prediction<sup>30</sup> derived from their theoretical studies: "In a disrotatory process, the predicted electronic effect found in the conrotatory reaction is diminished."

## CHAPTER III

### SUMMARY

The purpose of our research project was to probe the relationship between reactivity and structure in the electrocyclic reaction. Our research has provided unprecedented experimental evidence for torquoselectivity on a 6- $\pi$  electron system. At the same time, because of the special nature of the system, it was discovered that the reaction was pseudopericyclic rather than pericyclic in nature<sup>134</sup>. During the research, a combination of computational and experimental methodology was utilized successfully. Computational studies not only quantitatively and qualitatively confirmed the *torquoelectronic* nature of the observed kinetic selectivity of the studied 6- $\pi$  electron system, but also elucidated the unique *pseudopericyclic* nature of the reaction. This chapter will serve to consolidate the experimental and computational results.

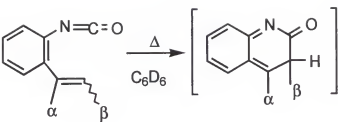
The geometry of the transition structure revealed the non-classical bonding interaction between the alkenic *p* orbital and one of the carbonyl non-bonded pairs on *sp* orbitals. Essentially, the bonding and non-bonding atomic orbitals interchange roles. The process of  $\sigma$ -bond formation gives rise to a disconnection in the cyclic array of overlapping orbitals because atomic orbitals which are switching functions are mutually orthogonal. *Pseudopericyclic* character was therefore recognized.

**Implications of the transition state.** In order to have insightful understanding of a chemical mechanism, an analysis of the geometries (therefore the energies) of the transition structure is crucial. The most direct criterion is the bond length between two reacting centers. The C-C bond-length ranges for normal organic molecules observed in X-ray structural analyses or calculated for transition structure are shown in Table 3-1. Table 3-1. The C-C bond-length ranges. The dotted line denotes a partial  $\sigma$  bond<sup>90</sup>.

	C··C	C—C	C=C	C=C	C $\equiv$ C	C $\equiv$ C
bond length (Å)	1.95-2.28	1.46-1.62	1.34-1.42	1.32-1.36	1.22-1.27	1.20-1.23

Under the same basis-set of calculation (MP2/6-31G\*//RHF/6-31G\*, Bartberger and Dolbier),<sup>89</sup> the forming C-C bond length differs within 0.1 Å among the isocyanate systems which were studied, as shown in Figure 3-2. A range of 1.86-1.96 Å of the forming C-C bond-length is about 20% shorter than a typical pericyclic reaction (2.1-2.3 Å). And they are about 0.4 Å away from a typical C-C  $\sigma$  bond (1.46-1.62 Å)<sup>90</sup>. It is an indication of the *lateness* of the bond forming. Thus, it can be generalized that maximum bonding is maintained in all of the studied transition structures.

The late transition states asserted that the reactions were endothermic (Figure 3-2). The endothermicity of the reaction could be a factor to diminish the influence of *torquoelectronics*. Because the more endothermic a process, the later its transition state, and the more likely that the kinetics of the process will be determined by the thermodynamics of the reaction, rather than by orbital interactions (the origin of the torquoselectivity), which generally exert their greatest influence in exothermic reaction which have early transition states.



Substituent		CC distance(Å)		E <sub>a</sub> of reaction	
α	β	<i>cis</i>	<i>trans</i>	<i>cis</i>	<i>trans</i>
H	H	1.883		19.20	
H	CH <sub>3</sub>	1.882	1.887	18.84	20.78
H	F	1.874	1.881	26.24	25.55
H	CF <sub>3</sub>	1.967	1.922	19.26	22.19
CH <sub>3</sub>	F	1.853	1.867	22.53	23.07
CH <sub>3</sub>	H	1.862		17.30	
CF <sub>3</sub>	H	1.866		22.79	
OCH <sub>3</sub>	H	1.896		16.34	
H	CHO	1.923	1.913	20.34	23.54

Figure 3-2. The forming bond lengths of the transition structures and the endothermicity of the reaction. Energies are in kcal/mol(MP2/6-31G\*\*/RGF6-31G\*\*+ZPE)<sup>89</sup>.

**Torqueelectronic selectivity.** After overcoming the steric-repulsion concerns,  $6\pi$  electron torquoselectivity was evaluated. The argument of importance of the electronic properties was settled by comparing the rate constants for *E*- and *Z*-isomers with the properties, both electronic and steric, of the substituents, as presented in Tables 2-4 and 2-5. From the results obtained thus far in these systems, there has unambiguously been demonstrated a consistent and kinetic preference for a  $\pi$ -donating group to rotate outwardly in these  $6\pi$  electron system; the electronic property is playing a more important role in controlling the rotation fashion.

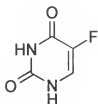
**Rotational isotope effects.** The monorotatory process also pinpointed the origin of the observed secondary kinetic isotope effect. When there is no steric impact on the

electrocyclization, the observed normal secondary deuterium kinetic isotope effects were interpreted as arising clearly from rotational motions of isotopic substituents. The studied electrocyclic reactions have a putative transition state, where methylene (for the parent system) rotation must occur in order for the reaction (ring closure) to occur. A deuteromethylene group has *less* motion to rotate than a methylene group. Thus, normal KIEs were observed for both the *cis* and the *trans* deuterated systems.

The very nice first order kinetic outcomes and the lack of reversibility combined with the weak normal KIEs demonstrated that the first electrocyclization step is the rate determining step of the whole process. Thus, it was safe to conclude that kinetic studies of this overall conversion provided information concerning only the electrocyclization step.

**Polar Effects.** One of the significant findings of this project was the observation of substantial polar effects on the reactions. For this isocyanate system, significant polar effects at the  $\alpha$ -carbon of the vinyl group were observed. Relative to the parent system, MP2 calculations revealed that putting electron donors  $\text{CH}_3$  and methoxyl group ( $\text{OCH}_3$  with  $\sigma_{\text{R}}^{\circ} = -0.43$ ) at the  $\alpha$ -carbon lowered the energy of activation by 3.7 kcal/mol and 7.9 kcal/mol, respectively. While, an electron acceptor ( $\text{CF}_3$ ) raises the energy of activation by 2.1 kcal/mol. These computational results supported our experimental results, as shown in Table 3-3. This polar effect can be understood in terms of donor/acceptor type interactions. Putting an electron donating group at the  $\alpha$ -position of the vinyl group can induce polarization of the transition state to some extent and results in a considerable lowering of the barrier to bond formation, which is rate-determining.


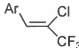
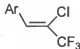

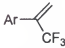
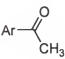
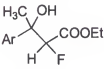
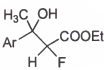
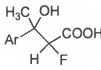
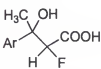
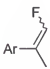
**Synthetic Explorations.** As discussed, extended kinetic studies on electrocyclic reactions were the main purpose of the project. To serve this purpose, some explorations were made to synthesize the precursors, especially for those fluorinated substrates. Due to its unique properties, fluorine atoms are possible to replace hydrogen in a wide range of hydrocarbon systems without gross distortion of the geometry of the system. (However, large perturbations of the molecular electronic distributions could be ensued.) Profound biological effects are often obtained when fluorine is substituted for hydrogen. One of the early studies was the synthesis of 5-fluorouracil in late 1950s<sup>135</sup>, which was found to exert considerable anti-tumor activity.

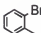


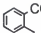
(5-FU)

In recent years, selectively incorporating fluorine atoms into organic molecules has become an area which attracts many organic chemists in material and pharmaceutical science. In exploring and synthesizing fluorine-containing molecules, concerns must be paid to the availability of the starting materials, the reaction conditions and the selectivity of reactions. The early fluorinating reagents, such as  $F_2$ <sup>136</sup>,  $HF$ <sup>137</sup>,  $XeF_6$ <sup>138</sup>,  $COF_2$ <sup>139</sup>,  $SF_4$ <sup>140</sup> and  $BrF_3$ <sup>141</sup>, normally react violently and reaction selectivities are usually poor. Introducing fluorine atoms directly into a molecule could also encounter technical difficulties. Using fluorine-containing building-blocks is now becoming an important alternative.

The reactions run during the research could be potentially useful in the fluoroorganic synthesis, as summarized in Figure 3-3. The reactions included: converting aldehydes and ketones to monofluoro olefins; preparing CF<sub>3</sub>-containing intermediates. Terminal HF-olefins<sup>142</sup> and trifluoromethylated<sup>143</sup> organic compounds are both of synthetic importance.

Starting Material <sup>a</sup>	Product	conditions	references
Ar-CHO		n-Bu <sub>3</sub> P/CH <sub>2</sub> Cl <sub>2</sub> /CFCl <sub>3</sub> then NaOH, 42%yield, 95%trans	133
Ar-CHO		Zn, CCl <sub>3</sub> CF <sub>3</sub> /THF, 50°C then AcOH, Zn, 50°C, 62%	115
	Ar-C≡CF <sub>3</sub>	NaNH <sub>2</sub> /t-butanol/benzene, 71%	115
Ar-C≡CF <sub>3</sub>		Zn(Ag)/CH <sub>3</sub> OH, reflux, 89%	116
Ar-I <sup>b</sup>		Pd(Ph <sub>3</sub> ) <sub>4</sub> /THF, 67%	104
		BrCFHCOOEt/Zn/THF, CeCl <sub>3</sub> (2%), 50%	127, 130
		NaOH/Ethanol(95%)(1eq) 64%	
		TsCl(1eq), pyr(2eq)/CHCl <sub>3</sub> , cis : trans=44:56	128, 129

a) Ar = 

b) Ar = 

## CHAPTER IV

### EXPERIMENTAL

#### General Methods

Experimental text discussing a “commercial” available material indicates such material was purchased from Aldrich, Fisher Science, PCR or SynQuest (Gainesville, Florida), and the material was used without further purification unless indicated in the text. A “dry” solvent was a material which was purified (distilled) off the appropriated drying agent and used immediately (or stored under an inert atmosphere). The following solvents and drying agents were used: diethyl ether (sodium benzophenone ketyl); tetrahydrofuran (THF) (sodium/potassium benzophenone ketyl), methylene chloride (Calcium hydride), triethyl amine (sodium benzophenone ketyl).

Nuclear Magnetic Resonance (NMR) chemical shifts were reported in parts per million (ppm) downfield from internal reference tetramethyl silane (TMS) for  $^1\text{H}$  and  $^{13}\text{C}$  spectrum and in ppm up field from internal reference  $\text{CFCl}_3$  for  $^{19}\text{F}$  spectra. All NMR spectra were obtained on Varian VXR300, Gemini 300 or Unity-500.  $^2\text{H}$  NMR spectra were obtained on Varian VXR300 in ppm with  $\text{CDCl}_3$  (7.26 ppm) as internal reference.

The kinetic studies were run in sealed NMR tubes (throw-away type #502 from Norrel Inc.). In order to eliminate the variation of the reaction condition, a group of NMR tubes were charged with the same stocked sample (with an internal standard) in

proper deuterated NMR solvent, and pyrolyzed simultaneously at an appropriate temperature to ascertain that the initial concentrations of the substrate were identical in all the tubes. The temperature of the oil-bath was measured with a thermocouple with an accuracy of  $\pm 0.1^\circ\text{C}$ . After a certain period of time, one of the tube was taken out from the oil-bath and was immediately frozen to  $-78^\circ\text{C}$  (a slurry of dry ice with isopropanol) to abort the reaction. The samples was thawed to room the temperature just before running the NMR. The peak change was recorded as its relative peak intensity with the respect to the internal standard. The plots for the kinetic studies were obtained from SigmaPlot (Scientific Graphing Software, V2.0) and errors of the measurements were interpreted from a QBasic program.

### Experimental Procedures

**2-Bromostyrene (50).** In a three necked 250-mL round bottom flask, which was equipped with a cooling condenser, a self-equalizing additional funnel and a rubber septum,  $\text{PPh}_3\text{CH}_3\text{Br}$  (41.59 g, 116.5 mmol) was dissolved in 100mL anhydrous tetrahydrofuran (THF). The whole system was flushed with  $\text{N}_2$  gas and the flask cooled to  $0^\circ\text{C}$ . *n*-Butyl lithium (from Aldrich, 2.5 M in hexanes, 44.8 mL, 112 mmol) was added to the flask with care through a syringe. After stirring for an hour, a solution of 2-bromobenzaldehyde (from Aldrich, 18.34 g, 99.1 mmol) in 100 mL THF was added via the additional funnel. An exothermic reaction took place and the color of the reaction mixture changed from colorless to orange. The reaction mixture was quenched with 200 mL brine after stirring at room temperature for 15 hours, and diluted with 100 mL

benzene. The organic phase was separated, and aqueous layer was extracted with benzene (100mL×2). The combined organic phase was washed with brine (100mL), and dried over anhydrous MgSO<sub>4</sub>. The solvent was removed by reduced pressure. Flash column chromatography with 10% ether in hexanes gave the pure product. Yield 13.76 g. (75.8%) <sup>1</sup>HNMR (CDCl<sub>3</sub>) δ 5.37 (d J= 11.1, 1H) 5.72 (d, J= 17.4, 1H) 7.5 (m 5H) <sup>13</sup>C NMR δ 137.449, 135.779, 132.842, 129.036, 127.440, 126.759, 123.581, 116.638

**2-Carboxystyrene (51).** In a 100-mL, 3-necked, round bottom flask, which was equipped with a cooling condenser, a self equalizing separation funnel and a rubber septum, activated magnesium (1.01 g, 42 mmol. Magnesium was washed with 10 HCl, distilled water, absolute alcohol and dry ether successfully and dried in the over prior to use.) was added. The system was flushed with nitrogen for 30 minutes. A solution of 2-bromostyrene (4.99 g, 27.3 mmol) in 20mL anhydrous ether was dripped into the flask just to cover the magnesium inside. The flask was warmed with a heat gun to initiate the reaction. More bromide solution was added when the reaction mixture was cloudy and slightly boiling. The bromide was added at a rate to maintain the boiling. After all the solution was added and refluxed for an hour, another 20 mL anhydrous ether was added to dilute the mixture. The reaction mixture was then quenched with dry ice. After the evolution of carbon dioxide had finished, the mixture was acidified with 10% HCl to pH 1. The organic layer was separated and aqueous phase was extracted with ether (20 mL×2). The organic phase was combined and the solvent was removed after drying over anhydrous MgSO<sub>4</sub>. A yellow solid was obtained (3.03 g, 75%). <sup>1</sup>HNMR (CDCl<sub>3</sub>) δ 5.37 (dd, J=11.1, 1.2, 1H), 5.60 (dd 17.1, 0.9 1H), 7.3 (m, 5H) <sup>13</sup>C NMR (CDCl<sub>3</sub>) δ 172.987,

140.632, 136.049, 133.166, 131.299, 127.581, 127.520, 127.080, 116.836. Elemental Analysis : Calculated for  $C_9H_8O_2$ , C 72.97%; H 5.41%. Found, C 72.67%; H 5.50%.

**2-Vinyl phenylisocyanate (52).** In a 5-mL, round-bottom flask, equipped with a drying tube, 2-carboxystyrene (0.40 g, 2.7 mmol) was mixed with oxalyl chloride (2M in  $CH_2Cl_2$ , 2mL, 4mmol). The mixture was stirred magnetically (bubbles formed significantly) overnight. The excess oxalyl chloride and the solvent methylene chloride were removed under vacuum. A yellow oily liquid was obtained.  $^1H$ NMR ( $CDCl_3$ )  $\delta$  5.46 (d, J 11.1 1H), 5.70 (dd, J 17.1, 0.6 1H) 7.25 (dd, J 18.6, 11.1 1H), 7.3 (m, 4H)  $^{13}C$  NMR  $\delta$  167.516, 140.199, 134.812, 134.190, 133.097, 131.412, 127.649, 118.634. The product was used for the next step without further purification. Sodium azide (0.15gram) was dissolved with a minimum amount of deionized water and cooled to  $0^\circ C$ . The acid chloride in 1mL dry acetone was added dropwise in a period of five minutes. After stirring magnetically at  $0^\circ C$  for 1.5 hours, the reaction mixture was diluted with 10mL ether, and about 5mL water. The organic layer was separated and the aqueous phase was extracted with ether (5mL $\times$ 2). The combined ether layer dried with anhydrous  $MgSO_4$ . Removal of the ether under reduced pressure gave a yellowish oily liquid. This liquid was further dried under high vacuum. This liquid was dissolved in  $C_6D_6$  and kept at room temperature for 10 hours. Proton NMR showed the conversion from azide to isocyanate was 100% complete.  $^1H$ NMR ( $CDCl_3$ )  $\delta$  5.40 (dd, J 11.1, 0.9 1H) 5.70 (dd, J 17.4, 0.9 1H) 6.90 (dd, J 17.7, 11.1 1H)  $^{13}C$  NMR  $\delta$  117.322, 116.791, 133.515, 131.800, 128.704, 127.490, 126.215, 126.002, 125.942.

**Quinol-2-one(56).** The kinetic experiments were run at five different temperatures: 103.1°C, 106.8°C, 109.4°C, 112.6°C and 115.7°C. Using methylene chloride as internal standard. The peak intensity of the isocyanate (starting material) was recorded relative to the peak intensity of the methylene chloride. After heating to infinite, the NMR conversion was 87%. <sup>1</sup>HNMR,  $\delta$  6.7 (d, 1H), 7.2 (t, 1H), 7.45 (d, 1H), 7.5(d, 1H), 7.55(t, 1H), 7.8(d, 1H), 12.4(b, 1H). (It is identical to the NMR published from Aldrich)<sup>144</sup>

Table 4-1. Data for the rate determining for the parent system, without pyridine

106.8°C	time (s)	1800	3300	5400	7200	9000	11400
	ln(rel-peak intensity)	0.728	0.586	0.420	0.250	0.120	-0.0753
103.1°C	time(s)	2400	4800	7200	9600	12000	14400
	ln(rel-peak intensity)	1.621	1.482	1.326	1.184	1.047	0.934
112.6°C	time(s)	-	-	3600	5400	7200	9000
	ln(rel-peak intensity)	-	-	0.133	-0.155	-0.310	-0.578
115.7°C	time (s)	1200	2400	3600	5400	7200	9000
	ln(rel-peak intensity)	0.550	0.370	0.194	-0.0603	-0.344	-0.627
109.5°C	time(s)	1800	3600	5400	7200	9000	10800
	ln(rel-peak intensity)	0.560	0.398	0.206	0.0505	-0.189	-0.295

Table 4-2. Data for the Arrhenius and Eyring plots, without pyridine

T(°C)	115.7	103.1	109.5	106.8	112.6
1/T ( $\times 10^{-3} \text{K}^{-1}$ )	2.571	2.657	2.613	2.632	2.592
ln(k)	-8.803	-9.753	-9.227	-9.393	-8.971
ln(k/T)	-14.767	-15.684	-15.174	-15.332	-14.927

Table 4-3. Data for the rate determining for the parent system, with pyridine

103.1°C	time (s)	2400	4800	-	9600	12000	14400
	ln(rel-peak intensity)	.253	.143	-	-.170	-.321	-.469
109.4°C	time(s)	1800	3600	5400	7200	9000	-

	ln(rel-peak intensity)	-0.0759	-0.281	-.442	-.650	-.771	-
115.7°C	time(s)	1200	2400	3600	4800	6000	7200
	ln(rel-peak intensity)	0.064	-0.220	-.335	-0.523	-0.793	-1.004

Table 4-4 Data for the Arrhenius and Eyring plots, with pyridine

T(°C)	109.4	115.7	103.1
1/T ( $\times 10^{-3} \text{K}^{-1}$ )	2.614	2.571	2.657
ln(k)	-9.234	-8.662	-9.753
ln(k/T)	-15.181	-14.625	-15.684

**2-Bromo- $\beta$ -fluorostyrene(107).** Into a 3-necked, 1L round bottom flask, equipped with a large condenser, a self-equalizing funnel and a rubber septum, n-tributyl phosphine (128mL 0.528mol) and anhydrous methylene chloride were added by syringe after the system was flushed with N<sub>2</sub> for 30 minutes. The flask was cooled to 0°C. CFC1<sub>3</sub> (16.6mL 0.182mol) was added by syringe in one portion. The cooling bath was removed after an hour. It was then stirred at room temperature for 4.5 hours, during which time, the color changed from colorless to clear bright yellow, with heat evolution. 2-Bromostyrene (25.17g, 0.136mol) was added dropwise over five minutes. After stirring at room temperature for 12 hours, NaOH (10% aqueous solution, 210mL) was added dropwise. After another 24 hours stirring at room temperature, the reaction was monitored by <sup>19</sup>FNMR. The organic phase was isolated and the aqueous layer was extracted with methylene chloride (50mL $\times$ 2). After washing with water (200mL), the

organic phase was dried over anhydrous  $\text{MgSO}_4$ . Removal of the solvent gave orange colored oily liquid. Four fractions were collected when the liquid was vacuum distilled: 1)  $35^\circ\text{C}/0.25\text{mmHg}$ , 0.3 g forerun; 2)  $35^\circ\text{C}/0.025\text{mmHg}$ , 2.9 g; 3)  $45^\circ\text{C}/0.025\text{mmHg}$ , 14.04 g; 4) greater than  $75^\circ\text{C}/0.025\text{mmHg}$ , 1.06 g. All four fractions showed the same  $^{19}\text{F}$  signals. Fractions 2) and 3) were combined and flash column chromatography (10% ether in hexanes) was performed to yield afford the product., (14.5 g, 53% yield. a mixture of 5% *cis* isomer and 95% *trans* isomer,  $^3\text{J}(\text{F},\text{H}) = 46.5 \text{ Hz}$ ,  $^{\text{cis}}\text{J}(\text{F},\text{H}) = 21.0 \text{ Hz}$ ).  $^1\text{HNMR}$  ( $\text{CDCl}_3$ ), 6.0(dd) 6.5-7.8 (m) Irradiating the mixture with *ca.* 2% benzophenone in chloroform for 4 hours gave 50:50 mixture of *cis* and *trans* isomers. Further vacuum distillation  $40^\circ\text{C}/0.05\text{mmHg}$  yielded a colorless liquid.  $^{19}\text{FNMR}$  ( $\text{CDCl}_3$ )  $\delta$  -124.3 (dd, 88.2, 21.0), -122.0 (dd, 88.2, 46.5)

**2-Carboxyl- $\beta$ -fluorostyrene(108).** Into a 3-necked 250mL round bottom flask, equipped with a condenser, a rubber septum and a glass stopper, 2-bromo- $\beta$ -fluorostyrene (1.55g, 7.7mmol) and THF (120mL) were charged. The flask, while flushing with  $\text{N}_2$ , was cooled to  $-78^\circ\text{C}$  with dry ice acetone bath. After 10 minutes, *t*-butyl lithium (Aldrich 9.10mL, 1.7 M in pentane) was added through a syringe with care in about 10 minutes. The reaction mixture changed from colorless to yellow and then blood red. After stirring at  $-78^\circ\text{C}$  for an hour, anhydrous  $\text{CO}_2$  was bubbled through the reaction mixture with stainless steel needle. The color changed immediately to golden yellow. The mixture was allowed to warm up to room temperature while  $\text{CO}_2$  was still bubbling through. The mixture was then acidified with 10% HCl to pH 1, extracted with methylene chloride (100mL $\times$ 3). The organic phase was washed with water (100mL) and dried over

anhydrous calcium chloride. Removal of the solvent to give a yellow solid. The solid was dissolved in 25 mL ether and it was extracted with 10% NaOH (10mL×3). The combined aqueous layer was neutralized with 10% HCl to pH 1. Ether extraction and removal of the ether gave a light yellow solid. (yield 9.4 g, 73.5%) For *trans* isomer (95%),  $^{19}\text{F}$ NMR ( $\text{CDCl}_3$ ,  $\text{CFCI}_3$ ) -124.6 (dd, J 19.53Hz, 83.01Hz);  $^{13}\text{C}$ NMR, 172.565, 152.428, 148.963, 135.082 (d, 48.8Hz), 133.319, 132.011, 127.691(d, 26.2Hz), 127.244 (d, 15.2Hz), 113.703 (d, 69.6Hz); High Resolution Spectra: Calculated for  $\text{C}_9\text{H}_7\text{O}_2\text{F}$ = 166.0430, Measured =166.0418.

**2- $\beta$ -Fluorovinyl-phenylisocyanate(109).** It was synthesized in the same way as for the parent hydrocarbon system.  $^{19}\text{F}$ NMR  $\delta$  -123.7 (dd, 88.2, 20.7) -120.7 (dd, 88.2, 46.8)

**3-Fluoro-quinol-2-one.** The kinetic experiments were run in  $\text{C}_6\text{D}_6$ , at 178.9°C, using monofluorobenzene as an internal reference.  $^{19}\text{F}$ NMR( $\text{C}_6\text{D}_6$ ),  $\delta$  -131.0 (d, 10Hz) Isolation of the product was unsuccessful.

Table 4-5 Data used to determine the rate of monofluoro system at 178.9°C

time(s)	1800	3600	5400	9000	12600	16200
ln(rel-peak) <i>trans</i>	-0.241	-0.523	-0.69	-1.507	-2.506	-3.031
ln(rel-peak) <i>cis</i>	-0.523	-0.586	-0.606	-0.714	-0.848	-1.036

**1-Bromo-2-((*E/Z*)-1-propenyl) benzene(85).** Into a 250mL 3-necked flask, equipped with a self-equalizing funnel, a rubber septum and a condenser (as  $\text{N}_2$ ) outlet to oil bubbler.  $\text{Ph}_3\text{PCH}_2\text{CH}_3\text{Br}$  (21.72g, 58.54mmol) was suspended in 50mL dry THF.

The mixture was stirred under N<sub>2</sub> and chilled to 0°C. Then *n*-ButylLi (2.5M in hexanes, 23.4mL, 58.50mmol) was charged with care through a syringe. (The color changed from white to yellow and than bloody red) After one hour, a solution of starting material, 2-bromobenzaldehyde (9.67g, 52.27mmol) in 50mL dry THF was dripped into the mixture via the self-equalizing funnel. Stirring was continued at room temperature for 24 hours. The reaction mixture was then quenched with brine (*ca.* 150mL) and extracted with methylene chloride(100mL, thrice). Organic layer was washed with brine, dried over magnesium sulfate (anhydrous). The solvent was evaporated under vacuum. The obtained yellow oily liquid solidified in refrigerator with some liquid. The liquid part was purified by flash chromatography (silica gel, 2 inch i.d.; 8 inch long). The first fraction, a light yellow oil, was collected as product. Yield, 9.46g, 91.8%. *cis* : *trans* = 45:55. <sup>1</sup>HNMR, the *trans* isomer, 1.90 (dd), 6.00 (dq), 6.60(dq); the *cis* isomer, 2.00 (dd), 6.30 (dq), 6.82(dq), and 7.1-7.7 (m)

**2-((*E/Z*)-1-Propenyl) benzoic acid(86).** Into a 250mL 3-necked round bottom flask, equipped with a rubble septum, a glass stopper and N<sub>2</sub> outlet to oil bubbler, the precedent product (1.59g, 8.07mmol) was dissolved in THF (100mL, anhydrous) and cooled to -78oC (isopropanol with dry ice) under N<sub>2</sub>. After 10 minutes, *t*-butyl lithium (1.7M in pentane, 9.5mL, 16.15mmol) was added into the mixture with care by a syringe in about 10 minutes period. (The color changed from colorless to brown). The mixture was stirred at that temperature for 1.5 hours. Anhydrous carbon dioxide was then bubbled through. (The color changed slowly to pink.) the temperature was kept at -78°C for another 10 minutes, then the flask was allowed to warm to room temperature by itself.

After acidification with 10%HCl (aqueous) to pH1, the reaction mixture was extracted with methylene chloride (100mL, thrice). The organic layer was washed with water, then rotary-evaporating off the solvent to obtain a yellow oil, which transformed to a light yellow solid under high vacuum. Yield, 1.17g, 89.5%. *cis* : *trans* = 44 :46,  $^1\text{H}$ NMR:  $\delta$  7.0-8.2 (multiplet), *cis* isomer, 1.76 (dd, J 7.15Hz, 1.64Hz), 5.88 (dq, 11.54Hz, 7.14Hz); *trans* isomer 1.95 (dd, 6.59Hz, 1.65Hz), 6.20 (dq, 15.66Hz, 6.87Hz). High Resolution Spectra: Calculated for  $\text{C}_{10}\text{H}_{10}\text{O}_2$ =162.0681, Measured =162.0679

**2- $\beta$ -Methyl-phenylisocyanate(87).** They were synthesized using the same methodology as for the fluorinated system.

**3-Methyl-quinol-2-one.** The kinetic experiments were run at 112.6°C in  $\text{C}_6\text{D}_6$ .  $^1\text{H}$ NMR  $\delta$  2.11(d, 1.1Hz, 3H), 7.1(dt, 1H, 1.37Hz, 7.14Hz), 7.31(d, 1H, 7.7Hz) 7.41(t, 1H, 10.25Hz), 7.56(dd, 1H, 1.37Hz, 7.97Hz), 7.75 (s, 1H), 11.80(b,1H);  $^{13}\text{C}$ NMR  $\delta$  16.459, 114.677, 119.5, 121.506, 126.848, 128.942, 129.807, 136.257, 137.881, 162.390; High Resolution Spectra:  $\text{C}_{10}\text{H}_9\text{NO}$  Calculated = 159.0684; Measured=159.0682

Table 4-6 Data for determining the rate constants for  $\beta$ -methyl system, at 112.6°C.

time(s)	1800	3600	5400	7200	10800	14400
ln(rel-peak) <i>trans</i>	0.655	0.388	0.338	0.192	-0.111	-0.298
time(s)	1800	-	5400	7200	10800	14400
ln(rel-peak) <i>cis</i>	0.9335	-	0.922	0.912	0.889	0.855

**1-Bromo-2-isopropenyl benzene(70).** Into a 250mL 3-necked round bottom flask, which was equipped with cooling condenser, self-equalizing additional funnel and

a rubber septum,  $\text{Ph}_3\text{PCH}_2\text{Br}$  (10.7 grams, 30mmol) was suspended in 50mL dry THF. The flask was flashed with  $\text{N}_2$  and cooled to  $0^\circ\text{C}$ . After *n*-butyl lithium (12mL, 2.5 M in hexanes) was charged with plastic syringe, the mixture was stirred for one hour. 2-Bromo-acetylphenone (5 grams in 50mL dry THF) was dropped into the flask form the equalizing additional funnel. The mixture was then stirred at room temperature for 15 hours. Quenching the reaction mixture with 100mL of brine and extracting the brine with methylene chloride (30mL, thrice) and rotary-evaporating off the solvent gave a yellowish oil. Running a short silica gel chromatography with 100% hexanes yielded a yellow liquid (the first fraction). 3.2 grams, 65.0%  $^1\text{H}$ NMR ( $\text{CDCl}_3$ )  $\delta$  2.00 (s, 3H), 5.00 (s, 1H), 5.37(s, 1H), 7.62 (d, 1H), 7.2-7.4 (m, 3H).  $^{13}\text{C}$ NMR  $\delta$  145.77, 144.80, 132.72, 129.69, 128.32, 127.20, 121.52, 115.98, 23.51.

**2-iso-Propenyl benzoic acid(71).** Into a 100mL 3-necked round bottom flask, equipped with a cooling condenser, self-equalizing additional funnel and a rubber septum, activated magnesium (1g, it was activated by washing successively with 5% aqueous hydrochloric acid, absolute ethanol and anhydrous ethyl ether) . The setup was then flushed with  $\text{N}_2$  and flame dried. A solution of 2-bromo- $\alpha$ -methylstyrene (1.5g, 7.6mmol) in 20mL dry ether was added to the flask to just cover the magnesium. A small crystal of iodine was also added at the same time. The reaction was self-initiated without external heating. The iodine color was discharged as the mixture maintained slightly boiling. The rest of the bromide was added at a rate to keep the boiling. The additional funnel was rinsed with another 20mL ether and the reaction mixture was kept boiling by warm water for an hour. The mixture was then quenched with dry ice. After the

evolution of the carbon dioxide finished, the mixture was acidified with 10% HCl to pH

1. The organic layer was separated and aqueous phase was extracted with diethyl ether (20mL, twice). The organic phase was combined and the solvent was removed after drying over anhydrous magnesium sulfate. A yellow solid was obtained. 0.88g, 71.5%.

$^1\text{H NMR}(\text{CDCl}_3)$   $\delta$  2.20 (s, 3H), 4.90 (s, 1H), 5.10 (s, 1H), 7.22(d, 1H), 7.28 (t, 1H), 7.50 (t, 1H), 7.90 (d, 1H);  $^{13}\text{C NMR}(\text{CDCl}_3)$   $\delta$  173.54, 146.51, 146.23, 132.53, 130.68, 129.68, 127.98, 126.94, 113.83, 24.22. High Resolution Spectra: Calculated for  $\text{C}_{10}\text{H}_{10}\text{O}_2=162.0681$ , Measured=162.0682

**4-Methyl-quinol-2-one.** The kinetic was run at 35.0°C from acyl azide in  $\text{C}_6\text{D}_6$ .

The peak decrease of the acyl azide was recorded from an acquisition array. Total 9

FIDs were collected. No internal standards were used to measure the peak.

$^1\text{H NMR}(\text{CDCl}_3)$  2.41(s, 3H), 6.50(s, 1H), 7.20(t, 1H), 7.30(d, 1H), 7.40(t, 1H), 7.60(d, 1H), 12.0(b, 1H)

Table 4-7. Data for estimating the rate constant of the  $\alpha$ -methyl system. Peak intensities were real from the array.

time(s)	600	1200	1800	2400	3000	3600	4200	4800	5400
ln(peak)	3.051	2.983	2.916	2.828	2.753	2.689	2.600	2.544	2.466

**Tri-n-butyl-vinyltin.** Tri-n-butyl tin(32,1g, 110.7mmol), AIBN (1.6g) and thiophene free benzene (80mL) was mixed in 800mL autoclave. The Autoclave was then cooled to -78°C and purged three times with  $\text{N}_2$ , and then cooled to -190°C with liquid nitrogen and about 10mL acetylene. The autoclave was then heated to 80°C with stir for

45°C, cooled and pressure was released. After benzene was removed by vacuum, tri-*n*-butyl-vinyl tin was then distilled under reduced pressure (95°C/1.0mmHg), yield 25g.

**Bromomethyltriphenylphosphonium bromide (Ph<sub>3</sub>PCH<sub>2</sub>BrBr).**

Dibromomethane (26.68g, 153mmol), triphenylphosphine (19.91g, 76 mmol) and toluene (100mL) was mixed in a 250mL round bottom flask equipped with a condenser. The reaction mixture was heated to reflux. After a couple of hours, some yellow oily substance formed at the bottom of the flask. The oily substance was removed by decanting the liquid out. The liquid was then refluxed for 24 hours. By cooling to 0°C, a white solid precipitated out, which was collected by suction. The filtrate was heated to reflux for another 24 hours. More solid was collected. Drying the combined solid product in an oven (100°C). 21g, 63.4%, <sup>1</sup>HNMR (CDCl<sub>3</sub>), δ 5.85(d, 5.77Hz), 7.6-8.0(m)

**2,β'-Dibromostyrene(61).** Into a 3-necked flask, Ph<sub>3</sub>PCH<sub>2</sub>BrBr (14.4g, 33.3mmol) and potassium *t*-butoxide (3.57g, 31.08mmol) were suspended in dry THF (30mL). The flask was flushed with N<sub>2</sub> and cooled to -78°C. The suspension was stirred rapidly for 2 hours at that temperature. 2-bromobenzaldehyde in 10mL THF was added through a self-equalizing funnel in a 5 minute time period. The mixture was stirred overnight. The temperature was raised slowly by itself to room temperature. The reaction mixture was then quenched with 50mL brine and the brine solution was extracted with methylene chloride (50mL in 3 portions). After washing the extract with another 50mL brine, it was dried over magnesium sulfate. The solvent was removed by rota-evaporation. Flash chromatography with silica gel (100% hexanes, the first fraction) yielded a yellow liquid. 4.2g, 72.1% yield, (*cis* : *trans* = 11:1, *cis*<sup>3</sup>J(H,H)= 7.8 Hz,

$trans^3J(H,H) = 13.9$  Hz),  $^1H$ NMR,  $\delta$  6.20 (d,  $J=9.0$  Hz); 6.40 (d,  $J=13.5$ Hz); 6.8-7.8 (multiplet). The second fraction was the starting material 2-bromobenzaldehyde.

**2-Bromo-phenylacetylene- $d_1$  (62).** Into a 3-necked round bottom flask, which was equipped with N<sub>2</sub> inlet, outlet and a self-equalizing funnel, the precedent dibromide (4.70g, 17.9mmol) was dissolved in dry THF (20mL). The joints were greased and sealed with Teflon tape. The flask was chilled to  $-78^\circ C$ . Potassium t-butoxide (4.00g, 35.7mmol, in 10mL THF) was added through the self-equalizing funnel dropwisely. The reaction mixture stirred for 4 hours and warmed up gradually to  $0^\circ C$ . (The mixture was red in color). Deuterated water (D<sub>2</sub>O, in excess) was added slowly. Some white solid was formed. The solvent was removed by rotary-evaporation. The obtained crude mixture was diluted with some hexanes. The liquid was decanted away from the solid. The hexanes extract was concentrated and flash chromatography yielded 2.88g (88.0%) light yellow liquid.  $^1H$ NMR showed the ratio of deuterium and protonium was 13:1.  $^1H$ NMR(CDCl<sub>3</sub>),  $\delta$  7.60 (m), 7.20(m), 3.40(s);  $^2H$ NMR(CD<sub>3</sub>OD), 3.48(s).

**2-Bromo- $\beta$ - $d_1$  styrene(63).** In a 3-necked flask, which was equipped with a balloon, a stopper and a connection to vacuum line, Lindlar catalyst (0.5g, Palladium on calcium carbonate, poisoned with lead, dried in oven) is suspended in methanol (5mL, dried over molecular sieve). 2-bromophenylacetylene (2g, 11.0mmol) is added. All the joints were well-greased. The balloon was first charged with N<sub>2</sub>. The system was then evacuated and purged with N<sub>2</sub> for more than three times. The balloon was in turn charged with hydrogen (at least 500mL). The system was again purged with H<sub>2</sub> for several times. The stop-cock was closed to the vacuum line and the one to the balloon was opened. The

mixture was stirred at room temperature for 24 hours. Deuterium NMR showed the completion of the hydrogenation. The catalyst was filtered off and solvent methanol was rotary-evaporated off. The obtained yellow liquid was purified by running a short silica gel column with 100% hexanes as eluting solvent. Yield: 1.8g, 89.0%,  $^1\text{H}$ NMR ( $\text{CDCl}_3$ )  $\delta$  7.65 - 7.10 (m),  $\delta$  5.80 (dd, J, 17.1, 0.9, associated with non deuterated isomer)  $\delta$  5.78 (d, J=17.1, *trans* deuterated isomer)  $\delta$  5.57 (dd, J, 11.4, .9, non deuterated isomer),  $\delta$  5.55 (d, J=11.4, *cis* deuterated isomer). The ratio of *cis*-deuterium, *trans*-deuterium and non deuterium products was 50 : 20 : 30.  $^2\text{H}$ NMR ( $\text{CHCl}_3$ ,  $\text{CDCl}_3$  as reference),  $\delta$  5.07 (d, J=9.6) for the *trans* isomer;  $\delta$  5.41 (d, 17.7) for the *cis* isomer.

**2-Carboxy- $\beta$ - $\text{d}_1$  styrene(64).** In the same way as the parent hydrocarbon system via Grignard reaction.  $^{13}\text{C}$ ( $\text{CDCl}_3$ )  $\delta$  172.48, 140.28, 135.89, 132.80, 131.10, 127.71, 127.35, 116.544, 116.27, 115.95;  $^1\text{H}$ NMR ( $\text{CDCl}_3$ , Unity-500),  $\delta$  8.02(d), 7.28-7.60 (m), 5.67 (dd, J, 17.5, 0.9, non-deuterated isomer),  $\delta$  5.65 (d, J=17.5),  $\delta$  5.39 (dd, J, 10.0, 0.9, non-deuterated isomer,  $\delta$  5.37 d, J=10). Product:  $^1\text{H}$ NMR( $\text{CDCl}_3$ , Unity-500) 6.75 (d, non-deuterated, 0.36), 7.82(d and s, non-deuterated and deuterated product, 0.71), 7.2-7.6 (m)

Table 4-8. Data for determining the deuterium isotope effects for  $\beta$ -substitution.

time(s)	1800	3600	5400	7200	9000	10800
ln(rel-peak) non-d	0.3647	0.2009	-0.0391	-0.2388	-0.3946	-0.5108
ln(rel-peak) <i>trans</i>	-0.8944	-0.9826	-1.2984	-1.4232	-1.5759	-1.7304
ln(rel-peak) <i>cis</i>	-0.03714	-0.1709	-0.3991	-0.5576	-0.7153	-0.8372

**Ethyl -2-Iodo-benzoate(74).** Into a three necked round bottom flask, which was equipped with a condenser (with drying tube on top), rubber septum and glass stopper, 2-iodobenzoic acid (10 g, 40mmol) was dissolved in ethanol (ca. 10mL). The mixture was not homogeneous at beginning. After the flask was cooled 0°C, thionyl chloride (4mL) was charged with care through syringe in 5 minute time period. When addition of SOCl<sub>2</sub> finished 1 drop of N,N-dimethylformaldehyde was added as catalyst. The flask was warmed to 70 °C. The reaction completion was monitored with TLC. Reaction was not completed after 4 hours, while overnight stirring and warming gave one spot in TLC (run in 50 : 50 ether and hexanes). The excess alcohol was removed by rotary-evaporation.. the obtained yellow oily liquid was then purified by short chromatography (silica gel, 6 inches long, about 2.5 inches inner diameter) with 50 : 50 mixture of ether and hexanes. Yield 10.8 g (97%). <sup>1</sup>HNMR(CDCl<sub>3</sub>), δ 1.50 (t, 3H), 4.50 (d, 2H), 7.20 (t, 1H), 7.45(t, 1H), 7.90(d, 1H), 8.10(d, 1H).

**Zinc-Silver couple, Zn(Ag).** To a well stirred refluxing solution of silver acetate (100mg) in glacial acetic acid (200mL), zinc powder (100g) was added all at once portion and the mixture was stirred for 30 seconds then quickly cooled by running tap water outside of the flask. Zinc-Silver couple so formed and was isolated by simple decanting, washed several times with anhydrous ethyl ether to remove excess acetic acid the dried under full vacuum, stored at room temperature.

**Making Pd(PPh<sub>3</sub>)<sub>4</sub>.** Palladium dichloride (0.5 g, 2.8 mmol) , triphenylphosphine (3.7 g, 14.1 mmol) and 36 mL DMSO were mixed in a three necked 50 mL round bottom

flask equipped with an outlet to oil bubbler, a rubber septum and a glass stopper. The system was flushed with gaseous nitrogen for 30 minutes. The yellow mixture was then heated slowly with oil bath and stirred fast with magnetic bar. When the oil bath reached 150 °C, a yellow homogeneous solution was obtained. The oil bath was taken away. Hydrazine monohydrate (0.6 mL) was added by means of syringe while the mixture was stirred. A vigorous reaction takes place with evolution of nitrogen gas. Yellow precipitate formed when the yellow solution was cooled by itself to room temperature. The precipitate was filtered under N<sub>2</sub>. The solid was with dry 50mL ethyl ether and 50mL absolute ethanol and dried with a slow N<sub>2</sub> stream overnight. Yield 2.9g, the yellow bright crystalline turned to slightly orange in the air. The product should be stored under N<sub>2</sub> and kept cold in refrigerator. The reactivity will be lost is the catalyst turned to reddish. The reactivity can be recovered by recrystallizing it from hot benzene.

**3,3,3-Trifluoroisopropenyl zinc reagent (76).** To a suspension of zinc(Ag) (2.5g, 38mol) in THF (20mL, anhydrous) was added trimethyl chlorosilane (0.5mL, fresh distilled) during stirring under N<sub>2</sub>. After 10 minutes, TMEDA (tetramethylethylenediamine) (6mL) was added and followed by 2-bromotrifluoropropene. After the addition, the mixture was heated to 60 degrees (temperature of the oil bath) for 9 hours. <sup>19</sup>FNMR showed the completion of the reaction ( $\delta$  -69.424ppm for starting material to  $\delta$  -59.952ppm). The mixture was used as such for the coupling reaction without determining the yield. <sup>19</sup>FNMR (CCl<sub>3</sub>F)  $\delta$  -59.952ppm. (Side note: On addition of trimethylchlorosilane, the Zn(Ag) couple became spongy and much more reactive.)

**Ethyl (2-(1-trifluoromethyl)vinyl) benzoate(77).** The precedent reaction mixture was filtered through celite ( it is important to get rid of the excess zinc.) under  $N_2$ . Into the filtrate, 0.2g of  $Pd(PPh_3)_4$  and ethyl 2-iodobenzoate (2.7g, 10mmol). The reaction was carried out under  $N_2$ , refluxing overnight to completion. (The reaction was monitored by  $^{19}F$ NMR, from starting zinc reagent (-60.0ppm) to product (-66.4ppm)). The resulting yellow mixture was then cooled and was poured into 100mL pentane. Some yellow solid precipitated out. The solid was triturated and decanted. The filtrate was concentrated and the product was purified with flash chromatography. Yield 1.70g (67%).  $^1H$ NMR( $CDCl_3$ ), 1.40 (t, 3H), 4.40 (q, 2H), 5.60(s, 1H), 6.10(s,1H), 7.4(d, 1H), 7.50-7.62(m, 1H), 8.20(d, 1H);  $^{19}F$ NMR ( $CCl_3F$ ,  $CDCl_3$ ) -66.366ppm

**2-(1-(Trifluoromethyl) vinyl) benzoic acid (78).** The previous product (0.7g) was mixed with NaOH (20%, 10mL aqueous solution), ethanol (5mL) was added for enhancing the solubility. The oil bath was set at  $90^\circ C$  to reflux the reaction mixture for 2 hours. A homogeneous solution was formed. (The reaction was monitored by  $^{19}F$ NMR, from starting material(-66.366ppm to product (-66.235ppm) The flask was then cooled diluted it with small amount of water, and then poured into 20% hydrochloric acid. The acidity of the resulting mixture was adjust to pH1. Extracting with methylene chloride, drying the extract and rotary-evaporating off the solvent gave light yellow solid. Yield 0.35g (57%).  $^{19}F$ NMR( $CDCl_3$ ,  $CFC_3$ )  $\delta$ -66.256;  $^1H$ NMR( $CDCl_3$ ) 5.61(s,1H), 6.18(s,1H), 7.40(d,1H), 7.60(t,1H), 7.65(t,1H), 8.20(d,1H); High Resolution Spectra: Calculated for  $C_{10}H_7O_2F_3=216.0398$ , Measured: 216.0424. The kinetic experiment was run at  $149.3^\circ C$ , using  $\alpha,\alpha,\alpha$ -trifluorotoluene as internal standard.  $^{19}F$ NMR( $C_6D_6$ ,  $CF_3Ph$ ,

-62.5ppm),  $\delta$ -66.874,  $^1\text{H}$ NMR 7.1.(s, 1H), 7.35(t, 1H), 7.45 (d,1H), 7.62(t, 1H), 7.88(d, 1H), 12.0(b, 1H)

Table 4-9 Data for determining the rate constant of  $\alpha$ -trifluoromethyl system, at 149.3°C.

time(s)	1200	2400	3600	4800	6000	7200
ln(rel-peak)	0.199	0.1404	0.0381	-0.0342	-0.118	-0.208

**2-Bromo-1-(2-chloro-3,3,3-trifluoropropenyl) benzene (91).** Into N,N-dimethylformaldehyde (20mL) solution of 2-bromobenzaldehyde (5.6g, 30mmol) were added 1,1,1-trichloro-2,2,2-trifluoroethane (6.8g, 36mmol) and zinc powder (2.1g, 32mmol). The mixture was stirred at room temperature for 1 hour then at 50°C for 24 hours. The mixture was then treated with acetic anhydride (4mL) and more zinc powder (3.93g, 60mmol). After the resulting mixture was stirred for 2 hours at 50 °C, pured into 10% hydrochloric acid (100mL) and extracted with diethyl ether (100mL $\times$ 3) . The ethereal extract was washed successfully with saturated sodium hydrogencarbonate aqueous solution and saturated sodium chloride aqueous solution and dried over magnesium sulfate. Running flash chromatography to yield 5.3 g product. (62.0%). *cis:trans* = 6.8:1. The *cis* and *trans* isomers were not isolated and proceeded to the next elimination reaction.  $^{19}\text{F}$ NMR ( $\text{CDCl}_3$ ,  $\text{CCl}_3\text{F}$ )  $\delta$  -67.6ppm (*trans*), -74.1ppm (*cis*).  $^1\text{H}$ NMR( $\text{CDCl}_3$ )  $\delta$  6.90 (s, 1H) 7.24 (t, 1H), 7.40 (t, 1H), 7.68 (d, 1H), 7.9 (d, 1H).

**2-bromo-(3,3,3-trifluoropropynyl) benzene(92).** Into a 100mL three necked round bottom flask, which was equipped with rubber septum, glass stopper and  $\text{N}_2$  outlet, sodium amide (2.73g, 70mmol) was added to benzene (50mL) solution of precedent

product (3.0g, 10mmol). The mixture was stirred under  $N_2$ . To the resulting mixture was added t-butyl alcohol (6.64mL, 70mL) at room temperature. The mixture immediately turned to thick. The mixture was stirred for 4 hours. (The reaction completion was monitored by  $^{19}F$ NMR.) after the completion, the mixture was pored into 100mL 10% hydrochloric acid. The aqueous layer was extracted with diethyl ether (50mL $\times$ 2). The combined organic layer was washed with saturated sodium hydrogencarbonate aqueous solution (50mL, twice) and dried over magnesium sulfate. Concentration followed by flash column chromatography gave 1.8g product (71%).  $^{19}F$ NMR ( $CDCl_3$ ,  $CCl_3F$ ),  $\delta$  - 50.663ppm.  $^1H$ NMR ( $CDCl_3$ )  $\delta$  7.2-7.8 (m). (Side note: Potassium t-butoxide as the base was *not* effective onto the elimination reaction.)

**1-bromo-2-((E)-(3,3,3-trifluoro-1-propenyl) benzene(93).** The precedent product (2.0g, 8mmol) was dissolved in methanol(100mL) with Zinc(Ag) couple (1.0g, 15mmol). The mixture was heated to reflux and stirred overnight. The completion of the reaction was monitored with  $^{19}F$ NMR. When the reaction was completed, the mixture was poured into 1M hydrochloric acid to dissolve the excess zinc. Extracting with diethyl ether and drying over anhydrous magnesium sulfate, followed by concentrating and running short flash column chromatography to give 1.8 g product. (89%)  $^1H$ NMR( $CDCl_3$ ) 5.85(m) 7.0(d), 7.2-7.4(m), 7.6(d);  $^{19}F$ NMR ( $CDCl_3$ ,  $CFC_3$ ) -58.390 (d,9.33Hz)

**2-((Z)-(3,3,3-trifluoro-1-propenyl) benzoic acid(95).**

$^1H$ NMR( $CDCl_3$ , TMS):  $\delta$  5.85 (dq, 12.20Hz, 8.30Hz, 8.3Hz), 7.40(d, 7.69Hz), 7.50(t, 10.99Hz), 7.62(t, 7.69Hz), 8.20(d,7.69Hz );  $^{13}C$ NMR ( $CDCl_3$ , TMS), 118.066(q,

33.21Hz, 34.36Hz), 124.682, 126.974, 128.658, 130.267, 130.237, 131.390, 133.150, 137.126, 139.980 (q, 7.72Hz), 171.363.  $^{19}\text{F}$ NMR ( $\text{CDCl}_3$ ,  $\text{CFCl}_3$ )  $\delta$ -57.762 (d, 9.877Hz)  
 Elemental Analysis: Calculated for  $\text{C}_{10}\text{H}_7\text{O}_2\text{F}_3$ : C 55.56%, H 3.24%; Found: C 55.287%, H 3.172%

**2-((E/Z)-(3,3,3-trifluoro-1-propenyl) benzoic acid(95).** Irradiating (254nm, 1.5 hours) in a quartz tube using chloroform as solvent to give a 1:3 mixture of the *cis* and *trans* isomer.  $^{19}\text{F}$ NMR ( $\text{CDCl}_3$ ,  $\text{CFCl}_3$ ),  $\delta$ -57.050 (d, 9.6Hz), 63.521 (d, 7.3Hz)

Table 4-9 Data for determining the rate constant of  $\beta$ -trifluoromethyl system, at 182.3°C.

time(s)	1200	3000	4800	6600	8400
ln(rel-peak) <i>trans</i>	-1.215	-1.319	-1.497	-1.688	-1.836
ln(rel-peak) <i>cis</i>	-1.661	-1.684	-1.764	-1.779	-1.867

**Ethyl 2-fluoro-3-hydroxy-3-phenyl-butyrate(101).** In a flame dried 100 mL 3-necked flask, which was equipped with cooling water condenser, glass stopper and rubber septum, Zn powder (1.75 g, activated by washing with 1N aqueous HCl, absolute ethanol, anhydrous ether successfully, and then dried under full vacuum.) and  $\text{CeCl}_3$  (dehydrated from  $\text{CeCl}_3 \cdot 7\text{H}_2\text{O}$  by flame dried under full vacuum.) were suspended in THF (anhydrous, 15mL). The mixture was stirred at room temperature under nitrogen. 2-Bromo acetyl phenone was charged with syringe. Into the resulting mixture, ethyl bromofluoroacetate was then added with care in a period of 5 minutes. Exothermic reaction occurred. In about 7 minutes, the reaction was so exothermic that it ended up with a vigorous refluxing, which subsided in about 10 minutes, resulting a yellow cloudy mixture.  $^{19}\text{F}$ NMR showed the completion of the reaction in 30 minutes. From doublet -

151ppm (starting material) to doublet -194ppm and doublet -201 ppm (product) and triplet -230ppm (reduction product, *ca.* 35%) By pouring the mixture into saturated  $\text{NH}_4\text{Cl}$ , extracting it with ethyl acetate (100mL in three portions) and evaporating off the solvent to obtain a gray oily liquid. A short column chromatography (silica gel, with 20:80 ethyl acetate in hexanes) was run to yield yellowish oily liquid, which formed yellow solid by standing in the fume hood.  $^{19}\text{F}$ NMR 194.794 (d, 46.53Hz), 200.522(d, 48,79Hz), ratio of two isomers is 41:59.

**2-Fluoro-3-hydroxy-3-phenyl-butyric acid (102).** The starting material (2.5g, 8.2mmol) was dissolved in 5 mL ethanol, stirred at zero degrees, then 8 mL 1N NaOH in ethanol was added to the mixture. It was stirred at room temperature to cloudy (over night).  $^{19}\text{F}$ NMR from the crude mixture showed the completion of the reaction. (From doublet -194 and doublet at -201 for starting material to doublet -185 and d -190ppm.) Rotary-evaporating off the ethanol after adding about 5mL water. After acidifying it with 1N HCl to PH4, the mixture was extracted with ether. (100mL in three portions.) Drying the ether layer with magnesium sulfate and evaporating off the solvent to yield a yellow solid (1.2g, 52.8%).  $^{19}\text{F}$ NMR( $\text{CDCl}_3$ ), -185.297 (d, 48.786Hz), -190.185 (d, 51.324Hz), ratio 38:62

**1-bromo-2-((E/Z)-2-fluoro-1-methyl-1-ethyl) benzene(103).**  $\text{CHCl}_3$ , starting material and pyridine were mixed in a sealable tube, then they were cooled to zero degrees. TsCl was then added by syringe slowly. The tube was sealed, and the mixture was stirred at room temperature for two hours. It was then warmed up slowly to 170 degrees.  $^{19}\text{F}$ NMR was checked. The reaction was completed when the temperature of oil

bath reached to 180 degrees for two hours. (From  $\delta$  -184 and  $\delta$  -190ppm to  $\delta$  -127 and  $\delta$  -129ppm). The mixture was then poured into  $\text{NH}_4\text{Cl}$  solution to wash off pyridine. The organic layer is evaporated. Flash chromatography with silica gel (20:80 ether in hexanes). First fraction to give the product.  $^{19}\text{F}$ NMR  $\delta$  -127.426 (d, 83.02Hz), -129.277(d, 85.45Hz), ratio of two isomer = 40:60.

**2-((E/Z)-2-fluoro-1-methyl-1-ethenyl) benzoic acid(104).** Into a three necked flask equipped with cooling condenser, rubble septum and a glass stopper, precedent product (0.15g) was dissolved in 10mL dry THF. The flask was flushed with  $\text{N}_2$  and was cooled to  $-78^\circ\text{C}$  and then t-butyllithium (1.7M in hexanes, 0.83mL) was charged with care through a syringe. (deep red in color) the mixture was stirred at  $-78^\circ\text{C}$  for 1 hour then it was quenched with anhydrous carbon dioxide. Color of the mixture changed to light yellow. The mixture was warmed up to room temperature by it self while  $\text{CO}_2$  was still bubbling through in about 30 minutes, and it was acidified with 10% HCl aqueous solution to pH1. Extracting with methylene chloride (10mL $\times$ 3), drying the solution and evaporating off the solvent to give a yellow solid (80mg, 64%).  $^1\text{H}$ NMR ( $\text{CDCl}_3$ ): *trans* isomer  $\delta$  2.01 (dd, 3.57Hz, 1.37Hz, 3H), 6.39(q, 1.65Hz, 1.38Hz,  $\frac{1}{2}\text{H}$ ), 6.70 (q, 1.65Hz, 1.37Hz,  $\frac{1}{2}\text{H}$ ); *cis* isomer 1.94 (dd, 4.39Hz, 1.64Hz, 3H), 6.43 (q, 1.65Hz, 1.37Hz,  $\frac{1}{2}\text{H}$ ), 6.75 (q, 1.37, 1.65Hz,  $\frac{1}{2}\text{H}$ ), 7.2-8.1 (m);  $^{19}\text{F}$ NMR( $\text{C}_6\text{D}_6$ ,  $\text{CFCl}_3$ ), -130.15(dd, 85.94, 3.96Hz), 130.70(dd, 89.90, 3.96Hz). High Resolution Spectra: Calculated for  $\text{C}_{10}\text{H}_9\text{O}_2\text{F}$  = 180.05866, Measured=180.0589

**3-Fluoro-4-methyl-quinone-2-one.**  $^1\text{H}$ NMR ( $\text{DMSO}-d_6$ )  $\delta$  2.38(d, 2.93Hz, 3H), 7.25 (t, 7.08Hz, 1H), 7.35(d, 8.3Hz), 7.50(t, 7.08Hz), 7.75(d, 8.05Hz),  $^{19}\text{F}$ NMR( $\text{C}_6\text{D}_6$ ,

FPh, -116.0), -136.5(s) High Resolution Spectra: Calculated for  $C_{10}H_8NOF=177.0590$ ,

Measured: 177.0636

Table 4-11. Data for determining the rate constant of  $\alpha$ -methyl- $\beta$ -fluoro system, at 101.6°C.

Time (s)	600	1200	1800	2400	3000	3600
ln(rel-peak) <i>trans</i>	1.203	1.020	0.762	0.504	0.245	0.121
Time (s)	2400	3000	7200	10800	13800	-
ln(rel-peak) <i>cis</i>	1.123	1.115	1.102	1.078	1.070	-

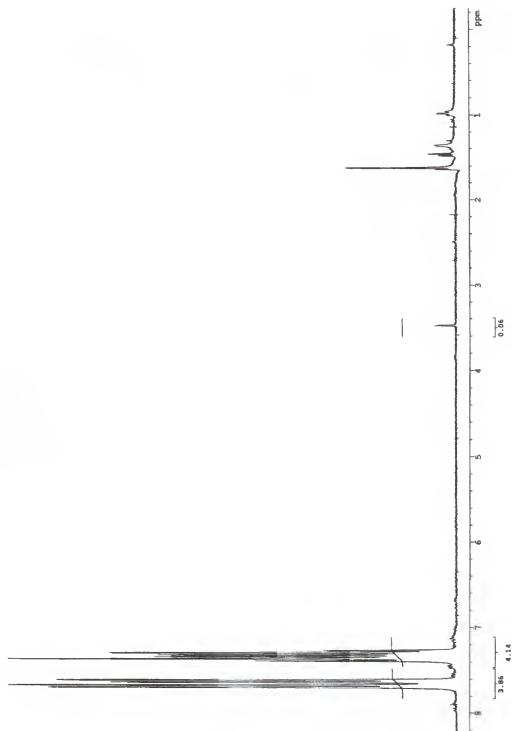
## APPENDIX

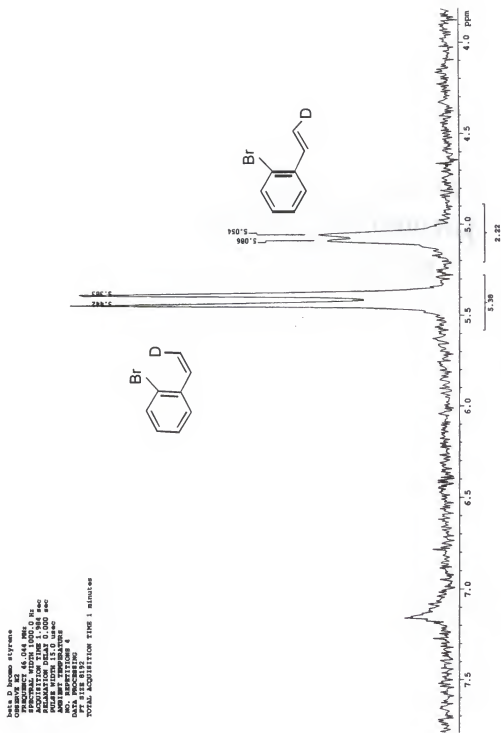
### SELECTED NMR SPECTRA

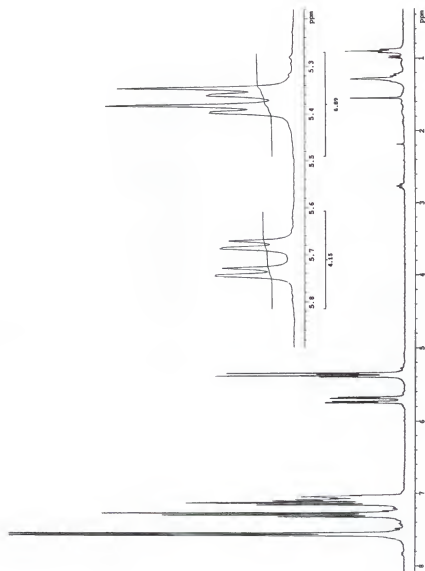
In the appendix, the spectra are presented numerically in their respective areas in this Chapter.



Figure A-1 Thermal Rearrangement of the Parent System (52) to (56)

Figure A-2 2-Bromo-phenylacetylene- $d_1$  (62)

Figure A-3 2HNMR of 2-Bromo-Styrene- $\beta$ - $d_1$

Figure A-4  $^1\text{H}$  NMR of 2-Bromostyrene- $\beta$ - $d_1$

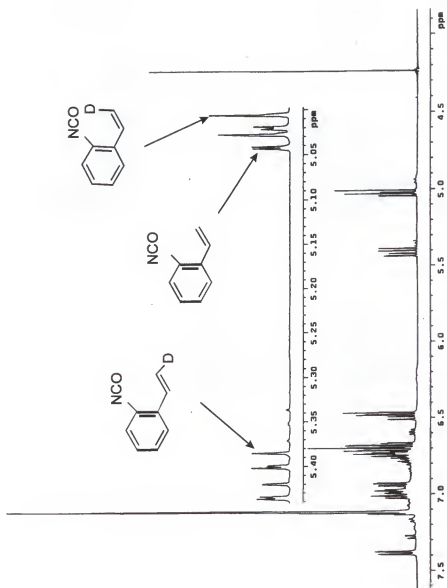
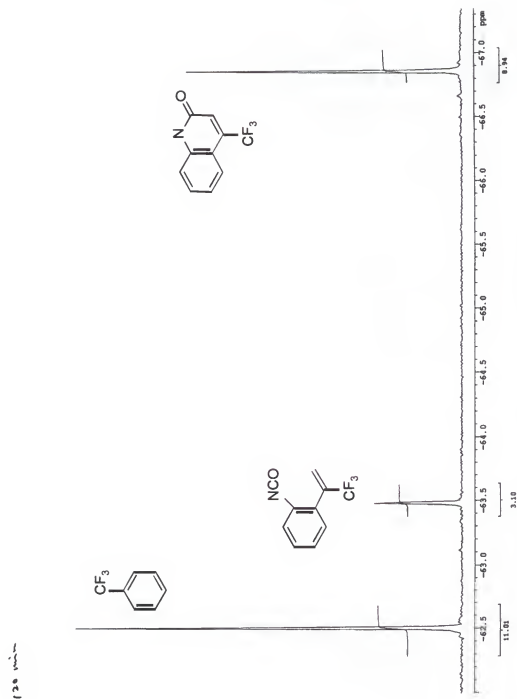
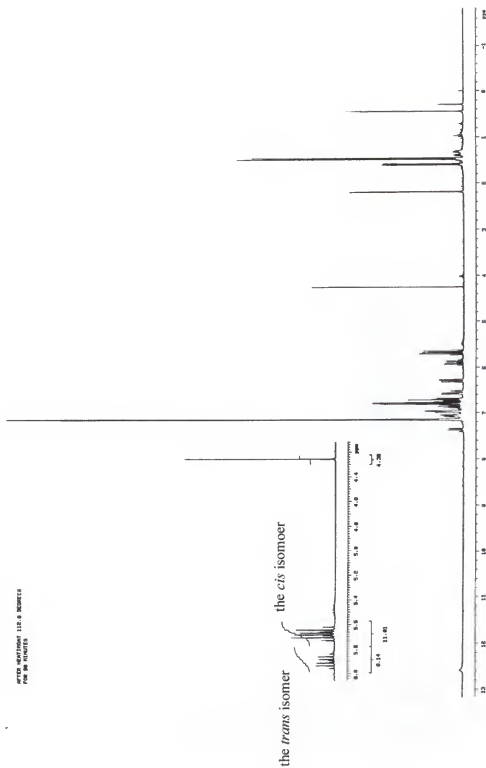


Figure A-5 Experiment of the Isotope Effect of the Thermal Rearrangement

Figure A-6 Thermal Rearrangement of  $\alpha$ -Tetrafluoromethyl Styrene (79)

Figure A-7 Thermal Rearrangement of  $\beta$ -methyl System (87)

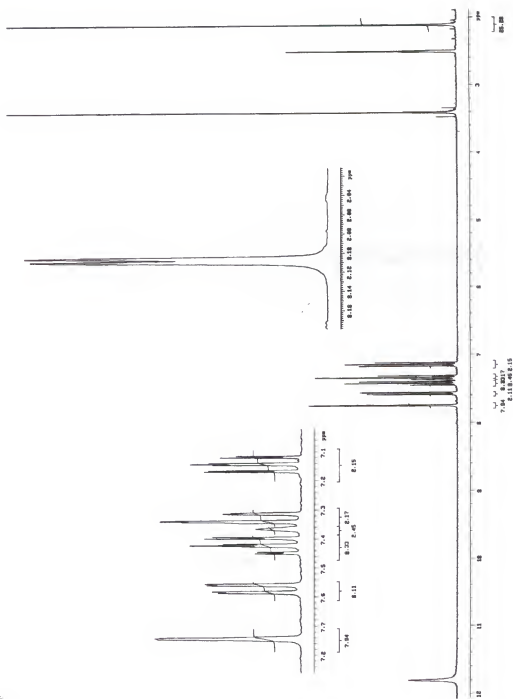


Figure A-8 3-Methyl-Quinol-2-one

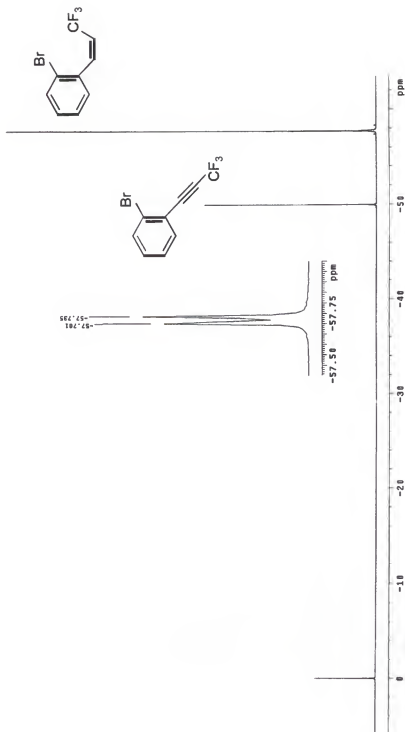


Figure A-9. Monitoring the Hydrogenation of (92) to (93)

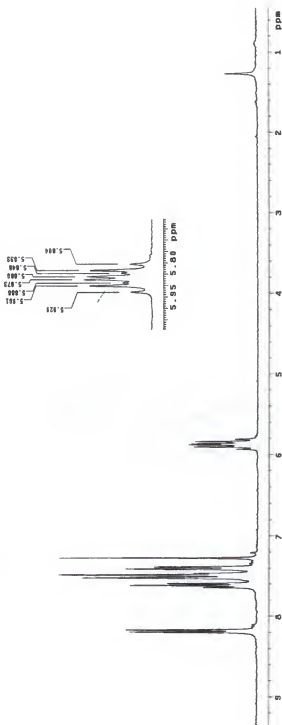
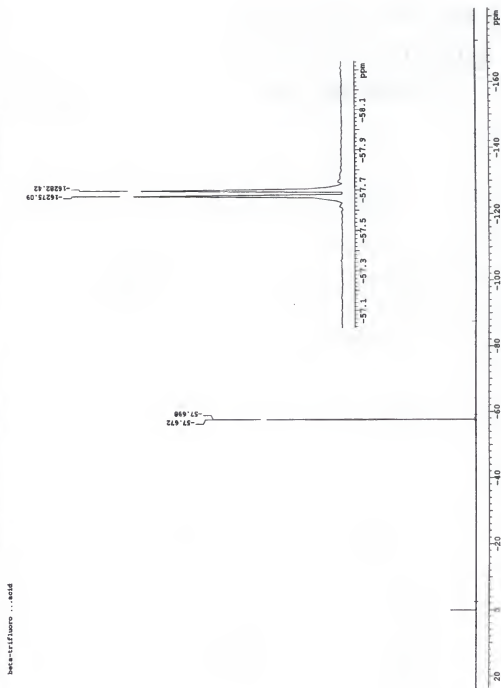


Figure A-10  $^1\text{H}$ NMR of 2-((Z)-(3,3,3-Trifluoro-1-Propenyl)benzoyl)benzoic Acid (94-cis)

Figure A-11  $^{19}\text{F}$ NMR of ((Z)-3,3-Trifluoro-1-Propenyl) benzoic Acid (94-cis)

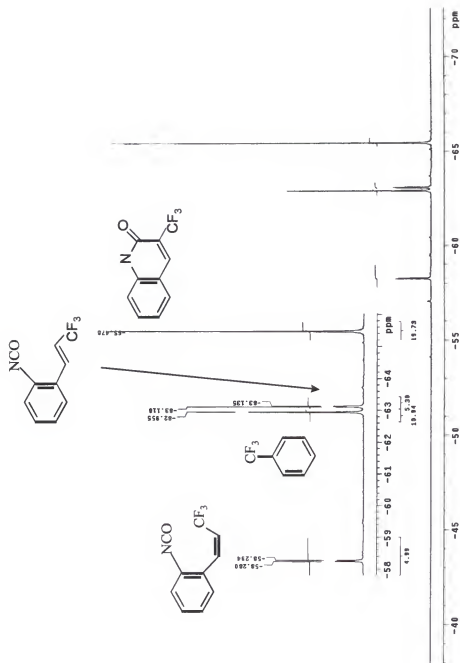


Figure A-12 Thermal Rearrangement of b-Trifluoromethyl System (96)

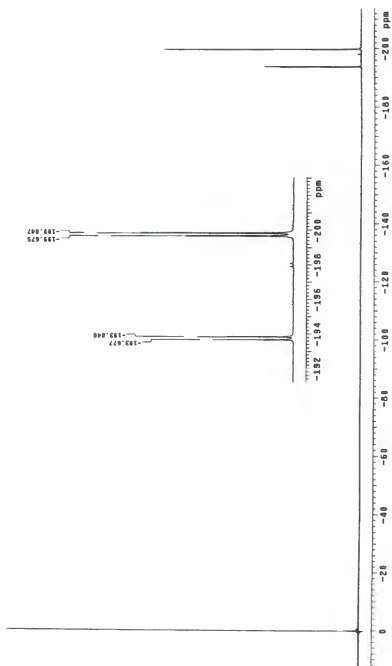


Figure A-13 Ethyl 2-fluoro-3-hydroxy-3-butyrate (101)

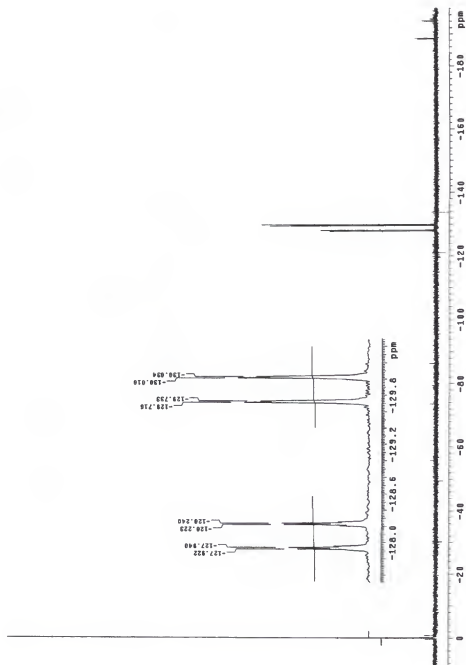


Figure A-14 1-Bromo-2-((Z/E)-2-Fluoro-1-Methyl-1-ethenyl) Benzene (103)

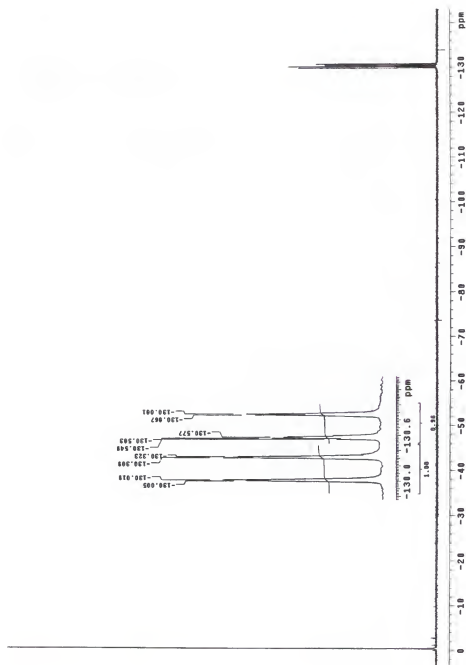


Figure A-15  $^{19}\text{F}$  NMR of 2-((E/Z) 20Fluoro-Methyl-1-Ethenyl) BenziocAcid

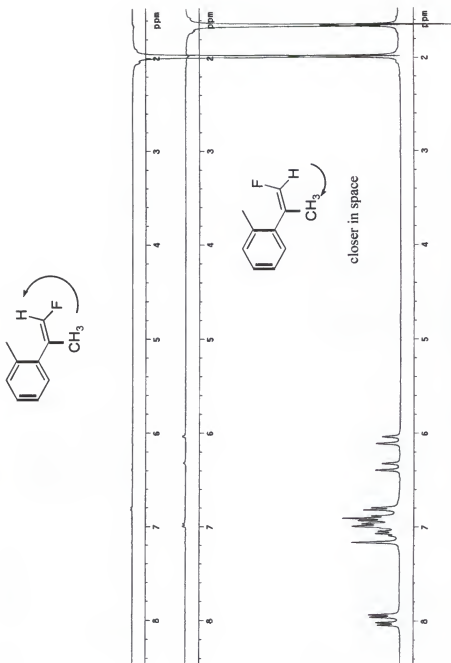
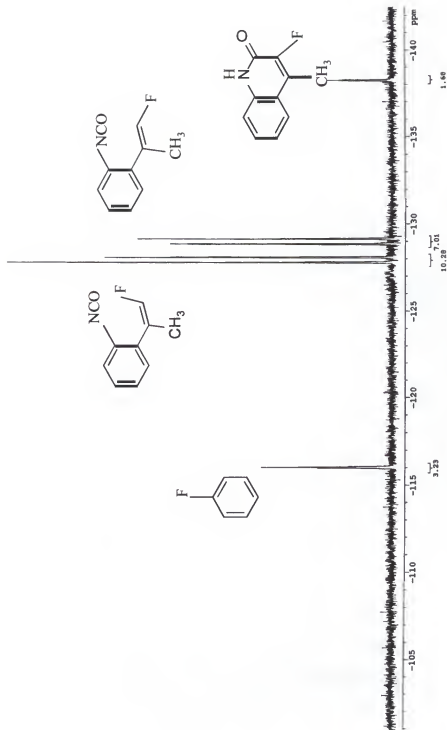


Figure A-16 NOE difference spectroscopy of (104)

101.6 degrees 30 minutes

Figure A-17 Thermal Rearrangement of  $\alpha$ -methyl- $\beta$ -fluoro System

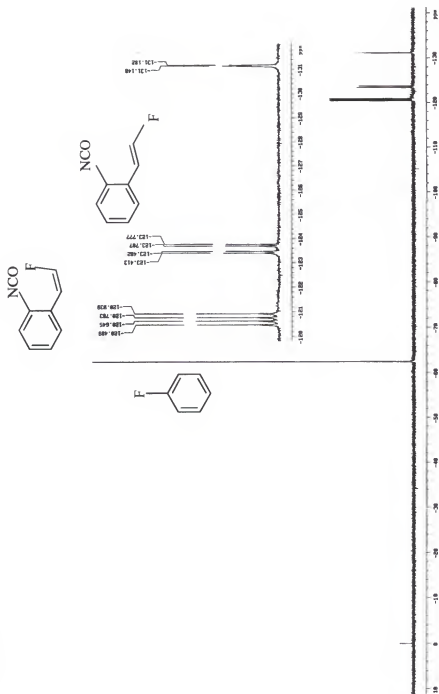


Figure A-18 Thermal Rearrangement of Monofluoro System (109)

## REFERENCES

1. Woodward, R. B. and Hoffmann, R., *J. Amer. Chem. Soc.* 87(1965), 395; Woodward, R. B. and Hoffmann, R., *J. Amer. Chem. Soc.* 87(1965), 2046; Woodward, R. B. and Hoffmann, R., *J. Amer. Chem. Soc.* 87(1965), 2511.
2. Woodward, R. B. and Hoffmann, R., *Conservation of Orbital Symmetry*, Verlag Chemie GmbH, Academic Press Inc. 1971
3. Breulet, J. and Schaefer III, H. F. *J. Amer. Chem. Soc.* 106(1984), 1221.
4. Branton, G. R., Frey, H. M. and Skinner, R. F., *Trans. Far. Soc.* 62(1966) 1546.
5. Winter, R. E. K. *Tetrahedron Lett.* 17(1965), 1207.
6. Criegee, R. Noll, K. *Liebigs Ann. Chem.* 1959, 1 627.
7. a) Vogel, E. *Liebigs Ann. Chem.* 1958, 615, 14; b) Cooper, W. Walters, W. D. *J. Am. Chem. Soc.* 80(1958), 4220.
8. Curry, M. J. and Stevens, I. D. R. , *J. Chem. Soc., Perkin Trans. II*, 10(1980), 1391.
9. Rudolf, K. Spellmeyer, D. C. and Houk. K. N. *J. Org. Chem.*, 52(1987), 3708
10. Houk, K. N.; Spellmeyer, D. C., Jefford, C. W., Rimbault, C. G., Wang, Y and Miller, R. D., *J. Org. Chem.* 52(1988), 2125
11. Pirkle, W. H. and McKendry, L. H., *J. Amer. Chem. Soc.*, 91(1969), 1179.
12. *The Chemist's Companion*, Editor, Gordon, A. J. and Ford, R. A., John Wiley and Sons, New York, NY (1972).
13. Pauling, L. *The Nature of the Chemical Bond*, Cornell University Press, Ithaca, NY(1960)
14. Smart, B. *Molecular Structure And Energetics*, Volume. 3 *Studies of Organic Molecules*. Editor, Liebman J. F. Greeberg, A. , VCH Publishes, Inc. (1986) 141.
15. Chambers, R. D. *Fluorine in Organic Chemistry*. Duram, U.K. 1973

16. Bondi, A. J. *Phys. Chem.* 68(1964), 441.
17. Dolbier Jr., W. R. *Advances in Strain in Organic Chemistry*, Volume 3, pages 1-58, 1993.
18. Dolbier Jr, W. R., Koroniak, H., Burton, D. J., Heinze, P. L., Bailey, A. R., Shaw, G. S. and Hansen, S. W., *J. Amer. Chem. Soc.* 109(1987), 219.
19. Dolbier, W. R. Jr., Koroniak, H. Burton, D. J. Heinze, P. L. *Tetrahedron Lett.* 27(1986), 4387
20. Dolbier, W. R. Jr., Gray, T. A., Celewicz, L. and Koroniak, H., *J. Amer. Chem. Soc.*, 112(1990), 363.
21. Smith, D. A. and Ulmer, II, C. W., *J. Org. Chem.*, 58(1993), 4118.
22. Lopez, R., Sordo, T. L., Sordo, J. A. and Gonzalez, J., *J. Org. Chem.* 58(1993), 7036.
23. Rondan, N. G., Houk, K. N. *J. Amer. Chem. Soc.* 107(1985), 2099.
24. Houk, K. N. in *Strain and Its Implications in Organic Chemistry*, Organic Stress and Reactivity, Kluwer Academic, Dordrecht, Netherlands, V 273, NATO ASI Series, Series C, 1988, 25
25. Spellmer, D. C., Houk, K. N., *J. Am. Chem. Soc.* 110(1988), 3412.
26. Buda, A. B., Wang, Y., Houk, K. N., *J. Org. Chem.* 54(1989) 2264.
27. Kallel, E. A., Wang, Y., Spellmeyer, D. C., Houk, K. N. *J. Am. Chem. Soc.* 112(1990), 6759
28. Rudolf, K; Spelmeyer, D. C., Houk, K. N. *J. Org. Chem.* 52(1987) 3708
29. Thomas IV, B. E. Evanseck, J. D., Houk, K. N. *J. Am. Chem. Soc.* 115(1993), 4165
30. Evanseck, J. D.; Thomas IV, B. E.; Evanseck, J. D.; Spelmeyer, D. C.; Houk, K. N., *J. Org. Chem.* 60(1995), 7134.
31. Dolbier, Jr., W. R.; Palmer, K. W., *Tetrahedron Lett.* 34(1993), 6201.
32. Dolbier, W. R., Jr.; Palmer, K. W. *J. Am. Chem. Soc.* 115(1993), 9349.
33. Lowry, T. H.; Richardson, K., S. *Mechanism and Theory in Organic Chemistry*, 3<sup>rd</sup> ed.; Harper and Row, Publishers; New York, 1987, p839.
34. Ross, J. A.; Seiders, R. P.; Lemal, D. M., *J. Amer. Chem. Soc.* 98(1976), 4326.

35. Bushweller, C. H.; Ross, J. A. Lemal, D. M., *J. Amer. Chem. Soc.* 99(1977), 629.
36. Wendrup, C.; Nettsch, K.-P., *Angew. Chem. Int. Ed. Engl.* 23(1984), No. 10, p802.
37. Okamura, W. H.; Peter, R.; Reischl, W. *J. Am. Chem. Soc.* 107(1985) 1034.
38. Elnagar, H. Y.; Okamura, H. H., *J. Org. Chem.* 53(1988), 3060.
39. Henriksen, U.; Snder, J. P.; Halgren, T. A. *J. Org. Chem.* 46(1981), 3767.
40. Burke, L. A.; Elguero, L. Leroy, G.; Sana, M. *J. Am. Chem. Soc.* 98(1976), 1685.
41. Birney, D. M., *J. Org. Chem.* 61(1996), 243.
42. Birney, D. M. *J. Org. Chem.* 59(1994), 2557.
43. Birney, D. M. *J. Am. Chem. Soc.* 119(1997), 4507
44. Birney, D. M. and Wagenseller, P. E. A. *J. Am. Chem. Soc.* 116(1994), 6262
45. Wagenseller, P. E.; Birney, D. M.; Roy, D. *J. Org. Chem.* 60(1995), 2853
46. Ham, S. and Birney, D. M. *Tetrahedron Lett.* 38(1997) 5925
47. Melander, L. Saunders, W. H., Jr., *Reaction Rates of Isotopic Molecules*; Wiley & Sons: New York, 1980.
48. Wiberg, K. B. in *Physical Organic Chemistry*, Wiley: New York, 1964, 273 and 351.
49. Saunders, W. H. Jr., In *Techniques of Chemistry*. Vol. 6: *Investigations of rates and Mechanisms of Reactions*; Bernasconi, C. F., ed.; Wiley-Interscience: New York. 1980;
50. Carpenter, B., *Determination of Organic Reaction Mechanisms*; Wiley-Interscience: New York, 1986.
51. Dolbier, W. R. Jr. In *Isotope Effects in Organic Chemistry*. Vol. 1: *Isotopes in Molecular Rearrangements*; Buncl, E., Lee, C.C., Eds.; Elsevier: New Yowk, 1975
52. Gajewski, J. J., In *Isotope Effects in Organic Chemistry*. Vol. 7: *Secondary and Solvent Isotope Effects*; Buncl, E., Lee, C.C., Eds.; Elsevier: New York, 1987.
53. Seltzer, S. *J. Am. Chem. Soc.* 85(1963), 360-1361; Seltzer, S. *J. Am. Chem. Soc.* 87(1965), 1534-1540
54. van Sickle, D. E.; Rodin, O. J., *J. Am. Chem. Soc.* 86(1964) 3091-3094.
55. Taagepera, M.; Thornton. E. R. *J. Am. Chem. Soc.* 84(1972), 1168-1177.

56. Gajewski, J. J.; Perterson, K. B.; Kagel, J. R.; Huang, Y. C. *J. Am. Chem. Soc.*, 111(1989) 9078-9081.
57. Dewar, M. J. S. Olivella, S.; Rzepa, H. S. *J. Am. Chem. Soc.* 100(1978) 5650
58. Lowry, T. H.; Richardson, K., S. *Mechanism and Theory in Organic Chemistry*, 3<sup>rd</sup> ed.; Harper and Row, Publishers; New York, 1987, p238
59. Streitweiser, A. Jr.; Jagow, R. H.; Fahey, R. C.; Suzuki, S. *J. Am. Chem. Soc.* 80(1958), 2326-2332.
60. Crawford, R. J.; Cameron, D. M. *J. Am. Chem. Soc.*, 88(1966), 2589.
61. Dai, S.; Dolbier, W. R.; Jr., *J. Am. Chem. Soc.* 94(1972), 3946.
62. Dai, S. H. Dolbier, W. R., Jr., *J. Am. Chem. Soc.* 92(1970), 1774.
63. Caldwell, R. A.; Misawa, H.; Healy, E. F.; Dewar, M. J. S. *J. Am. Chem. Soc.* 109(1987), 6869.
64. Olson, L. P.; Niwayama, S.; Yoo, H-Y; Houk, K. N.; Harris, N. J.; Gajewski, J. J. *J. Am. Chem. Soc.* 118(1996), 886-892.
65. Baldwin, J. E.; Reddy, V. P; Hess, B. A., Jr.; Schaad, L., *J. Am. Chem. Soc.* 110(1988), 8554-8555.
66. Baldwin, J. E.; Reddy, V. P; Schaad, L.; Hess, B. A., Jr., *J. Am. Chem. Soc.* 110(1988), 8555-8556
67. Wiest, O; Houk, K. N.; Black, K. A.; Thomas IV, B. *J. Am. Chem. Soc.* 117(1995), 8594-8599
68. Hammond, G. S. *J. Am. Chem. Soc.* 77(1955), 334.
69. Leffler, J. E. *Science*, 117(1953), 340.
70. Shaik, S. S.; Schlegel, H. B.; Wolfe, S. in *Theoretical Aspects of Physical Organic Chemistry*, John Wiley & Sons, Inc. 1992
71. Jefford, C. W.; Bernardinelli, G.; Wang, Y.; Spellmeyer, D. C.; Buda, A; Houk, K. N., *J. Am. Chem. Soc.* 114(1992), 1157
72. a) Lewis, K. E; Steiner, H., *J. Chem. Soc.* 1964, 3080; b) Pichko, V. A.; Simkin, B. Y.; Minkin, V. I.; *Dokl Phys. Chem. (Engl. Transl)* 292(1987), 910.
73. Marvell, E. N.; Caple, G.; Schatz, B.; Pippin, W., *Tetrahedron*, 29(1973), 3781

74. Gajewski, J. J. in *Hydrocarbon Thermal Isomerizations*, Editor: Wasserman, H. H., Academic Press, New York, NY, Vol 5, Organic Chemistry Series, (1981).
75. Vogel, E.; Grimme, W.; Dinne, E. *Tetrahedron Lett.* 21(1965), 391.
76. a) Cope, A. C.; Haven, A. C. Jr.; Ramo, F. L. Trumbull, E. R. J. Am. Chem. Soc. 74(1952) 4867; b) Lowry, T. H.; Richardson, K., S. *Mechanism and Theory in Organic Chemistry*, 3<sup>rd</sup> ed.; Harper and Row, Publishers; New York, (1987) 194
77. Hibino, S.; Sugino, E.; Adachi, Y.; Nomi K.; Sato, K., *Heterocycles*, 28(1989), 275
78. Daheiser, R.; Gee, S. K.; Perez, J, J. *J. Am. Chem. Soc.* 108(1986), 806
79. Szmuszkowicz, J. *J. Org. Chem.* 29(1964), 843
80. *Organic Synthesis*, Coll. Vol. 5 Editor: Horning, E. C., John Wiley and Sons (1965), 846
81. Some other ways to synthesize isocyanate: a) Bose, H.; Dutta, K. K; Sinha, M. Ray, P. K. *J. Indian Chem. Soc.* 67(1990), 172; b) Walbrick, J. M.; Wilson, J. W.; Jones, W. M., *J. Am. Chem. Soc.*, 90(1968), 2895; c) Kurita, K.; Matsumura, T.; Iwakura, Y., *J. Org. Chem.* 41(1976), 2070; d) Valli, V. L. K. and Alper, H., *J. Org. Chem.* 60(1995), 257; e) Sigurdsson, S. T.; Seeger, B; Kutzke, U; Eckstein, F., *J. Org. Chem.* 61(1996), 3883. f) Baumgarten, H. E. and Staklis, A. *J. Am. Chem. Soc.* 87(1965), 1141
82. Lowry, T. H.; Richardson, K., S. *Mechanism and Theory in Organic Chemistry*, 3<sup>rd</sup> ed.; Harper and Row, Publishers; New York, (1987), 494.
83. Linke, S.; Tisue, G. T.; Lwowski, W., *J. Am. Chem. Soc.* (1967) 6308
84. Felt, G. R. and Lwowski, W. *J. Org. Chem.* 41(1976), 96
85. Linke, S.; Tisue, G. T.; Lwowski, W., *J. Am. Chem. Soc.* (1967) 6303
86. Atkins, P. W. in *Physical Chemistry* Third Edition, W. H. Freeman and Company, New York. 1985
87. a) Huisgen, R.; Steiner, G. *J. Am. Chem. Soc.* 95(1973) 5054, 5055; b) Steiner, G.; Huisgen, R. *J. Am. Chem. Soc.* 95(1973) 5056; c) Connors, K. A. and Sun, S, *J. Am. Chem. Soc.* 93(1971), 7239; d) Isaacs, N. S., *Physical Organic Chemistry*, Longman Scientific & Technical and John Wiley & Sons, Inc. New York. (1988) 201
88. Isaacs, N. S. *Liquid Phase High Pressure Chemistry*, Wiley, Chichester, (1981)

89. Bartberger M. D. and Dolbier, W. R., Jr., unpublished results. The program for the calculations: Gaussian 94 (Revision C. 3) Frisch, M. J.; Trucks, G. W.; Schlegel, H. Gill, P. M.; Keith, T. A. et. al, Gaussian, Inc. Pittsburgh, PA, 1995.
90. Houk, K.N.; Li, Y.; Evanseck, J. D. *Angew. Chem. Int. Ed. Engl.* 31(1992) 682.
91. Isaacs, N. S. *Physical Organic Chemistry*, Longman Scientific & Technical, John Wiley & Sons Inc, New York, (1987), 264.
92. Pianetti, P. and Pougny, J. R., *Tetrahedron Lett.* 27(1986), 5853.
93. Matsumoto, M. and Kuroda, K. *Tetrahedron Lett.* 21(1981) 4021.
94. Marvell, E. N. and Li, T. *Synthesis* (1973), 457.
95. Wolinsky, J.; and Erickson, K. L. *J. Org. Chem.*, 30(1965), 2208.
96. Harthun, A.; Giernoth, R.; Elsevier C. J.; Bargon, J., *Chem. Commun.* (1996) 2483.
97. Smolin, . M., *Tetrahedron Lett.* (1961) 143.
98. Zollinger, H. *Adv. Pyhs. Org. Chem.*, 2(1964), 163.
99. Mitsuhashi, T *Polar Effects on the Lability of Carbon-Carbon Bonds in Structure and Reactivity*, Editors: Liebman J. F. and Greenberg, A., VHC Publishers, Inc. New York, (1988), 179.
100. Laidler, K. J., in *Chemical Kinetics*, third edition. Harper Collins Pulishers (1987) 280.
101. Moore, J. W.; Pearson, R. G., *Kinetic and Mechanism*, John Wiley & Sons: New York, 1981, p290.
102. *NMR Command and Parameter Reference*, Varian Nuclear Magnetic Resonance Instruments, (1995) 223.
103. Wen, J; Tian, M; Chen, Q., *Liquid Crystals*, 16(1994) 445.
104. Jiang, B. and Xu, Y. *J. Org. Chem.* 56(1991), 7336.
105. Rousseau, G.; Conia, J. M., *Tetrahedron Lett.* 22(1981) 649.
106. Nolttes, J. G. and Van Den Hurk, J. W. G., *J. Organomet. Chem.* 1(1964), 377.

107. a) Ingold, C. K. *J. Chem. Soc.* (1930), 1032; b) Taft, R. W., Jr. *J. Am. Chem. Soc.*, 74(1952), 2729, 3120; 75(1953) 4231; c) Swain, C. G. and Lupton, E. C., Jr., *J. Am. Chem. Soc.* 90(1968), 4328.
108. a) Unger, S. H. and Hansch, S., *Prog. Phys. Org. Chem.* 12(1976), 91; b) Charton, M. *J. Org. Chem.* 43(1978), 3993.
109. a) Hirsh, J. *Top. Stereochem.* 1(1967), 199; b) Eliel, E. L.; Allinger, N. L.; Angyal, S. L.; Morrison, G. A. *Conformational Analysis*; Wiley, New York, (1965), 44.
110. Smart, B. *Properties of Fluorinated Compounds in Chemistry of Organic Fluorine Compounds*, editor Hudlicky, M. and Pavlath, A. E. ACS Monograph 187, (1995) 979.
111. a) Jensen, F. R. Bushweller, C. H.; Beck, B. H. *J. Am. Chem. Soc.* 91(1969), 344; b) Taft, R. W.; Abboud, J. L. M.; Anvia, F.; Berthet, M.; Fujio, M. *J. Am. Chem. Soc.*, 110(1988), 1797.
112. Ruzicka, L. *Angew. Chem. Int. Ed. Engl.* 29(1990), 1320.
113. Ehrenson, S.; Brownlee, R. T. C.; Taft, R. W. *Prog. Phys. Org. Chem.* 10(1973), 1.
114. Silverstein, R. M.; Bassler, G. C.; Morrill, T. C. in *Spectrometric Identification of Organic Compounds*, fifth edition, (1991), 217.
115. a) Fujita, M. and Hiyama, T. *Bull. Chem. Soc. Jpn.* 60(1987) 4377, 4385; b) Huyama, T.; Sato, K.; Fujita, M. *Bull. Chem. Soc. Jpn.*, 62(1989), 1352.
116. Sondengam, B. L.; Charles, G.; Akam, T. M., *Tetrahedron Lett.* 21(1980), 1069.
117. Brace, N. O.; Marshall, L. W.; Pinson, C. J.; van Wingerden, G., *J. Org. Chem.*, 49(1984), 2361.
118. Kurobshi, M. and Ishihara, T., *Journal of Fluorine Chemistry*, 39(1988), 299.
119. Rong, G. and Keese, R., *Tetrahedron Lett.* 31(1990), 5615.
120. Huang, W. and Zhang, H., *Journal of Fluorine Chemistry* 50(1990), 133.
121. Haszeldine, R. N.; Keen, D. W.; Tipping A. E., *J. Chem. Soc (C)*, (1970), 414.
122. Brace, N. O., *Journal of Fluorine Chemistry*, 20(1982), 313.
123. Tekeyama, Y.; Ichinose, Y.; Oshima, K., *Tetrahedron Lett.* 30(1989), 3159.

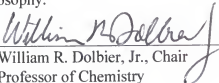
124. Hayashi, S.; Nakai, T.; Ishikawa, N.; Burton, D. J.; Naae, D. G.; Kesling H. S., *Chemistry Letters*, (1979) 893.
125. Naae, D. G. and Burton, D. J., *Synthetic Communications*, 3(3) (1973), 197.
126. Burton D. J. and Greenlimb, P. E., *J. Org. Chem.* 40(1975), 2796.
127. Shen, Y. and Qi, M., *Journal of Fluorine Chemistry*, 67(1994) 229.
128. Dolbier, W. R. Jr.; Ocampo, R.; Paredes, R. *J. Org. Chem.* 60(1995), 5378.
129. Ocampo, R; Dolbier, W. R. Jr.; Bartberger, M. D. Paredes, R., *J. Org. Chem.* 62(1997), 109.
130. Shen, Y. and Qi, M., *J. Chem. Research(S)*, (1993) 222.
131. Brandange, S.; Dahlman, O.; Morch, L. *J. Am. Chem. Soc.* 103(1981), 4452.
132. Rahman, A in *One and Two Dimensional NMR Spectroscopy*, Elsevier Science Publishers B. V. New York (1989).
133. Burton, D. J., *J. Am. Chem. Soc.* 107(1985), 2812.
134. L. Luo; Bartberger, M. D.; Dolbier, W. R. Jr. *J. Am. Chem. Soc.* 119(1997), 12366
135. Heidelberger, C. and Chaudhuri, N. K., *Nature*. 179(1957), 663.
136. a) Dennis, L. M.; Veeder, J. M.; Rochow, E. G., *J. Am. Chem. Soc.* 53(1931), 3263;  
b) Rudge, A. J., *The Manufacture and Use of Fluorine and its Compounds*. Oxford University Press, Oxford, (1962)
137. a) Finger, G. C. *Advances in Fluorine Chemistry* 2. Butterworths, London, (1961);  
b) Leech, H. R. *Chem. Ind (London)*, (1960), 242; c) Stuewe, A. H. *Chem. Eng. News*, 36(51), (1958), 35.
138. a) Tullock, C. W.; Fawcett, F. S. Smith, W. C. Coffman, D. D., *J. Am. Chem. Soc.* 82(1960), 539; Nyman, F. Roberts, H. L. *J. Chem. Soc.* (1962), 3180; Smith, W. C.; Tullock, C. W. Muetterties, E. L. *J. Am. Chem. Soc.* 81(1959), 3163.
139. a) Emeleus, H. J, and Wood, J. F., *J. Chem. Soc.* 76(1954), 3459; b) Fawcett, F. S. Tullock, C. W. Coffman, D. D, *J. Am. Chem. Soc.* 84(1962), 4275.
140. Schreiner, F. McDonald, G. N. Chernick, C. L. *J. Phy. Chem.* 72(1968), 1162.

141. *Methods of Introducing Fluorine into Organic Molecules* in *Chemistry of Organic Fluorine Compounds*, a critical review, Editor: Hudlicky, M. and Pavlath, A. E. ACS Monography 187 (1995)
142. McCarthy, J. R.; Huber E. W. Le, T; Laskovics, F. M.; Matthews, D. P., *Tetrahedron* 52(1996), 45.
143. a) Welsh, J. T. *Tetrahedron* 43(1987), 3123; b) Fugigami, T. J. *Synth. Org. Chem. Jpn.* 42(1982), 775.
144. *The Aldrich Library of  $^{13}\text{C}$  and  $^1\text{H}$  FTNMR Spectra*, Edition I, Editor: Ponchert, A and Behnke, J, Aldrich Chemical Company, Inc. Volume 3, (1993) 431.


## BIOGRAPHICAL SKETCH

Lian Luo was born in the year when the Culture Revolutions started, in Zhejiang Province, People's Republic of China. He was brought up in a cottage with his other four siblings. He received his B.S. in Chemistry from East China Normal University, Shanghai, in 1989. After the Student Movements, he managed to initiate his graduate studies under supervision of Dr. J. Martin E. Quirke, at the Florida International University, Miami, USA. In the fall of 1993, he moved to the University of Florida in Gainesville, Florida, joined the doctoral program in the Department of Chemistry and carried out new graduate researches with Dr. William R. Dolbier, Jr. Throughout his research, Luo found that chemistry was unfolding and it became more and more fascinating. Upon completion of his doctoral studies, Luo looks forward to the new chemistry adventures at Oak Ridge National Laboratory as a postdoctoral fellow.


I certify that I have read this study and that in my opinion it conforms to acceptable standards of scholarly presentation and is fully adequate, in scope and quality, as a dissertation for the degree of Doctor of Philosophy.

  
William R. Dolbier, Jr., Chair  
Professor of Chemistry


I certify that I have read this study and that in my opinion it conforms to acceptable standards of scholarly presentation and is fully adequate, in scope and quality, as a dissertation for the degree of Doctor of Philosophy.

  
Merle A. Battiste  
Professor of Chemistry


I certify that I have read this study and that in my opinion it conforms to acceptable standards of scholarly presentation and is fully adequate, in scope and quality, as a dissertation for the degree of Doctor of Philosophy.

  
Lisa A. McElwee-White  
Professor of Chemistry

I certify that I have read this study and that in my opinion it conforms to acceptable standards of scholarly presentation and is fully adequate, in scope and quality, as a dissertation for the degree of Doctor of Philosophy.

  
Robert T. Kennedy  
Associate Professor of Chemistry

I certify that I have read this study and that in my opinion it conforms to acceptable standards of scholarly presentation and is fully adequate, in scope and quality, as a dissertation for the degree of Doctor of Philosophy.

  
James F. Klausner  
Associate Professor Mechanical  
Engineering

This dissertation was submitted to the Graduate Faculty of the Department of Chemistry in the College of Liberal Arts and Sciences and to the Graduate School and was accepted as partial fulfillment of the requirements for the degree of Doctor of Philosophy.

May, 1998

---

Dean, Graduate School